JULY 2017

M.Sc. in Physics Engineering

PESHAWA O. HAMA

UNIVERSITY OF GAZİANTEP

GRADUATE SCHOOL OF

NATURAL & APPLIED SCIENCES

INVESTIGATION OF THERMOLUMINESCENCE (TL) RETROSPECTIVE DOSIMETRIC PROPERTIES OF SILICON CARBIDE (SiC) USED IN INDUSTRY APPLICATIONS

M.Sc. THESIS

IN

PHYSICS ENGINEERING

BY

PESHAWA O. HAMA

JULY 2017

Investigation of Thermoluminescence (TL) Retrospective Dosimetric Properties of Silicon Carbide (SiC) Used in Industry Applications

M.Sc. Thesis

in

Physics Engineering

University of Gaziantep

Supervisor

Assoc. Prof. Dr. Hüseyin TOKTAMIŞ

by

Peshawa O. HAMA

July 2017

REPUBLIC OF TURKEY
UNIVERSITY OF GAZİANTEP
GRADUATE SCHOOL OF
NATURAL & APPLIED SCIENCES
PHYSICS ENGINEERING

Name of the Thesis: Investigation of Thermoluminescence (TL) Retrospective Dosimetric Properties of Silicon Carbide (SiC) Used in Industry Applications.

Name of the student: Peshawa O. HAMA

Exam date: 31.07. 2017

Approval of the Graduate School of Natural and Applied Sciences.

Prof. Dr. A. Necmeddin YAZICI
Director

I certify that this thesis satisfies all the requirements as a thesis for the degree of Master of Science.

Prof. Dr. Ramazan KOÇ
Head of Department

This is to certify that we have read this thesis and that in our consensus opinion it is fully adequate, in scope and quality, as a thesis for the degree of Master of Science.

Assoc. Prof. Dr. Hüseyin TOKTAMIŞ
Supervisor

Examining Committee Member	Signature
Assoc. Prof. Dr. Hüseyin TOKTAMIŞ	----------
Assoc. Prof. Dr. Vural E. KAFADAR	----------
Assist. Prof. Dr. Necmettin NUR	----------

I hereby declare that all information in this document has been obtained and presented in accordance with academic rules and ethical conduct. I also declare that, as required by these rules and conduct, I have fully cited and referenced all material and results that are not original to this research.

Peshawa O. HAMA

ABSTRACT

INVESTIGATION OF THERMOLUMINESCENCE (TL) RETROSPECTIVE DOSIMETRIC PROPERTIES OF SILICON CARBIDE (SiC) USED IN INDUSTRY APPLICATIONS

HAMA, Peshawa O. Hama

M.Sc. in, Physics Engineering

Supervisor: Assoc. Prof. Dr. Hüseyin TOKTAMIŞ

July 2017

96 pages

During a nuclear accident or violent terror attack the dose measurement was not easily done at this moment because the data is not available to decide correct value of dose in the contaminated area. One of the alternative solution is by using retrospective dosimetry as a tool of accidental dosimetry for dose estimation. And many objects of the contaminated area are applicable as retrospective dosimeters. Although many electronic devices today are based on pure silicon substrates, a number of other substrates are used in various applications. SiC has been found to be widely useful as a substrate and wide band gap semiconductor in, high-temperature, high-frequency, and high-power electronic devices, as well as in short wavelength, radiation resistant optoelectronic devices. The aim of this study was to discuss the thermoluminescence (TL) properties of silicon carbide (SiC) used in industry applications for retrospective dosimetry purposes. Basic TL properties of these materials (e.g. dose response, heating rate, fading effect and reproducibility) have also been investigated.

Keywords: Thermoluminescence, Silicon Carbide, Retrospective Dosimetry.

ÖZET

ENDÜSTRİ UYGULAMALARINDA KULLANILAN SİLİKON KARBÜRÜN (SiC) TERMOLUMİNESANS RETROSPEKTİF DOZİMETRİK ÖZELLİKLERİNİN İNCELENMESİ

HAMA Peshawa O. Hama
Yüksek Lisans Tezi, Fizik Müh. Bölümü
Tez Yöneticisi: Doç. Dr. Hüseyin TOKTAMIŞ
Temmuz 2017
96 sayfa

Bir nükleer kaza veya şiddetli terör saldırısında bölgedeki doz ölçümü kolay değildir. Bunun nedeni kirlenmiş bölgeden alınacak dataların doğru ve sağlıklı bir şekilde temin edilmesinin imkansız olmasıdır. Bu tür doz ölçümlerinde alternative çözümlerden biri kaza dozimetresi olarak retrospektif dozimetrelerin kullanılmasıdır. Kirlenmiş bölgede toplanılan bir çok nesne geçmişe ait dozimetre olarak kullanılabilinir. Bir çok dozimetrik numune oluşumundan itibaren biriktirdiği dozlardan dolayı retrospektif dozimetre olarak adlandırılır. Günümüzde birçok elektronik cihaz saf silikon tabanlı olmasına ragmen diğer silikon tabanlı malzemlerin kullanıldığı farklı uygulamalar mevcuttur. Silikon karbür (SiC) endüstüride geniş uygulama alanları bulunan, geniş bant aralığına sahip ve radyasyona dayanıklı bir optoelektronik malzemedir. Bu çalışmanın amacı endüstüri uygulamalarında kullanılan silikon karbürün retrospektif dozimetrik amaç doğrultusunda termolüminesans özelliklerini irdelemektir. Aynı zamanda bu malzemenin doz cevap ilişkisi, ısıtma oranı, sönümleme etkisi ve tekrarlanabilirlik gibi temel termolüminesans özellikleride araştırılmıştır.

Anahtar Kelimeler: Termolüminesans, Silikon Karbür, Retrospektif dozimetre.

To my parents and my family

ACKNOWLEDGEMENT

First and foremost, I would like to acknowledge Almighty God who granted me wisdom, health and strength to overcome life's difficulties and actualizing my set targets and academic achievement.

I would like to express my heartfelt thanks and deep gratitude to my supervisor, **Assoc. Prof. Dr. HÜSEYIN TOKTAMIŞ**, for the continuous support of my M.Sc., study and research, for his ongoing advice, encouragements, the great moral motivation, patience, brotherly treatment and insight throughout the writing of this research work. My gratitude is due to the head and staff of the Engineering Physics Department for their assistant and support during the years of my study and research. I would like to express my thanks to Fetas Metallurgy Company from Turkey to support me by SiC to this study.

I would like to show my gratitude and my love to my family for their support and love through the duration of my M.Sc. life. They have given me an endless enthusiasm and encouragement. I am similarly indebted to all my friends. Especially, my wife **ASKLA**, that they helped me in completion of my thesis.

Finally, I would like to thank to those who have helped me in one way or another.

TABLE OF CONTENTS

Page

LIST OF FIGURES

Page

LIST OF TABLES

Page

CHAPTER 1

INTRODUCTION

1.1 Introduction

The physical properties of a solid can be determined by influence the defect in a material structure. An essential understanding of the defect structure is necessary for the selecting properties of the material and also for the explanation of many physical properties. The defect structure of a material should be studied by several different methods, such as (electrical, thermal, optical …etc.). The study of defects or impurity states can lead to a basic understanding of the nature of the defects and to a characterization of the material with its associated defects. Such a study can result not only in the identification and understanding of defects itself but also can lead to techniques which control the defects for suitable applications.

Thermoluminescence is one of the useful methods for studying the cyclic processes among defects. Thermoluminescence is known as processes of emitting light in an insulator or semiconductor that occurs during the heating of a material, after a previous absorption of energy from the radiation. [1,2]
On the other hand vacancies, dislocations and interstitials influenced by impurity in materials can act as luminescence centers or charge traps . After irradiated the sample carriers are trapped in these traps, by increasing the temperature charge is released energy with emitting wave often in the form light. This emission of light can be recorded as a function of temperature which is measured by a photomultiplier tube circuit, and it is called glow curve.

The glow curve has valuable information about the intrinsic defect. Analysis of the glow curves gives a value for the energy level at which the trap is situated (activation energy). The area under the curve reveals the number of recombination of electron-hole pairs which have taken place in the crystal. The first glow curve in TL dosimeter

was determinded by Randall and Wilkins in 1945. The first determinded glow curve showed multiple peaks and later it was realised its very rare for a single glow curve peak to appeare in TL dosimetry [3].

However, the final glow curve structure are depends on those factors like the mixture of dosimeter types of dopants, type of ionizing radiation, compound, position of defect centers after irradiation, level of radiation dose, and annealing [4,5].

The maximum point of the Glow curve peak not only varies with the heating mechanism and with the materials compositions, but also greatly affected by the intrinsic (traping) parameters such as the radiation dose, concentration of traps , activation energy (E), heating rate (β), and frequency factors (s) [6,7].

In general, application of thermoluminescence involved at three major area as, radiation dosimetry, age determination, and geology, with developing technology, simultaneously thermoluminescence application was grown, the most important utilization area of thermoluminescence is the radiation dosimetry, the most important application areas [8];

i. Personnel Dosimetry (extremity dosimetry, whole-body dosimetry, tissue dosimetry)
ii. Environment Dosimetry (terrestrial dosimetry, retrospective dosimetry and space dosimetry)
iii. Clinical Dosimetry (diagnostic radiology, radiotherapy)
iv. High Dose (food sterilization, nuclear reactors, materials testing)

In today's world, energy needs and developing technologies are increasing rapidly in a proportional manner. Dosimeters are necessary equipment to measure absorbed dose in the nuclear plants, hospitals and research investigations and they need to develop for giving the best results. There are several types of dosimeters and two of them are accidental and personal dosimeters. In the worst case scenario, we can measure the magnitude of the radiation by using accidental dosimeters which are spread around the areas of a nuclear accident or terrorist attack. In such a case, we can take the appropriate steps in these accidents by measuring the magnitude of the radiation accurately using accidental dosimeters. We can decide where the radiation is intense

by comparing the radiation values or magnitudes in different regions and after these measurements we can decide correctly whether these regions are safe or not.

In addition, personnel who work in places such as oncology, radiology, laboratories, etc., should limit the radiation doses they are exposed to during while performing their duties. Increased dosage levels may harm the health of personnel, so the value to be received from personal dosimeters which the personnel is wearing becomes important. In these situations, we need to use appropriate personal dosimeters to ensure their health. In addition,with the advancement of technology, humans needs are also advancing.

Due to the physical properties of synthetic Silicon Carbide (SiC) and increasing its benefits and applications in industry, the SiC may be a good candicate retrospective dosimeter.

The development of SiC high-temperature devices is in, jet engine ignition systems, aircraft, and automotive engine sensors, deep well drilling transmitters and a number of industrial process measurement and control systems. The distributed smart electromechanical controls which are capable of harsh ambient operation which based on uses of SiC will enable considerable reduced maintenance, jet-aircraft weight savings, higher fuel efficiency, reduced pollution, and increased operational reliability [45].

The applications of SiC high-power devices are in power supplies, surge suppressors, and solid-state lamp ballasts [46]. SiC electronics performance could enable the public power wire to supply increased demon for consumer electricity request without constructing extra generation plants and improve the quality of the power and the reliability of operation due to smart power management. More effective electric motor drives which will help the systems of industrial production as well as transportation systems for example diesel-electric railroad locomotives, electric automobiles, electric mass-transit systems, and nuclear-powered ships.

The uses of SiC High-frequency power devices are in cellular phone base stations, high-frequency power supplies, small lightweight RF , microwave transmitters,and phased array radar systems, where ordinary GaAs-based devices are not able to operate exactly because of high temperatures demands and high power densities [47].

The main applications for SiC, in optoelectronic devices are blue LASER diodes, low-intensity blue light emitted diodes (LEDs) and high-intensity blue LEDs which are substrates for gallium nitride (GaN) [48].

1.2 Thesis Outline

This thesis consists of 6 chapters arranged as following:

• Chapter 1 introduces the context and contains luminescence and thermoluminescence., and the other two sections devoted to description of radiation dosimetry types and retrospective dosimeter and Silicon carbide properties are used in this study.

• Chapter 2 is dedicated to general view of Thermoluminescence Mechanism in detail explanation, and described the output signal of process (glow curve). In the second part of this chapter, explained retrospective dosimeter and SiC benefits and properties, and clarified the well-known model to simplify analysis in Thermoluminescence phenomenon.

• Chapter 3 separated into two sections first, Thermoluminescence Models which described in detail. Second, involved four methods to find out Trap Parameters.

• Chapter 4 includes the material synthesis and doping procedures, Equipment's, Radiation Source with a brief characterize of Irradiation Procedure.

• Chapter 5 presents the results on the study of the experiments stated in Chapter 4 with some determination of trap parameters. These results include the outputs from characterization analysis as well as thermoluminescence measurements.

• Chapter 6 discusses the main findings of this study and recommendations.

CHAPTER 2
LITERATURE SURVEY

2.1 Luminescence

When radiation is incident on an insulator or wide band-gap semiconductor, some of its energy are absorbed and re-emitted as light of a longer wavelength “Stoke's law” this process is called luminescence, or these materials and substances that are capable of emitting light, particularly in the visible range are termed “luminescent”. In nature, most of the materials possess luminescent properties[1].

The wavelength of the emitted light is characteristic of the luminescence substance and not of the incident radiation. Usually, most studies of luminescence phenomena are concerned with the emission of visible light but other wavelength can be emitted, such as (ultra-violet or infra-red) [1]. Sometimes luminescence emission resulting from heat, or by chemical reactions, electrical energy, subatomic motions, and stress on a crystal. The various luminescence phenomena are named according to method of excitation energy. Such as thermoluminecence (by heat), photoluminescence (by U.V. and infrared light) , radioluminescence (by ionizing radiation), cathodoluminescence (by electron beam), etc…

The emission phenomenon of the light takes place after characteristic time (τ_c) which this parameter (τ_c) allows us to subdivide the process of luminescence into two parts phosphorescence and fluorescence. As illustrated in Figure 2.1. The (τ_c) of fluorescence is smaller than (10^{-8}s) but phosphorescence is greater than (10^{-8}s) by this difference we can distinguish between the phosphorescence and fluorescence. Fluorescence emission is basically a spontaneous process because its (τ_c) value is smaller than (10^{-8}s), which after simultaneously absorbing the radiation immediately ceases when the radiation ceases

Phosphorescence emission is the time interval which is starting the radiation absorption till reach to maximum intensity (t_{max}) and the (τ_c) value of the

phosphorescence is greater than (10^{-8}s) and has been seen to continue for some time after removing the excitation. However, it is more complex to distinguish between phosphorescence and fluorescence when the time of delay is too short.

And the phosphorescence itself can be subdivided into two main kinds [10]. One is the short period phosphorescence ($\tau c < 10^{-4}$ s) and another one is the long period phosphorescence ($\tau c > 10^{-4}$s). Another different between the fluorescence and the phosphorescence is the effect of temperature on the decay of luminescence clearly through practical viewpoint. Phosphorescence is heavily dependent on temperature, whereas the fluorescence is not dependent on temperature [1].

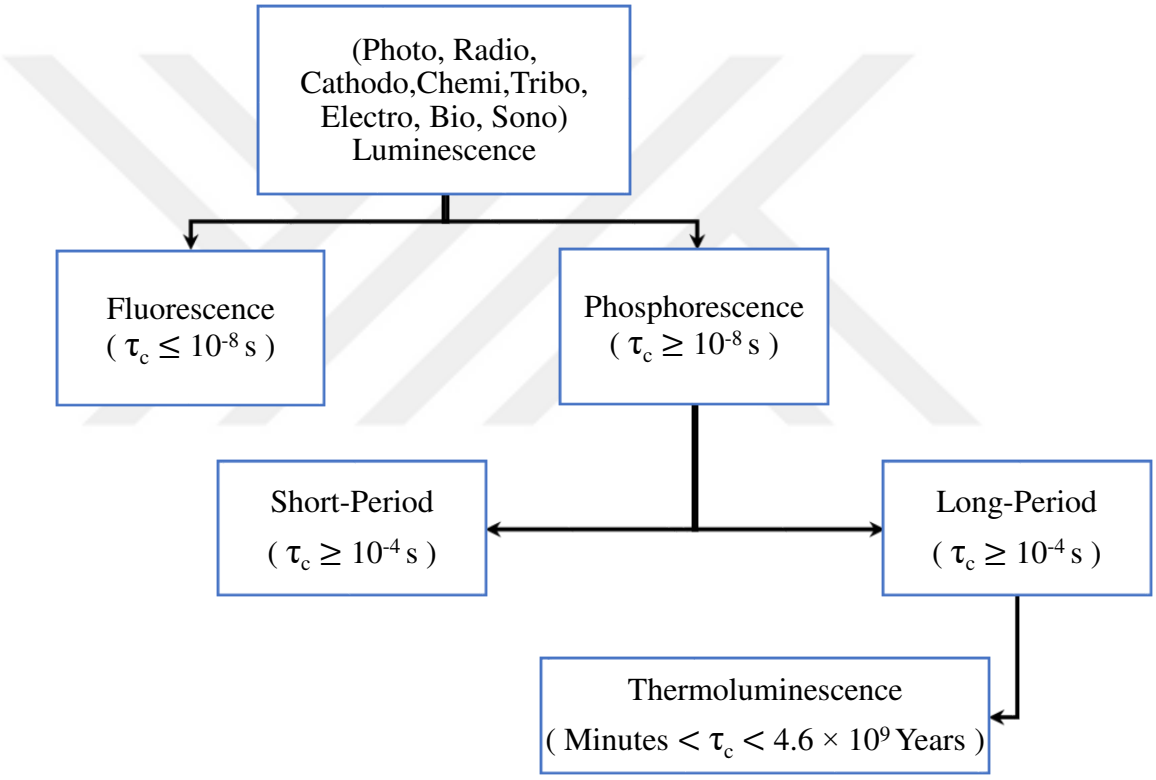

Figure 2.1 The family tree of the phenomenon of luminescence.

Luminescence phenomena are usually described by utilizing energy band theory. So, it can explain the luminescence emission by transferring the energy from radiation to the electrons of the solid material, an electron after acquiring sufficient excitation energy makes a transition from the ground state (g) to the excited state (e) (transition (1) in Figure 2.2a), and when excited electrons come down to its ground state emits luminescence photon (transition (2)). If the average time between excitation and

emission (Lifetime) are less than 10^{-8}sec which is described in Figure 2.2a is called "fluorescence". And this process is independent of temperature, but some luminescence processes cannot be described in Figure 2.2a. Instead, as shown in Figure 2.2b the diagram of the energy level is adapted by the existence of a metastable level (m) which is in forbidden energy band gap between the excited state (e) and the ground state (g). When an electron excited from the ground state (g) to an excited state (e) may be trapped in (m) and stay in it till it is given enough energy (E) to turn to the excited state (e) and is subject to a natural transition back to the ground state (g), with subsequent light emission. Thus, this trapping phenomenon results in a longer delay (seconds to years) between excitation and emission. The average time spent by the charge inside the trap at temperature (T) is given by:

$$\tau = s^{-1}\, exp^{(-\frac{E}{kT})} \tag{2.1}$$

(s) is a constant and (E) is the difference of energy between the trap (m) and excited state (e) (called the trap depth); (k) is Boltzmann's constant. Thus, the process of phosphorescence is dependent on temperature exponentially [1]. This process of luminescence is called "phosphorescence". Energy (E) can be supplied either thermally or optically. The former is called Thermally Stimulated Luminescence (or thermoluminescence, TL) whereas the latter is named Optically Stimulated Luminescence (or OSL).

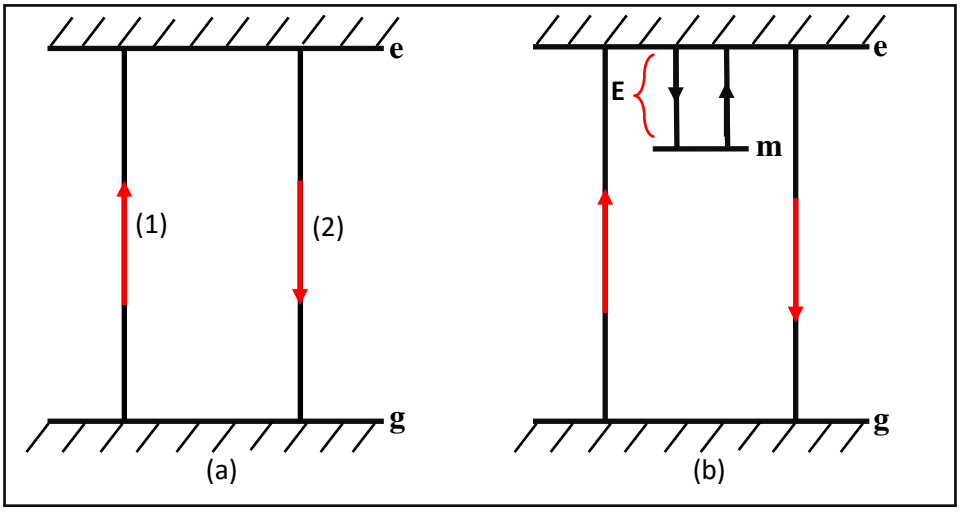

Figure 2.2 The energy level diagram of (a) fluorescence production and (b) phosphorescence production.

The description of wide band gap materials is based on a band model that concerns absorption and storage of ionizing radiation energy and release of the stored energy as the emission of a photon by thermally or optically stimulation. In the band model, absorption of radiation energy means creation of electron-hole pairs. The property of storing energy is due to the presence of crystal defects such as vacancies and impurities. The defects are able to capture the electrons and holes generated in the irradiation process.

A crystal defect is classified as a trap center if the defect is able to capture a charge carrier and re-emit it back to the band it comes from. A crystal defect where carriers of opposite sign can be captured, resulting in an electron-hole recombination, is classified as a recombination center. For the trap center, we assume that only transition between the center and the conduction band and valence band are possible. For recombination centers, we assume that only recombination of conduction electron and a valence hole is possible. Finally, an electron-hole pair is assumed initially to consist of a conduction electron and a valence hole. Exchange of charge carriers between the crystal defects is assumed to take place through the conduction and valence band [11,12].

Figure 2.3 shows the typical transitions used in simulations presented in the dissertation. During the ionizing irradiation of the crystal, electron –hole pairs are generated by excitation of electron from the valence band to the conduction band. The excited electrons are freely moving in the crystal until they are captured by an electron trap center T_1 and T_2, or by a recombination center R. A hole generated in the valence band is captured into either a hole trap center T^h or the recombination center R. Recombinations are assumed to be accompanied by emission of photons, i.e. luminescence. However, nonradiative recombinations are also possible.

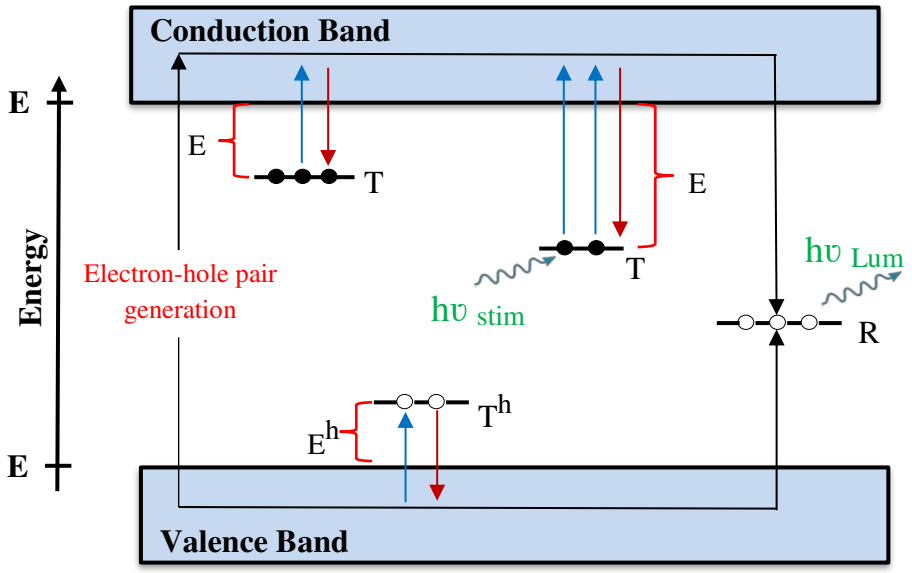

Figure 2.3 Basic concepts of irradiation, thermally and optically process between trap centers and recombination centers in a simple phenomenological band model. The transitions define whether a defect is a trap center T or a recombination center R. A recombination of an electron into an R center is assumed to be followed by photon emission[13].

The captured electrons and holes can be free into the valence or conduction band thermally by heating the crystal, and then make a transition to the recombination center R. This process is named thermoluminescence. Alternatively, external light exposure of the crystal can release captured electrons from a trap center to the conduction band from where they can recombine into the recombination center R. This phenomenon is termed optically stimulated luminescence (OSL).

2.2 Thermoluminescence

The substances like insulators or high band gap semiconductors artificially or accidentally are exposed to radiation, and the radiation causes absorb energy at a given temperature, and emit this energy in the form of visible light while heating the sample. This thermally stimulated phenomenon can be called as luminescence or thermoluminescence. However, the mechanism of thermoluminescence (TL) is not simple as this explanation [8, 14].

Since the early 1950s, thermoluminescence has been used widely to measure nuclear radiation doses [15], following the commercial availability of sufficiently sensitive and

reliable photomultiplier tubes. And in the early 1960s, thermoluminescence was next applied to archaeological dating [16, 17], and in the beginning of 1980s thermoluminescence used to geological dating [18]. Techniques and methods used in thermoluminescence dating are reviewed by Aitken [19].

Thermoluminescence is a process differs from the light emitted spontaneously from a substance when it is heated to glow. Say over 200 ^{o}C (or at high temperatures) a solid substance emits (infrared) radiation of which the intensity of it increases with increasing temperature, this process is called black body radiation. To emit the light in stimulate, it needs to add some energy levels among the forbidden energy gap, these energy levels create caused of lattice defects by insert some impurities into host lattice in thermoluminescence materials which these states are called “metastable state”. The lattice defects are the most important parameters to understand the thermoluminescence phenomenon. They occur naturally or artificially and induce electronic states in the forbidden band [20, 21].

2.3 Thermoluminescence (TL) Mechanism

Thermoluminescence (TL) method is a relatively complex process since it includes a trap and a luminescence center. The fundamental thermoluminescence phenomenon is given in the Figure 2.4 [8]. As can be seen from Figure 2.4, there are two bands within the system. One of them is the conduction band which is an energy band in a solid, electrons are freely mobile in this band and they can produce a net electric current. And the other is valence band which is the farthest energy band that contains electrons when a solid is in the ground state [8]. Due to radiation which is applied to thermoluminescent material, raises electrons from the valence band and trapped in some energy level in the forbidden gap near to the conduction band (electron trap) is happened. Simultaneously, resulting holes may be trapped at other energy levels that are also within the forbidden gap which are named as the “hole trap” or “recombination center” [8, 14], and the light must be emitted when these trapped electrons out of the trap and come down to the lower energy level by heating the sample [2].

In totality, thermoluminescence can be defined by two steps. First stage by absorption of energy from any radiation source the system is change from equilibrium to excited state. And the second stage by release of energy the system come back to the equilibrium, and is called relaxation of the system [14].

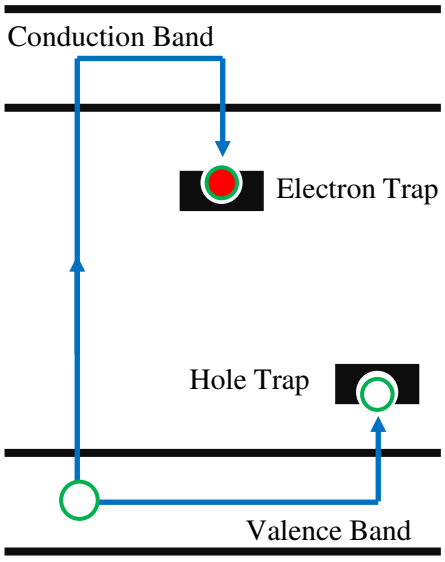

Figure 2.4 Schematic energy level diagram of a phosphor exhibiting thermo-luminescence.

2.3.1 Energy Storage in TL Materials

There are two ways for the steadying of this absorbed energy, when the sample was irradiated. Which are electronic excitation and displacement damage. At the end of both processes, the radiation produced defects are formed according to the structure of material. Radiation produced defects are localized electronic states occupied by non-equilibrium concentration of electrons [9]. All material has localized electronic energy states before, and after irradiation in which some of these states are occupied by electrons in non-equilibrium concentration of electrons. In this case, these occupied energy states are named radiation induced defects. According to McKeever, when researches are reserved into thought, they display that the electronic excitation rather than non-ionizing displacement damage, was caused of the defect construction [14].

Energy storage formed by electronic excitation, whose take place by the electron-hole pair construction and excitation construction. Which formed of mobile holes and electrons inside this material after radiation.

In addition, there happens a mid-gap state produced by imperfections which may be formed by radiation induced defects or pre-existing defects, which this gap is originate between conduction band and valence band. There are two kinds of defects called

electron trap and hole trap in the crystal which are localized at mid gap states. According to thermoluminescence phenomena [2, 14, 22]. In the mid gap, the electron trap is supposed close to the conduction band and the hole trap is close from the valence band.

Figure 2.5 shows the energy storage mechanism. The electrons pass from valence band to conduction band and in the valence band hole develops positively charged area after irradiation process. And electron find its way into an electron trap and hole occupies its associated trap, when electron reaches the conduction band. In this process, Hole traps are called luminescence center [2, 14, 22, 23].

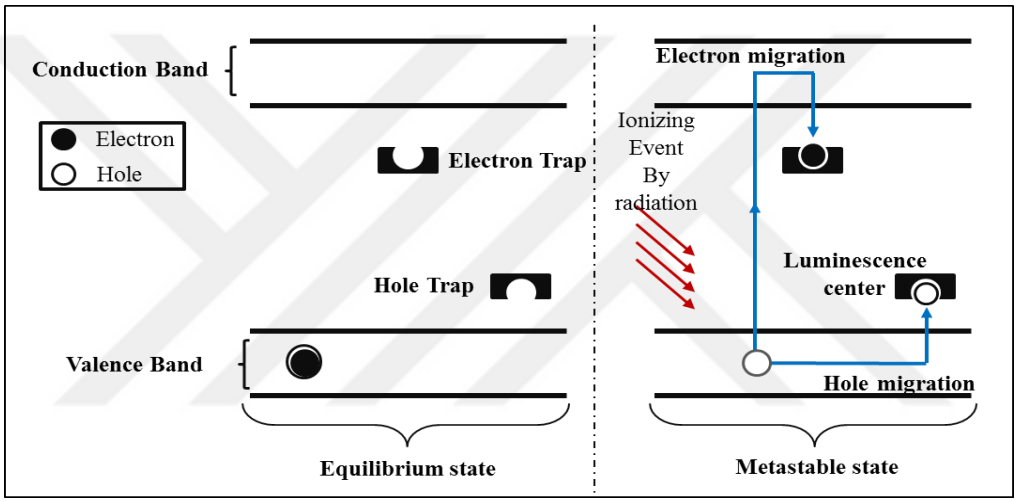

Figure 2.5 Energy-level diagram of the energy storage stage for thermoluminescence processes.

2.3.2 Energy Release in TL Materials

Now both types of carriers trapped in lattice imperfections in the crystalline solids. In electron trap electrons remain for a long time when the crystals are stored at room temperature. After increasing heat, the electron trapped in the electron trap is released to conduction band, and electron is become free to re-trap with the created hole in the hole trap. In this case hole trap is called as re-combination center [2]. This process is showed in the Figure 2.8.

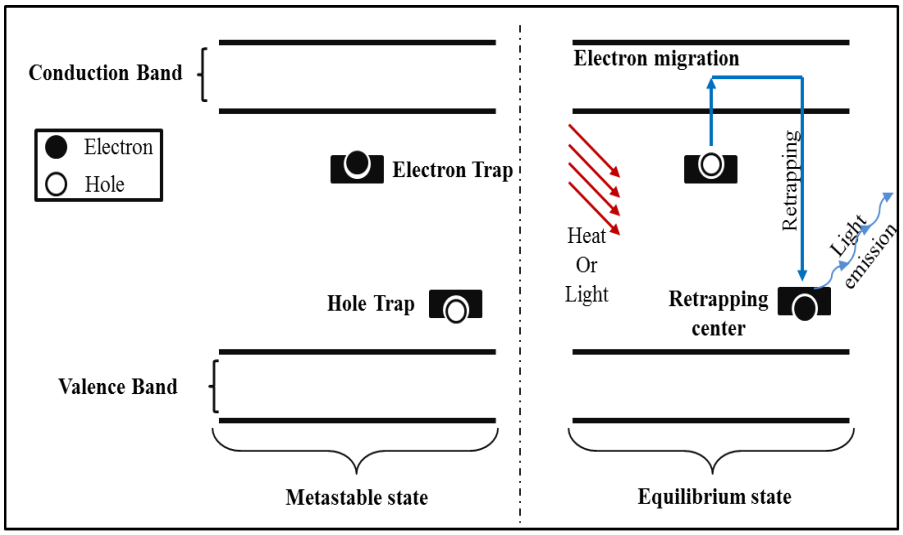

Figure 2.6 Energy-level diagram of the energy release stage for thermoluminescence processes.

2.3.3 Glow Curve

Thermoluminescence signal is expressed as a curve. This curve is called glow curve which can be defined as a graphical illustration of the luminescence intensity as a function of temperature [2]. After light emitting the shape of the glow curves is one or more peaks produce and some of them may overlap.

Generally, materials give one or more peaks on the glow curve. According to same cases the shape of the glow curve is depends on the material mixtures, the type of impurities, radiation induced defect centers, dose and type of ionizing radiation strongly in dosimetric materials [20, 24, 25]. There are numerous parameters that affect the shape of the glow curve, such as dose level of the radiation, thermal treatment (annealing) of the phosphor, pre-irradiation to high doses, pre-treatment with certain chemicals. The unit of peak intensities in glow curve is an arbitrary unit. Hence, they can be used mainly in comparative manner [4, 8, 14]. The magnitudes and appearances of the glow curves depending on the response of the light sensitive device, and the filter there are many filters are use between the detector, sample and heating rate.

In addition, when the sample is irradiated it has only one-shot result. A second thermoluminescence emission cannot be recorded by cooling and reheating it unless it is not irradiated again [2].

A study of these glow peaks yields information about trapping sites and recombination centres in the crystal, for example in thermoluminescence dosimetry (TLD), this curve gives information about the radiation dose to which the phosphor has been exposed.

2.4 Retrospective Dosimetry

An unexpected nuclear accident's possible risk or very strong or sudden terror attack needs different methods and processes possibly is applied in emergency. The assessments should be given fast and with reliability of the dose after the event in order to start arrangements and intervention soon.

The word retrospective generally refers to events already have appended. It is basically derived from a Latin word, "retrospectare", which means 'to look back', [27].

During a nuclear accident, the measurement was unarranged and the data is not available one of the alternative solution is by using retrospective dosimetry as tools of accidental dosimetry for dose estimation. And many objects of the affected area are applicable as natural dosimeters [28]. Because of their involving in measuring dose derived from past many dosimetry techniques are described as retrospective [27] Luminescent materials can be used for retrospective dosimetery by using TL analysis. There are several materials in the environment that have luminescence properties, but it is recommended to not just depend on natural substances in such situation, there should be a special attention to personal belongings carried by victims, who received the dose. Many objects are applicable for being natural dosimeters in our environment because of having suitable thermoluminescent (TL) properties [28]. Luminescent dosimetry is not used only in personal as a reliable method, but it is used in environmental and retrospective dosimetry as well. Thermoluminescence is known as processes of emitting light that is investigated. In spite, the fact that the dealing with nuclear materials have become less danger of not using in a peaceful way indicates a threat to the human race.

Scientific investigations are impacted by environmental disasters as result researchers are forced to develop subservient methods in emergency situation. People who have been in place where an explosion or emission of unpredicted nuclear or radioactive materials will be seriously affected. In order to be sure that the result is less dangerous there should be previous arrangements before the events. As possibilities for

retrospective estimation of received dose, lots of methods are thought, while few of them are suitable and applicable in real emergency. Most of materials and personal objects can be used for retrospective dosimetry purposes according to the prove mentis of the investigations. [29, 30, 31]

2.5 Silicon Carbide (SiC)

The semiconductor materials that permit devices to operate at much higher frequencies, voltages, and temperature than traditional semiconductor materials are known as Wide-band gap semiconductors that allow more influential electrical mechanisms to be construct and cost less as well as releas, further energy efficient. "Wide-band gap" indicates higher voltage electronic band gaps extensively larger than one electron volt. The correct threshold of "wideness" frequently depends on the context, "wide" band gap particulary refers to substans with a band gaps of at minimum 3 ev.

Carborundum (SiC) is one of the wide band gap semiconductor, Carborundum is a only compound of silicon and carbon. Carbon and silicon have only this chemical compound together . The origin of SiC was produced from sand (SiO_2) and carbon after a high temperature electro-chemical reaction. Grains of SiC can be bonded together by sintering to produce very hard ceramic.

The device applications with high temperature, high power, and high frequency device applications, prefer silicon as semiconductors more than any other semiconductor materials, however Silicon Carbide (SiC) has recently paid attention materials in a huge number of industrial and military submissions because of providing great benefits over other semiconductor materials [32]. SiC is the most important semiconductor material for high frequency electronic devices, high power, high temperature, short wavelength optoelectronic, and radiation resistance because of it is physical and electronic properties. [33]. Semiconductor device technology has been progressed in the fields of electronic and optoelectronic applications partly because of profitable accessibility of SiC substrates of increasing diameter and quality. In spite of the improvements made in this area, numerical simulation depends on accurate device models are a need to further improved design and optimization of SiC devices.

Carborundum is not known as an earth inert, while it is only obtained in peace of rocks from outer space, but it is produced from sand (SiO_2) and graphite in an industrial level [34]. It is used as abrasive material since in 1893. The publishing of a tiny article of Round authorized "A Note on Carborundum " was the detection and recognition of a SiC LED happened in 1907. [35]. In 1955 Lely method used for obtaining bulk crystalline SiC. [36, 37].

Here produced SiC powder is become gas at 2500^{o}C in a graphite container below main purity situation. It sublimes then on an absorbent graphite barrier inside the container establishing hexagonal platelets. This method was protracted later as sowed redirection technique by Tsvetkov and Tairov in the late 1970s [38]. The last method, more commonly named physical vapor transport, was supplementary distinguished in [39]. For making large diameter SiC boules, and several variations of these techniques are today used at several workshops worldwide. Bulk single crystals of SiC with 100 mm in diameter are organized today [40].

2.6 Physical and Electrical Properties of SiC

SiC can be defined as indirect semiconductor have a wide band gap and high saturation electron drift velocity and high breakdown voltage. Inertia and high hardness are two physical properties of SiC. While all SiC variations have same thermal and mechanical characteristics, their optical and electrical properties are highly different from polytype to other polytype [41]. The operation of electronic devices that made form at very high temperatures without suffering from the conduction intrinsic affects 10-35 times of magnitude lower than Si because of the wide band gap energy. SiC can resist an electric field 5 to 20 times bigger than Si or GaAs without going through the avalanche breakdown [42]. The construction of high power and high voltage devices come from this high breakdown electric field. And also permit the devices to be located very close together, providing high device stuffing density for integrated circuits. Silicon carbide is a very good thermal conductor. In detail, at room temperature, the thermal conductivity of Si larger than any metal, bigger than Si about 3-13 times [43]. Because of this characteristic SiC devices can work at very high-power levels and still disintegrate the large quantities of excess heat produced. The work of SiC devices is at high frequencies because of the higher saturated electron drift velocity which is 2-2.5 times that of Si [44].

2.7 Applications and Benefits of SiC Device

Because of wide range in the applications and exciting in new developments in SiC technology are being realized. The development of SiC high-temperature devices is in, jet engine ignition systems, aircraft and automotive engine sensors, control systems and in manufacturing technique quantity. In today technology, SiC was used and distributed in smart electromechanical controls which are capable of harsh-ambient operation which based on uses of SiC will enable considerable reduced maintenance, jet-aircraft weight savings, higher fuel competence, reduced pollution, and increased effective dependability [45].

The uses of SiC high-power devices are in power supplies, solid-state lamp stabilizers, and surge suppressors [46]. SiC electronics performance might enable the public power wire to supply improved consumer electricity request without constructing extra generation plants, and improve the quality of the power and the reliability of operation due to smart power management. More effective electric motor drives which will help the systems of industrial production as well as transportation systems for example electric mass-transit systems, nuclear-powered ships, electric automobiles, and diesel-electric railroad locomotives.

The uses of SiC high-frequency power devices are in cellular phone base stations, high-frequency power supplies, phased array radar systems, microwave transmitters and lightweight RF, where ordinary GaAs-based devices are not able to operate exactly because of high temperatures demands and high-power densities [47]. The main SiC uses in optoelectronic applications are in blue laser diodes, and in low and high intensity blue LEDs [48].

2.8 Band gap energy of SiC

The existent energy gap (E_{gx}) for 4H- and 6H-SiC, has been mentioned and measured by using photoluminescence method at $T = 4.2\,K$ the $E_{gx} = 3.265\,eV$ [49] and $E_{gx} = 3.023\,eV$ [50] respectively. The absorption measurements value has α-SiC (most likely 6H-SiC) depended on temperature are $E_{gx} = 2.6\,eV\ to\ 3.03\,eV$ at temperatures from $T = 77K$ to $717K$ [50]. The smallest energy gap is 2.86 eV at 300 K.

The 4H-SiC temperature dependence is concerned to be similar to the 6H-SiC temperature dependence while there is no other experimental data. Recently there are no values about the binding energy Ex of free exaction in any α-SiC polytype that measured reliably. [51]. This value, however, needed so as to obtain the indirect band gap, which is given by

$$E_g = E_{gx} + E_x \tag{2.2}$$

The obtained results by comparing a theory with experimental data shows the values of E_x from $10 - 80\ meV$ [51]. Hence, a mean indirect band gap for 4H- and 6H-SiC might be measured by shifting E_{gx} by $20\ meV$ and $40\ meV$, respectively.

Fig. 2.12 shows the temperature dependence of the band gap energy in α-SiC.

Table 2.1 The measured of temperature dependent on excitation energy gap in α-SiC

SiC Polytypes	$Eg\ [eV]$	$\alpha - Eg\ [eV/K]$	$\beta - Eg\ [K]$	$TL\ [K]$
4H-SiC	3.265	3.3×10^{-2}	1.0×10^{5}	4 - 700
6H-SiC	3.023	3.3×10^{-2}	1.0×10^{5}	4 - 700

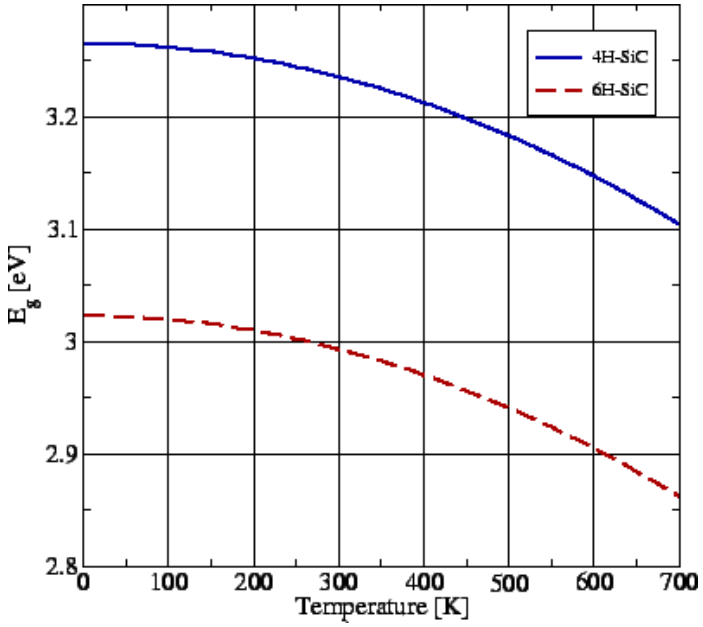

Figure 2.7 Temperature dependence of band gap energy in α-SiC[51].

CHAPTER 3

MODELS IN THERMOLUMINESCENCE

The equation (3.1) was obtained from One-trap One-Recombination Model

$$I(t) = \frac{mA_m ns\ \exp^{\left[-\frac{E}{KT}\right]}}{(N-n)A_n + mA_m} \tag{3.1}$$

Analytically, we can't solve the equation (3.1) without simplifying assumptions, hence in this section we will discuss some assumptions for solving this equation in detail, these assumptions include three part that named first-order kinetics, second-order kinetics, and general-order kinetics.

3.1 1st Order Kinetics (Randall-Wilkins Model)

Randall and Wilkins [3, 52] assumed neglected re-trapping ($(N-n)\,A_r$) during the heating stage i.e. they assumed ($mA_m \gg (N-n)A_n$) and by applying this assumption, equation (3.1) becomes:

$$I(t) = -\frac{d_n}{d_t} = sn\exp^{\left(-\frac{E}{kT}\right)} \tag{3.2}$$

The above differential equation describes movement of carriers inside the lattice as a first-order process, for constant temperature also probability is constant ($p = \exp^{\left(-\frac{E}{kT}\right)}$), and can be determine intensity by integration of equation (3.2).

$$I(t) = I_0\exp^{(-tp)} \tag{3.3}$$

Where: I_0 is the initial intensity at initial time. If temperature change with time, also intensity is varied and the solution of equation (3.2) becomes:

$$I(t) = -\left(\frac{dn}{dt}\right) = n_0 s\exp^{\left\{-\frac{E}{kT_{(t)}}\right\}} \times \exp^{\left\{-s\int_0^t \exp^{\left\{-\frac{E}{kT(t)}\right\}}dt\right\}} \tag{3.4}$$

Where: n_0 is the total number of trapped electrons at time $t = 0$, usually TL is observed as temperature is raised as a linear function of time according to

$$T(t) = T_0 + \beta t \tag{3.5}$$

Where, (β) is the constant heating rate and (T_0) is the temperature at the time ($t = 0$). Then, the intensity I(T) as a function of temperature becomes as;

$$I(T) = -\frac{1}{\beta}\left(\frac{dn}{dt}\right) = n_0 \frac{s}{\beta} \exp^{\left\{-\frac{E}{kT}\right\}} \times \exp^{\left\{-\frac{s}{\beta}\int_{T_0}^{T} \exp^{\left\{-\frac{E}{kT}\right\}} dT\right\}} \tag{3.6}$$

Equation (3.6) is a famous (Randall–Wilkins) expression in first-order single glow peak, but the integral on the right-hand side is not elementary in the case of linear heating. However, Chen showed that how the integral can be approximated by asymptotic series evaluated [53]. In practical applications, it is suitable for describing the glow peak in terms of the parameters which are easy to solve experimentally, Kitis et al [54]. Showed that the Equation (3.5) can be very accurately approximated by:

$$I(T) = I_m \exp^{\left[1+\frac{E}{kT}\frac{T-T_m}{T_m} - \frac{T^2}{T_m^2} \exp^{\left\{\frac{E}{kT}\frac{T-T_m}{T_m}\right\}}\left(1-\frac{2kT}{E}\right) - \frac{2kT_m}{E}\right]} \tag{3.7}$$

The properties of Randall–Wilkins Equation (3.6) showed in Figure 3.1, this figure include some graphical curve which it is come from an example in this article [55]. When luminescence take place at first, by increases temperature, intensity also increases till reach the maximum point after this point intensity decreases (increases intensity means recombination between electrons and holes are growth, and depletion of charge carriers effected to decrease of intensity), hence the shape of intensity looks like a peak shape.

The difference of intensity I (t) can be observed in the Figure 3.1a, and it can be noted that the maximum temperature (T_m) fixed at all of peaks. This is a characteristic of all first-order TL curves, to found maximum temperature it can take ($\frac{dI}{dt} = 0$) (or, somewhat easier($\frac{d \ln I(T)}{dt} = 0$)), from this condition one gets:

$$\left(\frac{\beta E}{kT_m^2}\right) = s \exp^{\left\{-\frac{E}{kT_m}\right\}} \tag{3.8}$$

(n_0) does not appear from equation (3.8) it means that (T_m) is independent of n_0. But in Figure 2.14a, can be seen that each point of the curve is proportional to n_0, also $n_0$is an important parameter in application of dosimetry, and it is easy to find out that the n_0 is equal to the area under the glow peak.

$$\int_0^{\infty} I(t)dt = -\int_0^{\infty} \frac{dn}{dt} dt = -\int_{n_0}^{n_\infty} dn = n_0 - n_\infty \qquad (3.9a)$$

(n_∞) is zero for ($t \to \infty$). The maximum intensity for a first-order kinetics have derived by [56]

$$I_m = n_0 \frac{\beta E}{kT_m^2} \exp^{(-\frac{E}{kT_m} \exp^{\frac{E}{kT_m}})E_2(x)} \qquad (3.9b)$$

Where $E_2(x)$ is the exponential integral of second-order, and from this equation appear that the peak height is not only proportional to n_0, also it is proportional to β.

In Figure 3.1b activation energy (E) changes from (0.8eV) to (1.2eV), when activation energy increases, the peak shifts to higher temperatures with decrease of I_m and increase width, but area does not change (because n_0 is constant). This shift happens because charge carriers needed more energy (temperature) to release to the state if traps are deeper (E is bigger). In Figure 3.1c the same changes can be seen but in the opposite way by change frequency factor (s), when a trapping center has a high value of (s) mean that charge carriers can be free in a lower temperature (so needs few energy) and this is clearly appearing in a first peak. Also in Figure 3.1dshows effect of the heating rate(β) on the shape of glow curves as it is illustrating by change (β)from (0.5 to 2K/s) the peak shifts to higher temperature with decrease the high and increase in width.

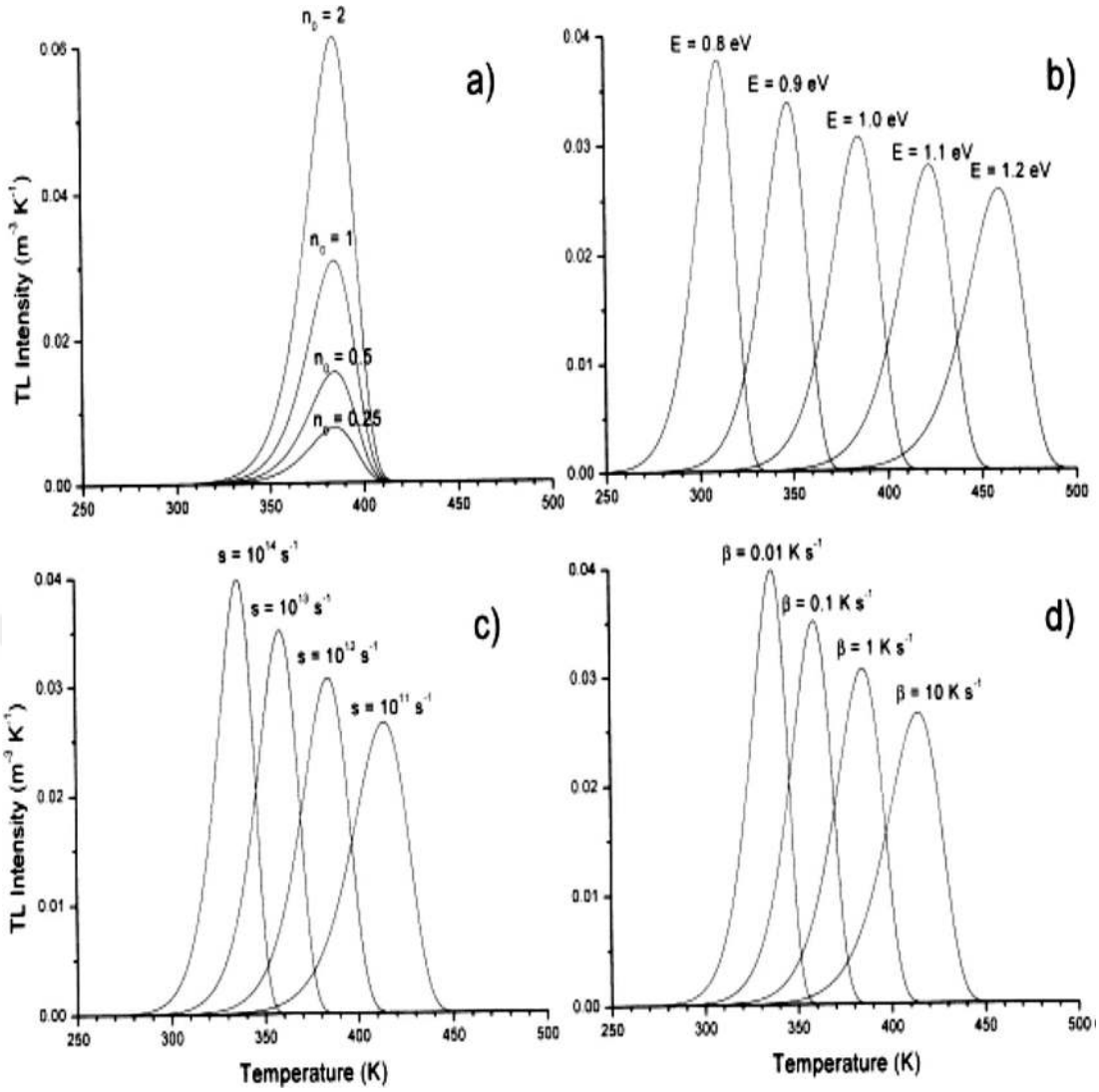

Figure 3.1 Properties of the Randall and Wilkins first-order thermoluminrscence (TL) equation, showing variation with; (a) the trapped charge carriers concentration after irradiation (n_o), (b) activation energy (E), (c) the escape frequency (s), and (d) the heating rate ($\boldsymbol{\beta}$). Parameter values: (n_o=1 m^{-3}) (E=1 eV) (s=1×10^{12} s^{-1}), of which one parameter is varied while the others are kept constant, and ($\boldsymbol{\beta}$ =1 K/s) for (a, b, and c) [55].

3.2 2nd Order Kinetics (Garlick-Gibson Model)

The possibility which re-trapping dominates was considered by Garlick and Gibson [57]. ($mA_m << (N-n)A_n$). Also, they suppose that the trap is far from the saturation, i.e. ($N \ll n$) and($n = m$). By these assumptions, the equation (3.1) becomes.

$$I(t) = -\frac{dn}{dt} = s\frac{A_m}{NA_n} n^2 \exp^{\left\{-\frac{E}{kT}\right\}} \tag{3.10}$$

From the equation (2.23), it is clear that the (dn/dt) is proportional to (n^2) and that means a second-order reaction, and by the additional some assumptions, as the probability of recombination and re-trapping are equal$(A_m = A_n)$, with a constant temperature, and after some mathematical equation the above equation becomes [66].

$$I(T) = \frac{n_0^2}{N}\frac{s}{\beta} \exp^{\left\{-\frac{E}{kT}\right\}} \left[1 + \frac{n_0 s}{N\beta} \int_{T_0}^{T} \exp^{\left\{-\frac{E}{kT'}\right\}} dT'\right]^{-2} \tag{3.11}$$

This equation is the (Garlick–Gibson) thermoluminescence (TL) equation for the second-order kinetics. As it can be seen in Figure 3.2a, the shape of these glow curves is nearly symmetric, but the part in the end of the curve in high temperature is slightly wider than the part in low temperature. This wide curve caused of in second-order reaction considered that concentrations of released electrons are re-trapped before they recombine and make a delay in the emission of luminescence and this emission is spread out over a broader temperature range. The initial concentration (n_0) is a multiplicative constant in the case of first-order but in here furthermore it affected on the shape of curves in different dose levels. And can be seen in Figure 3.2a, $T_m$is changed by varied (n_0), It can be derived that the temperature shift [58].

$$T_1 - T_2 \approx T_1 T_2 \left(\frac{k}{E}\right) \ln f \tag{3.11}$$

(T_1) is the temperature of maximum intensity at a specific dose and (T_2) is the temperature of maximum intensity at (f) times higher dose. From the above equation (3.11) it follows further that for a given increase of the dose the shallower the trap.

Figures (3.2b, c, and d) describes the variation in position and size of a second - order peak as a function of (E), (s/N), and (β) respectively. As in the case of the first-order kinetics, the area under the curve is proportional to the initial concentration (n_0) but the peak height is no longer directly proportional to the peak area, despite deviation is small.

Although similarity between both of first and second-order to find the trap depth is that can be use 'initial rise method' which the term dominating the temperature dependence in the initial rise is ($\exp^{-E/kT}$).

Garlick–Gibson thermoluminescence (TL) equation for second-order kinetics like first-order kinetics can be approximately written in terms of maximum intensity (I_m) and maximum temperature (T_m) [54].

$$I(T) = 4I_m \exp^{\left[\frac{E}{kT}\frac{T-T_m}{T_m}\right]} \times \left[\frac{T^2}{T_m^2}\left(1-\frac{2kT}{E}\right)\times \exp^{\left\{\frac{E}{kT}\frac{T-T_m}{T_m}\right\}} + 1 + \frac{2kT_m}{E}\right]^{-2} \quad (3.12)$$

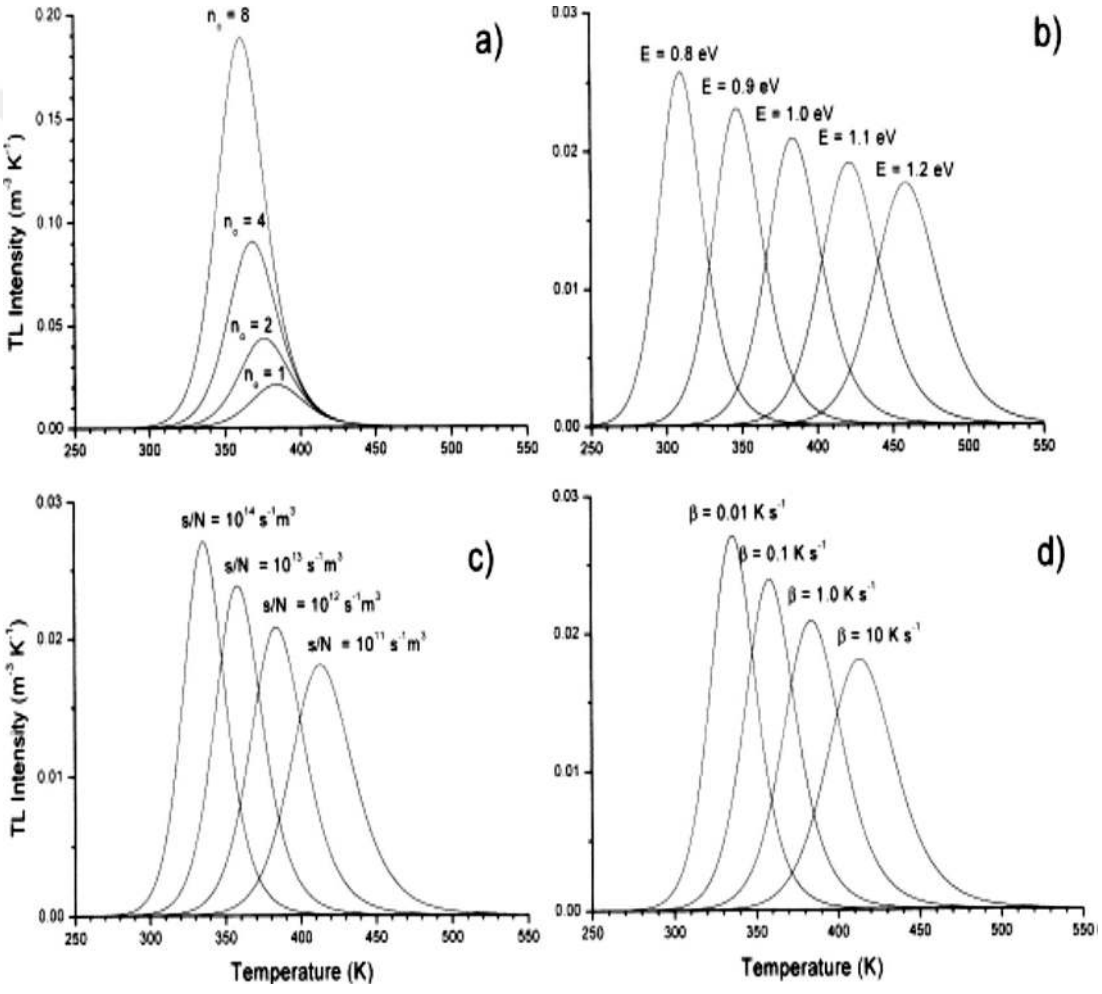

Figure 3.2 Properties of Garlick–Gibson second-order TL equation, showing variation with: (a) the trapped charge carrier concentration (no) after irradiation; (b) activation energy (E), (c) (s/N), and (d), the heating rate (**β**). Parameter values: (no=1 m-3) (E=1eV) (s/N=1×1012 s-1 m3), of which one parameter is varied while the others are kept constant, and (**β** =1 K/s) for (a, b, and c) [55].

3.3 General-Order Kinetics (May-Partridge Model)

In sections (3.1, and 3.2) the first and the second-order reaction of the (TL) equation have been derived by using some simplifying assumptions. However, in reality thermoluminescence peak will fit neither the first-order nor the second-order kinetics, because experimentally do not hold these simplifying assumptions. May and Partridge [59]. Used an empirical expression in the case of (general-order kinetics), and this is

$$I(t) = -\frac{dn}{dt} = n^b \acute{s}\ \exp^{-\frac{E}{kT}} \tag{3.13}$$

Where the dimension of (s') is ($m^{3\,(b-1)}\ s^{-1}$) and (b) is defined as the parameter of the general-order and is not necessary (1) or (2). Integration of equation (3.13) for ($b \neq 1$) yields:

$$I(T) = \frac{s''}{\beta}\ n_0\ \exp^{\{-\frac{E}{kT}\}} \left[1 + (b-1)\frac{s''}{\beta} \times \int_{T_0}^{T} \exp^{\{-\frac{E}{kT}\}} d\acute{T}\right]^{\frac{-b}{b-1}} \tag{3.14}$$

Where ($s'' = s'\ n_0^{(b-1)}$) in unit (s^{-1}), equation (3.14) includes the case of second-order, if ($b = 2$) and changes to the first-order equation when ($b = 1$), according equation (3.13) (s') has a dimension and changed with respect to the order (b). So, in this case can be dealt as the first-order when ($b \rightarrow 1$) and go to the second-order when ($b \rightarrow 2$), look at Figure 3.3.

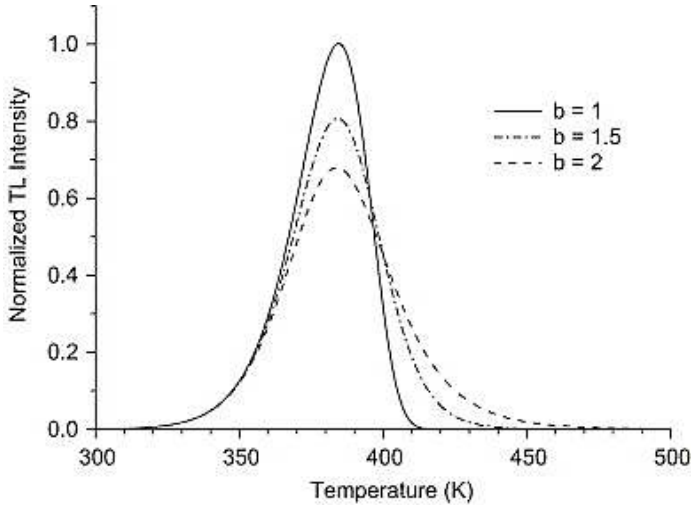

Figure 3.3 Comparison of first-order (b=1), second-order (b=2), and intermediate-order (b=1.5).

The temperature shift represented as:

$$T_1 - T_2 \approx T_1 T_2 \left(\frac{k(b-1)}{E}\right) \ln f \qquad (3.15)$$

(T_1) is the temperature of maximum intensity at a specific dose and (T_2) is the temperature of maximum intensity at (f) times higher dose. And for the general-order equation can be written in terms of (I_m) and (T_m), that has been derived [60].

3.4 Trap Parameters Determination Methods

It is important for knowing parameters of thermoluminescence, generally it have four parameters, the first two parameters which are the main physical parameters (activation energy E and frequency factor s) and named as the trapping parameters, and are fixed by the properties of the trapping center. The last two parameters can be determined experimentally by select a certain dose (n_0) and as well as through the reading of the signal at a certain heating rate (β). Determination of trapping parameters was an importance topic in half a century. In this chapter, it will be briefly discussed some methods to find out trap parameters. There are different ways to assess the trapping parameters from the glow curves [3, 61, 62]. When one glow peak is highly isolated from the other glow peaks, the experimental methods like (Initial Rise Method (IR), Variable Heating Rates Method (VHR), Three Points Method (TPM), Isothermally Decay Method (ID), and Peak Shape Method (PSM)) are appropriate ways for determining these parameters. In the case of overlapping peaks there are basically two methods to get these parameters. First, is the Partial Thermal Cleaning Method and the second, is the Computer Glow Curve Deconvolution Method (CGCD) program. In most cases, it cannot be used the partial thermal cleaning way for isolating the interest peak completely without making any perturbation on it. Therefore, (CGCD) program become so popular way to assess the trapping parameters from thermoluminescence glow curves in recent years [63]. Because of this reason we used this technic to find the kinetic parameters.

Computer glow curve deconvolution (CGCD) method is one of the most important ways to derive values of parameters E, s, and b these methods of computerized curve fitting it is more accurate in values wit*h apparent success in use. The procedure is beginning, by find out the approximate positions of the most prominent peaks in the

glow-curve and estimate each value of E, s, and b by using one of the analytical method and a theoretical curve is computed by using the general-order equation for b ≠ 1, or the first-order equation for b=1.

The computed curve is compared with the actual experimental curve and estimated a root mean square (RMS) deviation between them. The next action is changing E, s, and b values until a minimum value of the RMS deviation is obtained. This method can be used in largely overlapping peak's glow curve without acting to heat treatment therefore it is useful and better than experimental methods. It utilized two different models in a computer program. First, the glow curve is approached to the first-order thermoluminescence (TL) kinetic by using below expression,

$$I(T) = n_0 s\, exp^{\left(-\frac{E}{kT}\right)}\, exp^{\left[\left(-\frac{s\,kT^2}{\beta\ E} exp^{\left(-\frac{E}{kT}\right)}\right)*(0.9920-1.620\frac{kT}{E_a})\right]} \tag{3.16}$$

Second, the glow curve is approached with general order thermoluminescence (TL) kinetics by using below expression,

$$I(T) = n_0 s\, exp^{\left(-\frac{E}{kT}\right)}\ \left[1+\left(-\frac{(b-1)s}{\beta}\frac{kT^2}{E} exp^{\left(-\frac{E}{kT}\right)}\right)*(0.9920 - 1.620\frac{kT}{E_a})\right]^{\frac{b}{b-1}} \tag{3.17}$$

Where all of $(n_0, s, E, k, T, \beta, and\ b)$are annotated previously. Summation of overall peaks and contribution of background can lead to composite glow curve formula as described below:

$$I(T) = \sum_{i=1}^{n} I_i(T) + a + b\ exp^{(T)} \tag{3.18}$$

Where $I(T)$ is the fitted total glow curve, (a) allows for the electronic noise contribution of the planchet and dosimeters infrared to the background. Starting from the equation (3.18), the procedure of the least square minimization and also the figure of Merit (FOM) was used for judging the fitting results on whether they are good or not. Like,

$$FOM = \sum_{i=1}^{n} \frac{|N_i(T) - I(T)|}{A} = \sum_{i=1}^{n} \frac{|\Delta N_i|}{A} \tag{3.19}$$

Where $(N_i(T))$ is i-th experimental points (total n=200 data points), $(I(T))$ is i-th fitted points, and (A) is the integrated area of the fitted glow curve. from many experiences [8]. It can be said that if the (FOM) values are between (0.0%) and (2.5%) the fit is good, and for (2.5 %) and (3.5%) the fit is fair, and if greater than (3.5%) the fit is bad. To have a graphic representation of the agreement between the experimental and fitted glow curves, the computer program also plots the function,

$$X(T) = \frac{N_i(T) - I_i(T)}{\sqrt{I_i(T)}} \tag{3.20}$$

Which is a normal variable with an expected value (0) and $(\sigma = 1)$ where $(\sigma^2(T) = I_i$

CHAPTER 4

EXPERIMENTAL EQUIPMENTS AND PROCEDURES

The equipments, materials and experimental procedures utilized in this study are described below in details.

4.1 XRD Result

The XRD result has been taken from METU (ODTU) in department of chemistry from Ankara-Turkey, and the properties of XRD instrument is given in table 4.1.

Table4.1: Properties of XRD instrument.

Sample	SiC
Goniometer	Miniflex goniometer
Attachment	Standard sample holder
ScanningMode	2theta/theta
ScanningType	Continuos Scanning
X-Ray	30kV/15mA
Divergence slit	Variable
Scattering slit	4,2deg
Receiving slit	0,3mm

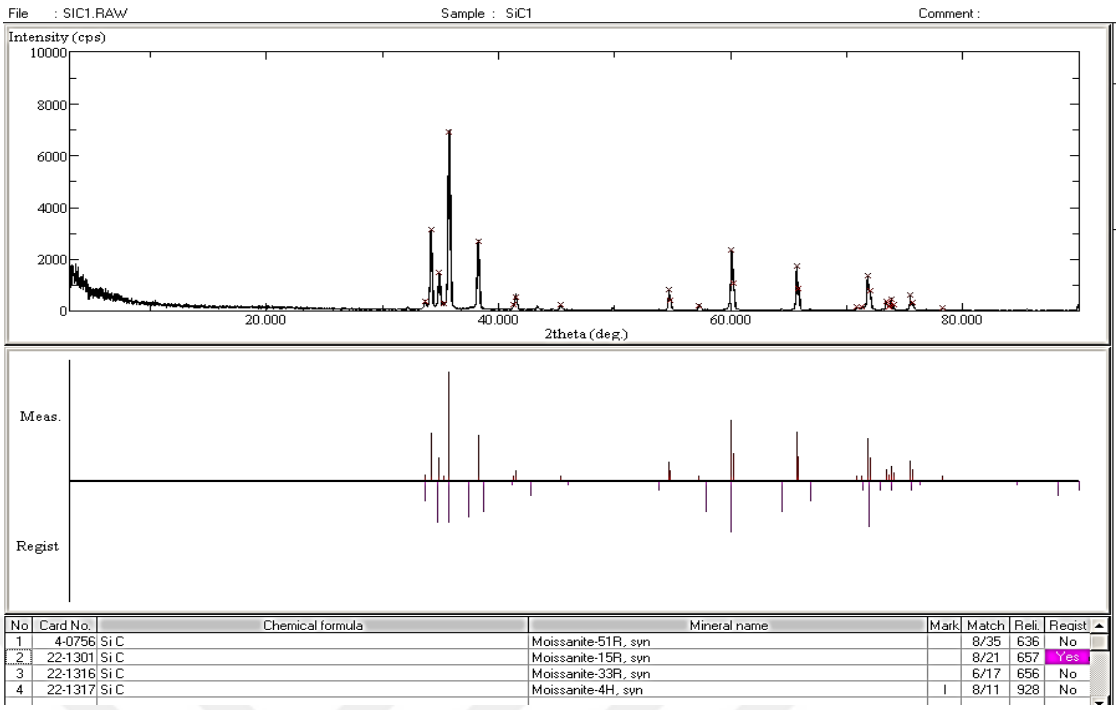

No.	Card No.	Chemical formula	Mineral name	Mark	Match	Reli.	Regist
1	4-0756	Si C	Moissanite-51R, syn		8/35	636	No
2	22-1301	Si C	Moissanite-15R, syn		8/21	657	Yes
3	22-1316	Si C	Moissanite-33R, syn		6/17	656	No
4	22-1317	Si C	Moissanite-4H, syn	I	8/11	928	No

Figure 4.1 XRD pattern of Silicon Carbide.

4.2 Equipments in Laboratory

The thermoluminescence laboratory has two main rooms:

1. Sample preparation room
2. Iirradiation and reading room

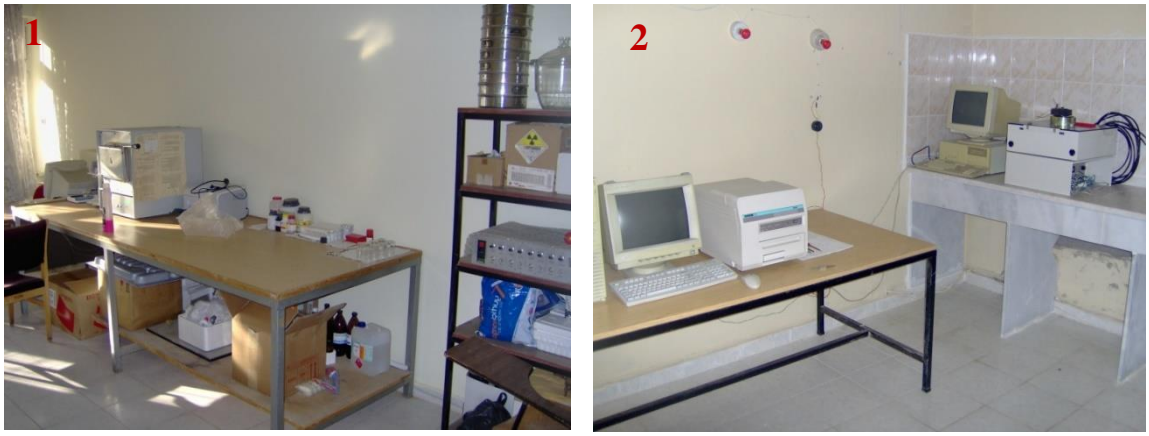

Figure 4.2 TL laboratory

4.2.1 Radiation source and irradiator

The ^{90}Sr - ^{90}Y β radiation source is a part of irradiation equipment located in our TL and OSL laboratory. The irradiation equipment is an additional part of the 9010-optical dating system which is interfaced to a PC using a serial RS-232 port to control the irradiation duration. The samples were irradiated at room temperature and our β radiation source irradiated materials with $0.04\mathrm{Gy}/s$.

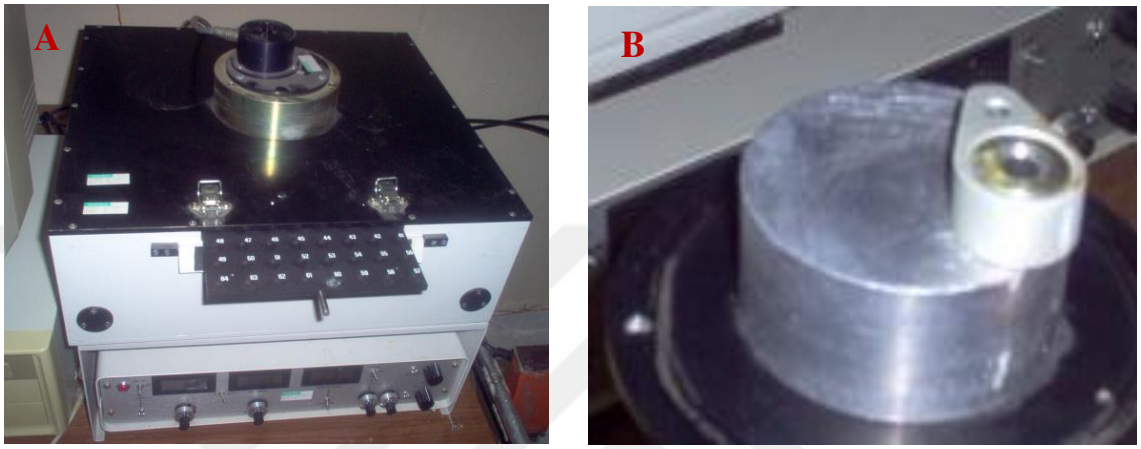

Figure 4.3 (**a**) 9010 Optical Dating System (irradiator), (**b**) ^{90}Sr-^{90}Y β (beta)-source.

Figure 4.4 ^{90}Sr - ^{90}Y β radiation source and computer.

4.2.2 Equipments used before irradiation process

Figure 4.5 Some of the used equipments: oven, chemicals, sieves and digital balance.

4.2.3 Harshaw 3500 TL Reader and Peak Analyzer

The Harshaw 3500 includes a sample drawer for a single element TLD dosimeter, a linear, programmable heating system and a cooled photomultiplier tube with associated electronics to measure the thermoluminescence light output [64]. It is the device where the irradiated materials are heated and the intensity of the light output measured. Using the software program Win-Rems, we can set the starting and ending temperatures of the heating process, and the temperature increments. Search Response Database (RSP) is used to view the results. Temperature settings are made with the Time Temperature Profile (TTP). The glow curves were obtained by using a Harshaw QS 3500 Manual type thermoluminescence reader interfaced to a PC, where the thermoluminescence signals were analyzed. The basic block diagram of reader is shown in Figure 3.5.

Figure 4.6 Harshaw 3500 TL Reader.

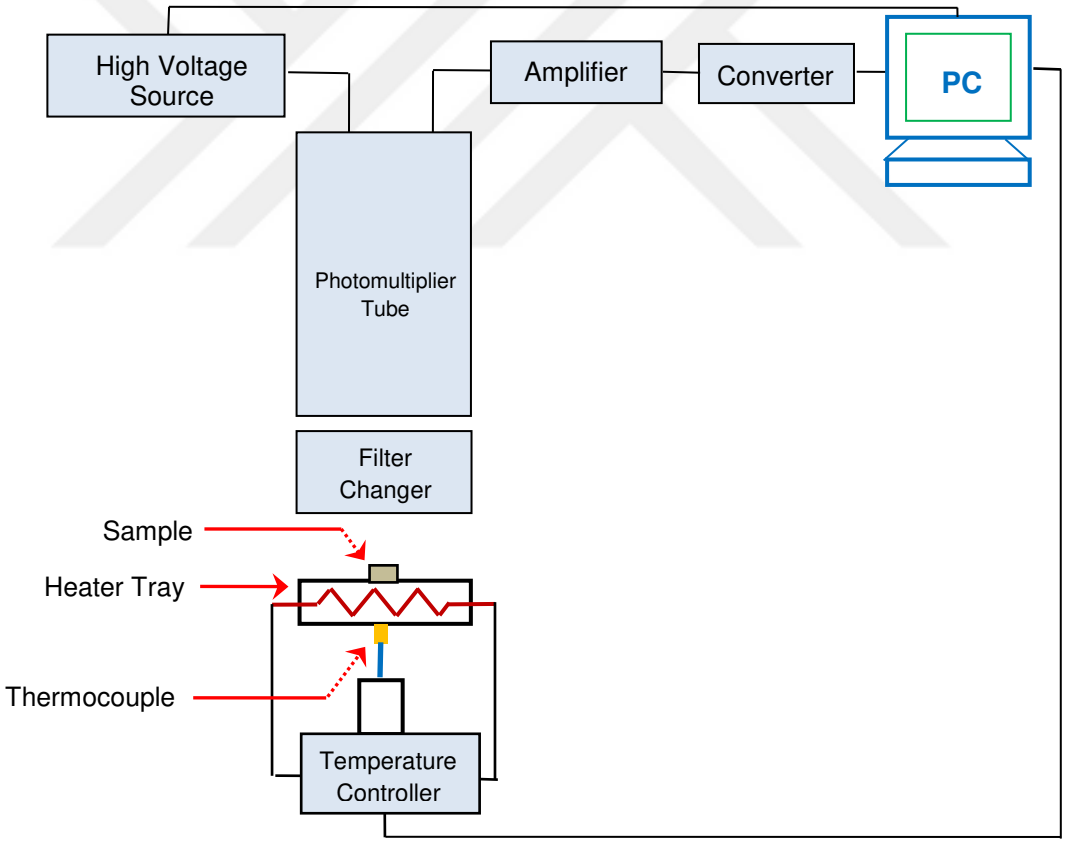

Figure 4.7 Basic block diagram of TL reader [65].

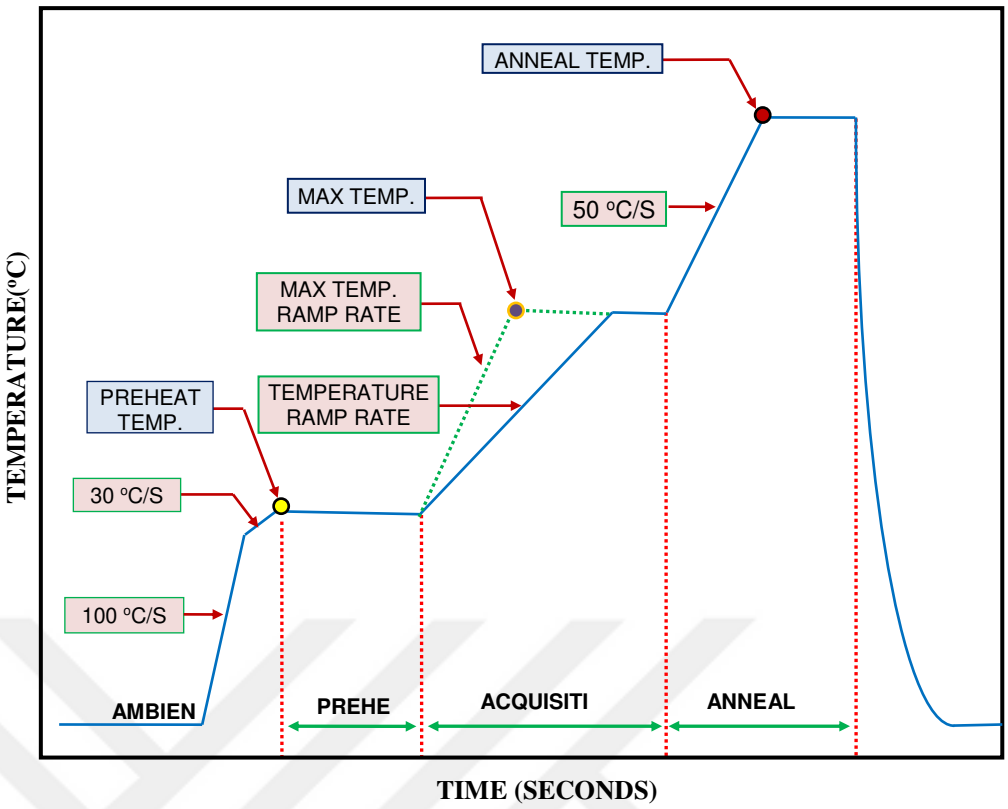

Figure 4.8 Typical time temperature profile (TTP) [65].

4.2.4 Fading Box

The samples are placed in a box in a completely dark environment to protect from light contamination. This box is called a fading box. The samples were faded at room temperature in fading boxes with dark ambient.

Figure 4.9 Fading box and fading cupboard

4.3 Material

The Silicon Carbide samples used in this study were in the form of powder that purchased from Fetas Metallurgy Company from Turkey. It is black Silicon Carbide. The chemical structure is given in table 4.2.

Table 4.2 Chemical Structure of the Silicon Carbide due to Fetas Company.

SiC	O_3, Free C	Si-SiO_2	AI_2, O_3
>98%	<0,3%	<0,4% <0,1%	<0,5%

Figure 4.10 Silicon Carbide sample are used in this study.

4.4 Procedure

4.4.1 Determination of Particle Size

First, the samples (SiC) need to be separated from each other according to particles size, and sieves instrument is used for this process. The purpose of the selecting dimensions process is to separate the particles size of SiC, and which one has the best TL intensity. At the end of this process, the particle sizes or grain size which obtained for SiC are separated for 50-75µm, 75-100µm, 100-125µm, 125-200µm, 200-250µm, 250-400µm, and 400-1000µm dimensions.

4.4.2 Natural Dose

The purpose of this experiment is the evaluation of the traps (resetting process) which are located in the forbidden gap of the SiC. In this experiment, the samples cannot be subjected to any radiation. The samples are heated up from 30℃ to 400℃ in 1℃ / s increments in Harshaw 3500 TLD Reader. This heating process evacuates the traps and leaves them empty of all residual thermoluminescence radiation.

4.4.3 Dose Response

The purpose of the Dose Response process is to get a relation between TL intensity and applied dose. First the sample is irradiated by the ^{90}Sr-^{90}Y β radiation source about 2.4 Gy for the radiation process. After the radiation process, sample is put into the Harshaw 3500 TLD reader for reading. The TLD reader heats the sample from 30℃ to 400℃ with heating rate of $1\,℃/s$ $(\beta = 1\,℃/s)$ and analyzes the thermoluminescence light output from the sample and the glow curve of the sample. Then the sample's traps need to be emptied for another irradiation process and to take background emission to subtract from the total emission. Therefore, we use the TLD reader again and it heats the sample from 30℃ to 400℃ in 1℃/s increments for the resetting process. Each process is repeated for (12, 36, 72, 144, 288, 576, 1152, 2304, and 4608) Gy minutes radiation dose.

4.4.4 Heating Rate Effect

This is similar to the Dose Response case. The differences are constant radiation dose and different heating rates (β). First the sample is irradiated by the radiation source about 36 Gy for radiation process. After the radiation process, the sample is put into the TLD reader for reading. The TLD reader heats the sample from 30℃ to 400℃ with heating rate of $1\,℃/s$ $(\beta = 1\,℃/s)$ and analyzes the thermoluminescence light output from the sample. Then the sample's traps are emptied, using the TLD reader resetting procedure outlined previously, then irradiate it again using a constant 36 Gy. After each radiation process has been completed, the heating rate (β) was increased to $1℃/s$, $2\,℃/s$, $3\,℃/s$, $4\,℃/s$, $5\,℃/s$, and $6\,℃/s$ for reading.

4.4.5 Cycle Measurements

In this case, the radiation dose and heating rate (β) are held constant. $36\ Gy$ was used for the radiation process and $\beta = 1\ ℃/s$ for reading. First the sample is put into the radiation source, and after the radiation process has been completed, it is put into the TLD reader for reading. The TLD reader heats the sample from 30℃ to 400℃ with heating rate of $1\ ℃/s$ and analyzes the thermoluminescence light output from the sample. Then the sample's traps are emptied, the process is repeated nine times, and the results are checked for consistency.

4.5.6 Fading Effect

First the sample is irradiated by the radiation source about $36\ Gy$. After the radiation process, the samples are placed in a box in a completely dark environment to protect from light contamination and held for different time intervals. First, the sample is kept for 15 minutes in the dark. After that waiting process, our sample is put into TLD reader for reading from 30℃ to 400℃ with heating rate of $1\ ℃/s$. Then the process is repeated for five samples keeping in the dark for 30, 240, 480, 1440, and 2880 minute.

CHAPTER 5

EXPERIMENTAL RESULTS AND DISCUSSIONS

In this chapter, we examined the experimental results under five cases which are:

- Determination of Particle Size
- Dose Response
- Heating Rate Effect
- Cycle of Measurements
- Fading Effect

5.1 Determination of Particle Size

5.1.1. Variation of Glow Curve

In this study, the particle size (grain size) of SiC particles has been investigated. Firstly, the purpose of the selecting dimensions process is to measure the particles size of SiC, and which one gives the best TL peak intensity. Figure 5.1 shows the effect of different particle sizes on TL glow curves of the sample. The particle size values vary between 50 μm to 1000 μm, each sample at different particle size has same TL glow curve shape but with different intensities.

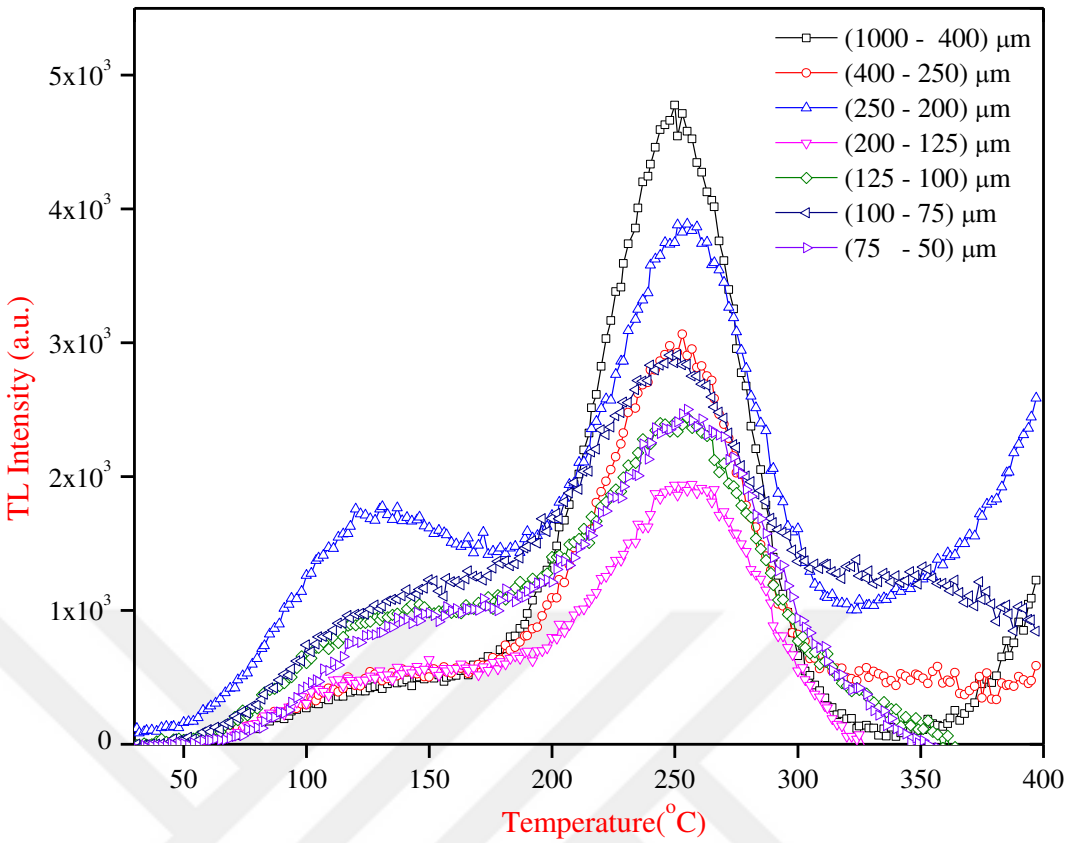

Figure 5.1 Glow curves of SiC measured at different grain sizes with β=1°C/s after beta irradiation of 36Gy.

5.1.2 Variation of Thermoluminescence Peak Intensity

In this study, the effects of the different grain size on the thermoluminescence peak intensity were investigated.

Figure 5.2 shows the variations of the thermoluminescence peak intensity as a function of grain size for the SiC sample. In the figure 5.1 two separated peaks are seen, the peaks are located around ≈ 130°C and ≈ 250°C. As shown in figure 5.2, the TL peak intensity of intermediate temperature peak is bigger than lower temperature peak, and no significant change is observed in the TL peak intensity of the low temperature peak except 200-250 µm. For the intermediate temperature (≈ 250°C) the TL peak intensity increases with fluctuations. As a result, the largest TL peak intensity is observed at 400-1000 µm. Therefore, it is good to use the particles size between 400-1000 µm in all experiments.

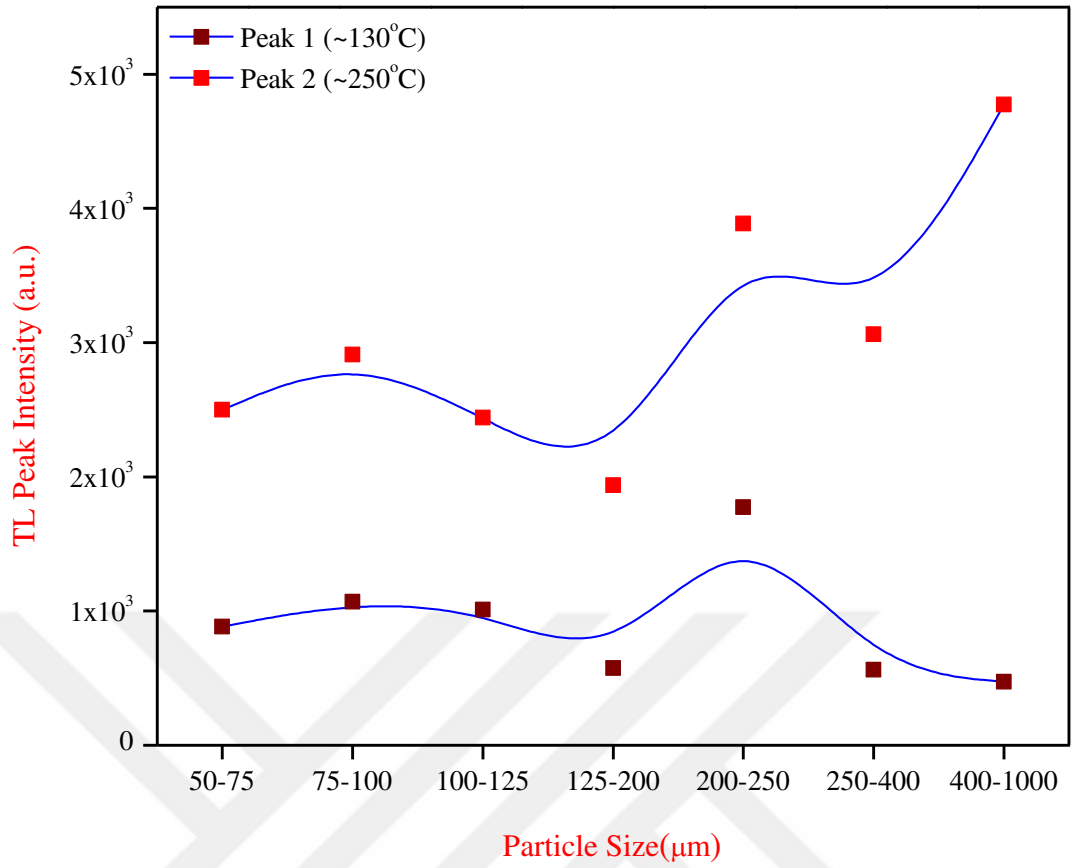

Figure 5.2 Variation of the thermoluminescence peak intensities for different particle sizes for SiC with β=1°C/s after beta irradiation of 36Gy.

5.1.3 Variation of Area under the Glow Curve

The sample whose particle size is about (200-250) μm has the biggest area in both low and intermediate peaks, but we don't need the low peak temperature in the dosimetric work because of higher fading. We used the particle size (400-1000) μm in all experiments because it has sharp intermediate TL peak, and it's good for TL dosimetry.

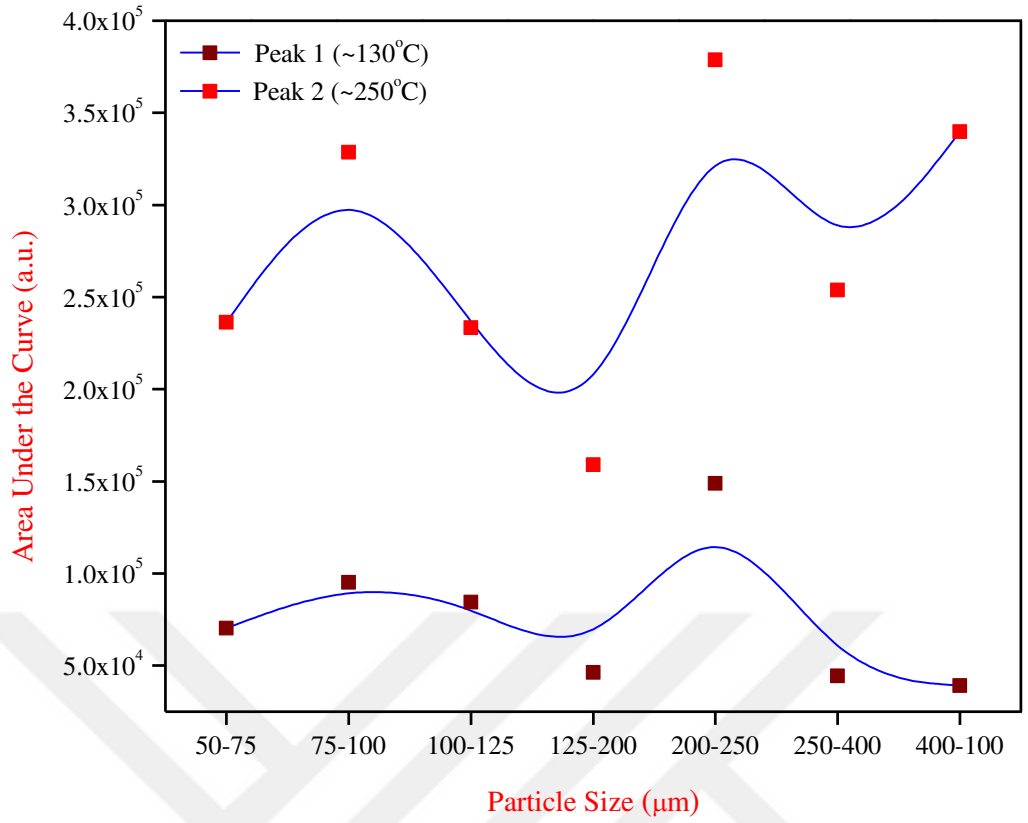

Figure 5.3 Variation of the area under the curve for different particle sizes for SiC with β=1°C/s after beta irradiation of 36Gy.

5.2 Dose Response

The glow curves of samples were examined by using different doses in this part of the experiments.

5.2.1 Variation of Glow Curve

In this study, the dose response behavior of SiC has been investigated. 100 mg of the sample was irradiated at room temperature by β-ray source between ≈ 12Gy and ≈ 4.6kGy to check the dose dependency influence on the glow curves shape. And figures 5.4 and 5.5 shows some of the selected glow curves after different dose levels. The experimental observations have clearly shown that the peak temperature of intermediate TL peak shifts to lower temperature region with increasing dose level, and the shape of glow curves do not change by using different doses. No extra peaks are produced.

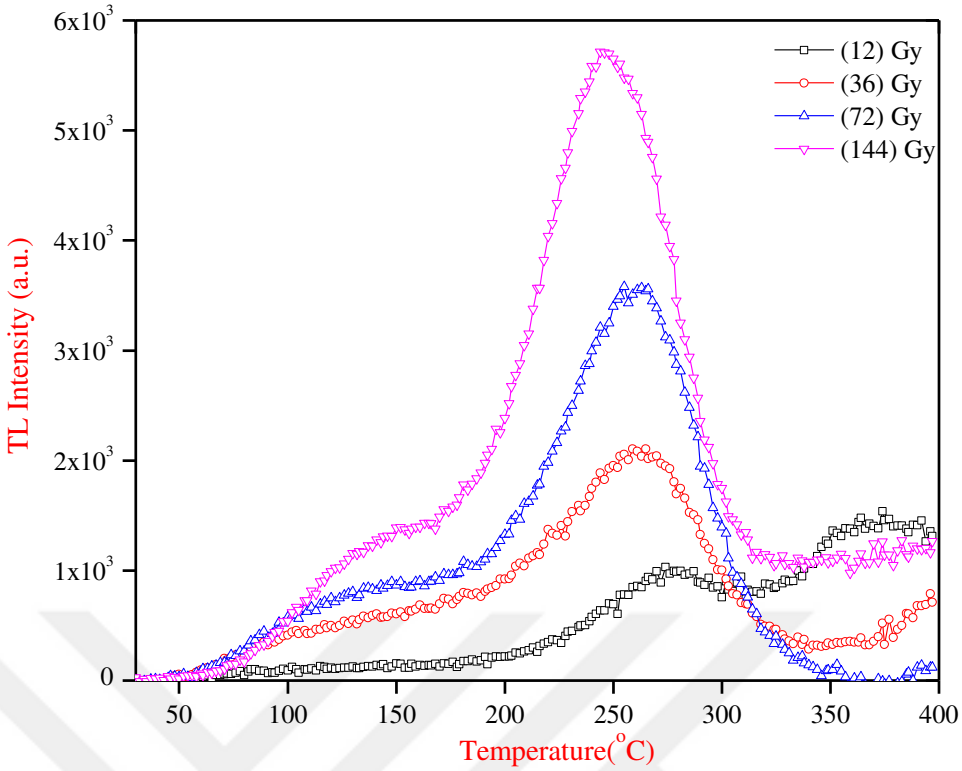

Figure 5.4 Glow curve variations for SiC sample measured after exposed to different dose levels (12, 36, 72, and 144) Gy with heating rate (1°C/s).

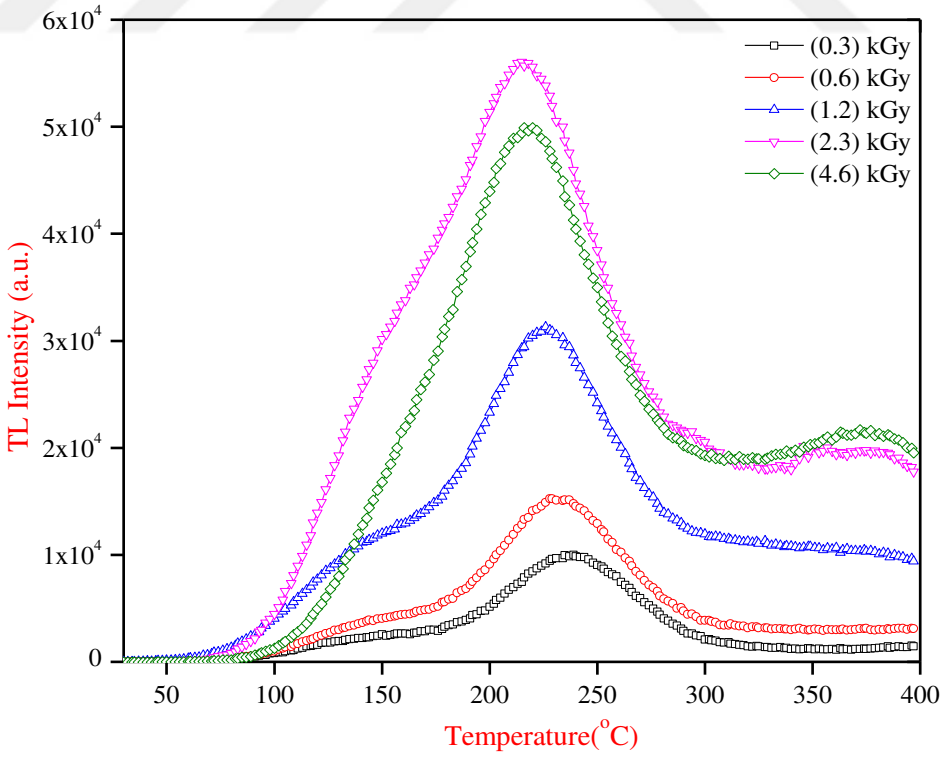

Figure 5.5 Glow curve variations for SiC sample measured after exposed to different dose levels (0.3, 0.6, 1.2, 2.3, and 4.6) kGy with heating rate (1°C/s).

5.2.2 Variation of Peak Temperature

In this part of the experiment, the effects of the different doses on the peak temperatures of thermoluminescence peaks were examined.

Figure 5.6 shows the variation of peak temperature as a function of doses for the SiC sample, if the dose increases, the peak temperature decreases because the structure of traps may change with increasing dose. This change occurs in the forbidden band gap. In the other word, with increasing dose levels the intermediate glow peak temperature gradually shifted to the low temperature sides. This peak temperature shifting is about 54°C was starts from ≈ 275°C to 221°C for different dose levels.

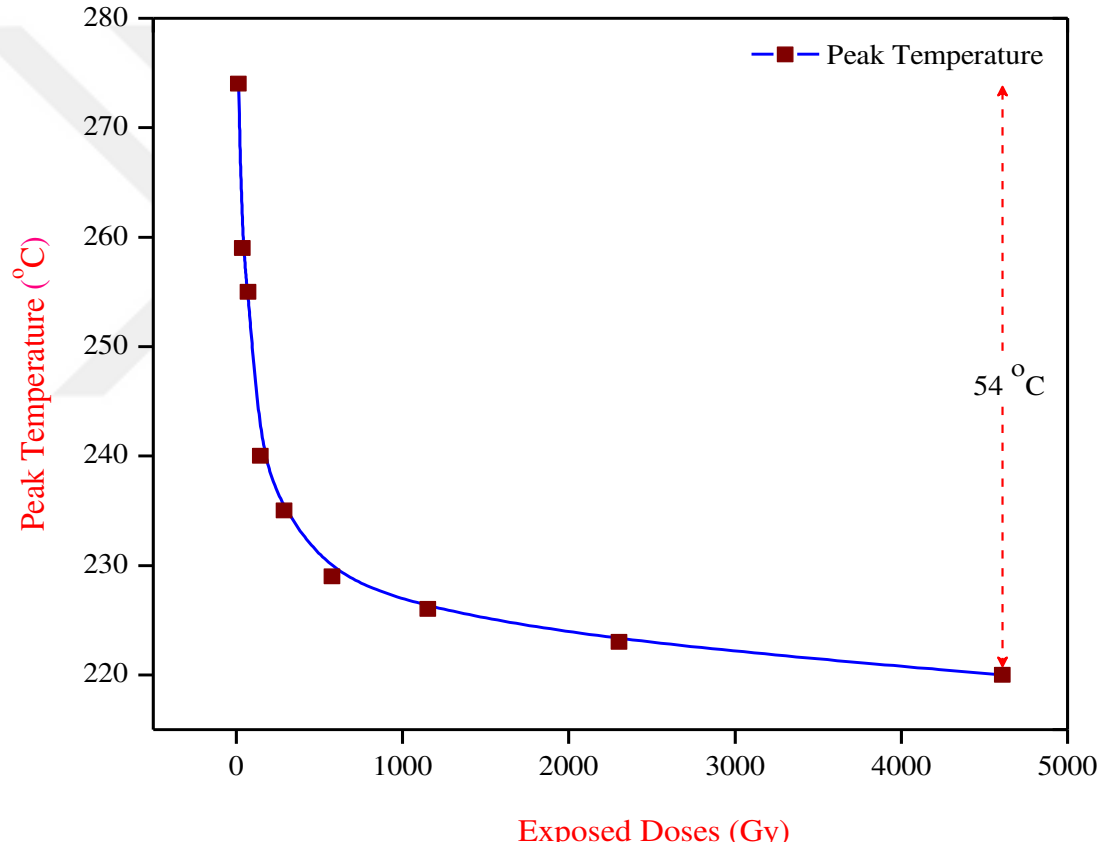

Figure 5.6 Variations of the peak temperature for different doses for SiC with β=1°C/s.

5.2.3 Variation of Thermoluminescence Peak Intensity

In this part of the experiment, the effects of the different doses on the thermoluminescence peak intensity were investigated.

Figure 5.7 shows the variations of the thermoluminescence peak intensity as a function of doses for the SiC sample. If the dose increases, the thermoluminescence peak intensity increases. In the low dose region to the high dose region. From 12 Gy, to 2.3 kGy, the TL peak intensity linearly increases and reaches to saturation region between 2.3 kGy to 4.6 kGy . Therefore, SiC sample has a big linear region.

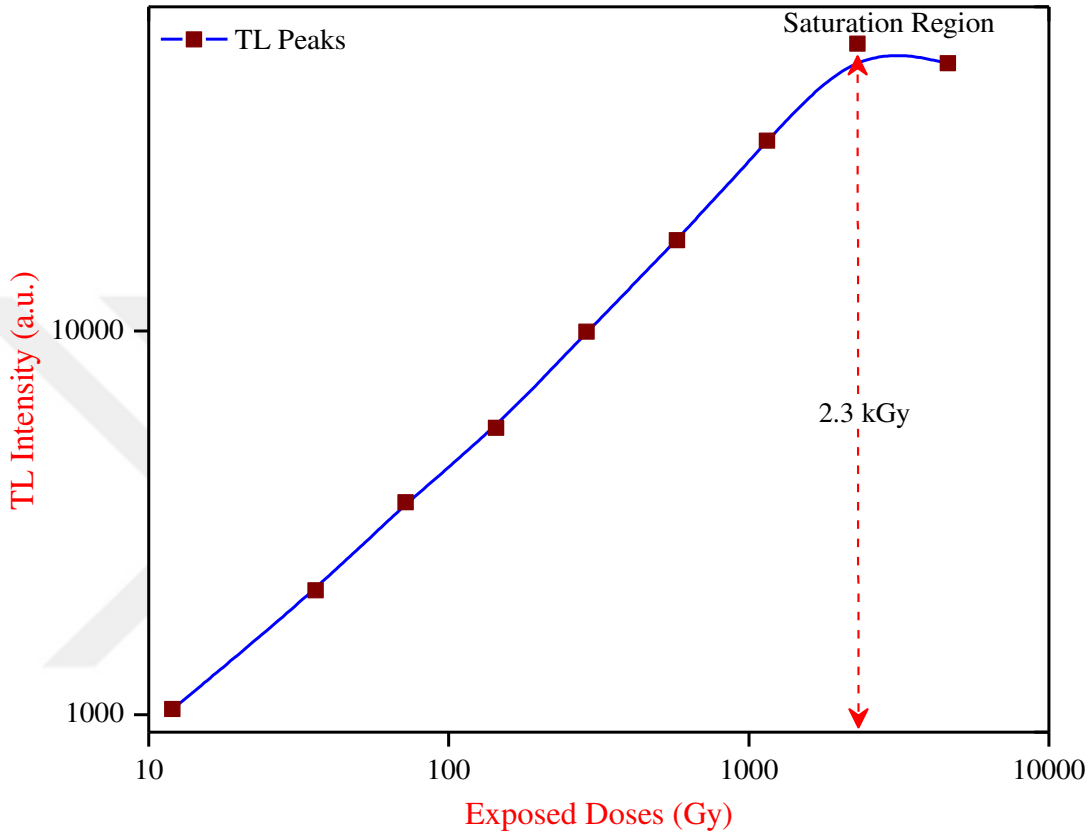

Figure 5.7 Variations of the maximum thermoluminescence peak intensity for different doses for SiC with β=1°C/s.

5.2.4 Variation of Area under the Curve

In this part of the experiment, the effects of the different doses on the area under the curve were examined.

Figure 5.8 shows the variation of area under the curve as a function of doses for the SiC sample. In the low dose region, from 12 Gy to 72 Gy, peak area increases with increasing dose and acts as a super-linear. From 72 Gy to 0.6 kGy peak area increases linearly with increasing dose. For high dose region, from 0.6 kGy, to 2.3 kGy the graph line becomes sub-linear. And between 2.3 kGy and 4.6 kGy the graph reaches to saturation region.

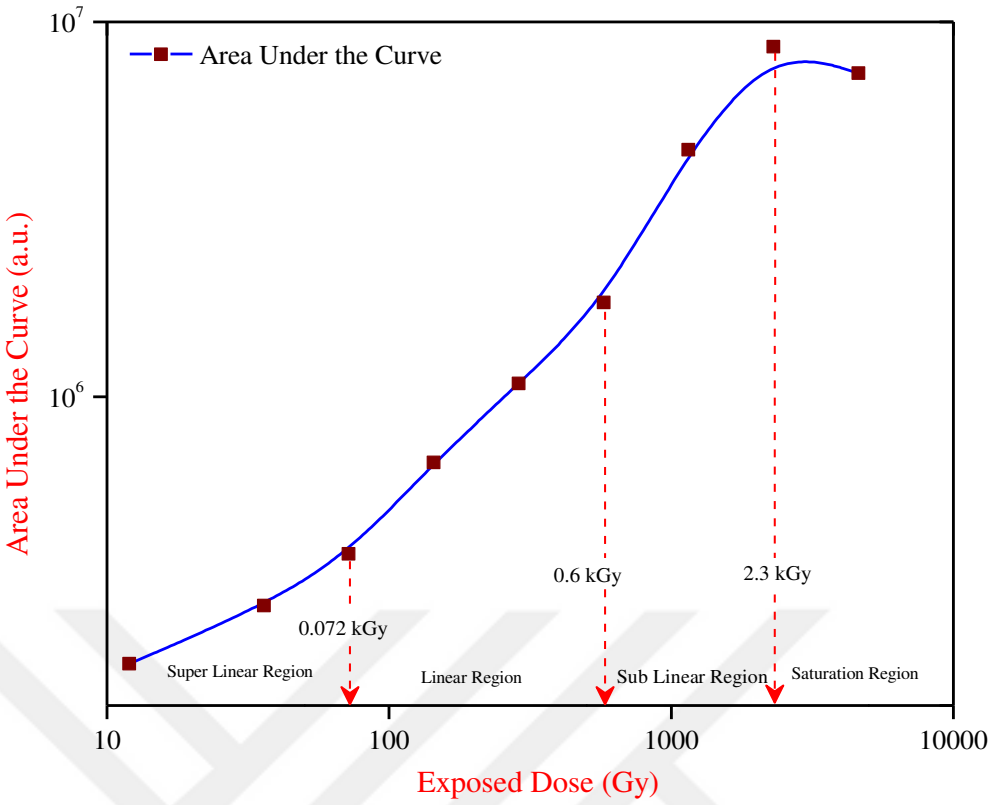

Figure 5.8 Variations of the area under the curve for different doses for SiC with β=1°C/s.

5.3 Heating Rate Effect

The glow curves of samples were examined by using different heating rates during read out in this part of the experiment. In studying the dosimetric parameters heating rate is one of the essential necessities for readout thermoluminescence dosimeters (TLD). And also controlled heating rate is more important. Therefore, heating rate becomes an important factor in reading the dosimetric properties [66]. The first examination for showing the effect of heating rate on the TL response readout by Pradhan and Kitis et al [67, 68]. They ascribed that by increasing heating rate to thermal quenching of luminescence in TLD the TL response is decrease.

5.3.1 Variation of Glow Curve

Another process in this experiment is aimed to understand the effect of linear heating rate on the glow curve features of SiC. In this section, the glow curve behavior of SiC has been investigated at different linear heating rates from 1°C/s to 6°C/s. Samples were irradiated with β-ray about 36Gy, glow curves were recorded for different heating rates of 1, 2, 3, 4, 5, and 6 °C/s, and it is shown in Figure 5.9. From the figure, it can

be understood the different linear heating rates shift the thermoluminescence glow peak to higher temperature region with increasing heating rate, and the width of peak increases with increasing heating rate, as described in theory. And also, with increasing heating rate TL peak intensity decreases. It has been recommended that it is because the effect of thermal quenching which reduces the effectiveness of the luminescence when increases temperature because of the increased non-radiative transition probability [69].

Figure 5.9 shows variation of glow curve as a function of heating rate for the SiC sample, the shape of glow curves does not change by different heating rate. No extra peaks are produced by different heating.

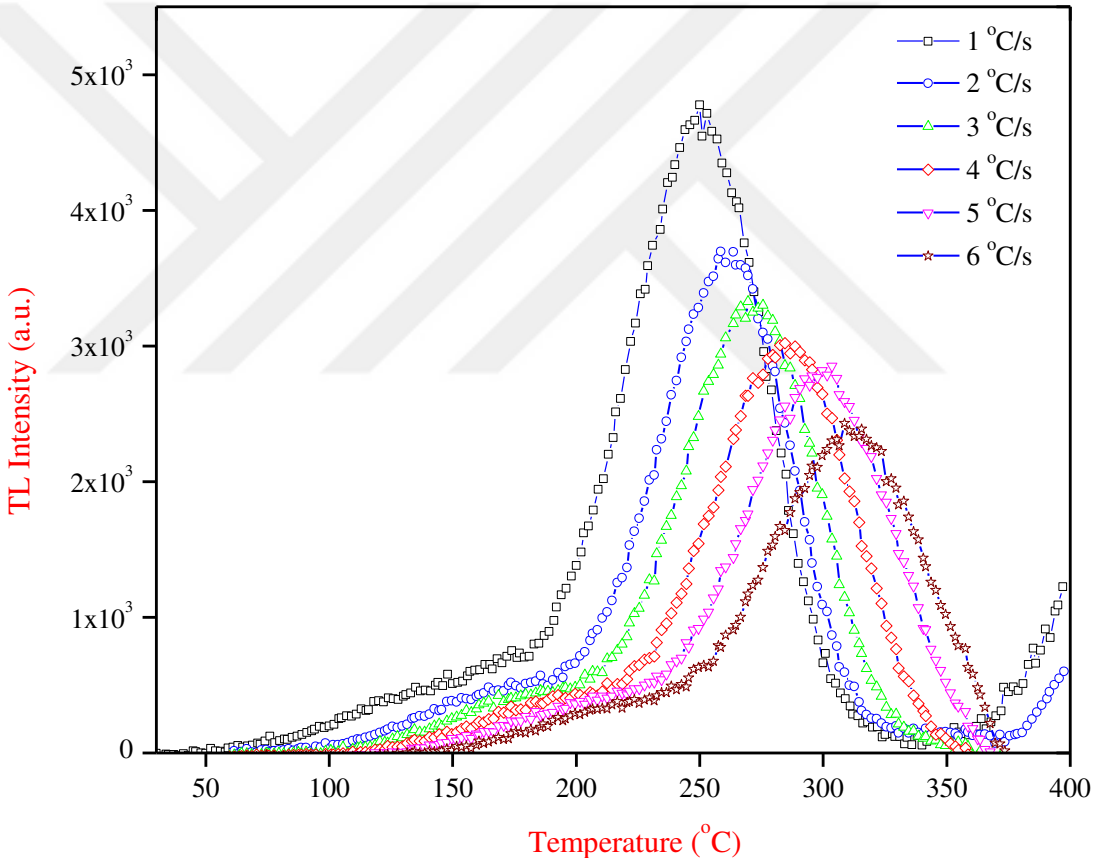

Figure 5.9 Glow curve variations for SiC measured at different heating rates (1, 2, 3, 4, 5 and 6 °C/s) after β irradiation of 36Gy.

5.3.2 Variation of Peak Temperature

In this part of the experiment, the effects of the different heating rates during read out on peak temperature were examined with heating rate (β) of 1 ℃/s . Figure 5.10 shows the variation of the peak temperature as a function of heating rates for the SiC sample, if heating rate increases, peak temperature increases until heating rate of 6 ℃/s. and it is clearly show that the peak temperature change linearly with heating rate. The peak temperature generally increases linearly. Therefore, SiC sample has acceptable results for this study because of linear behavior.

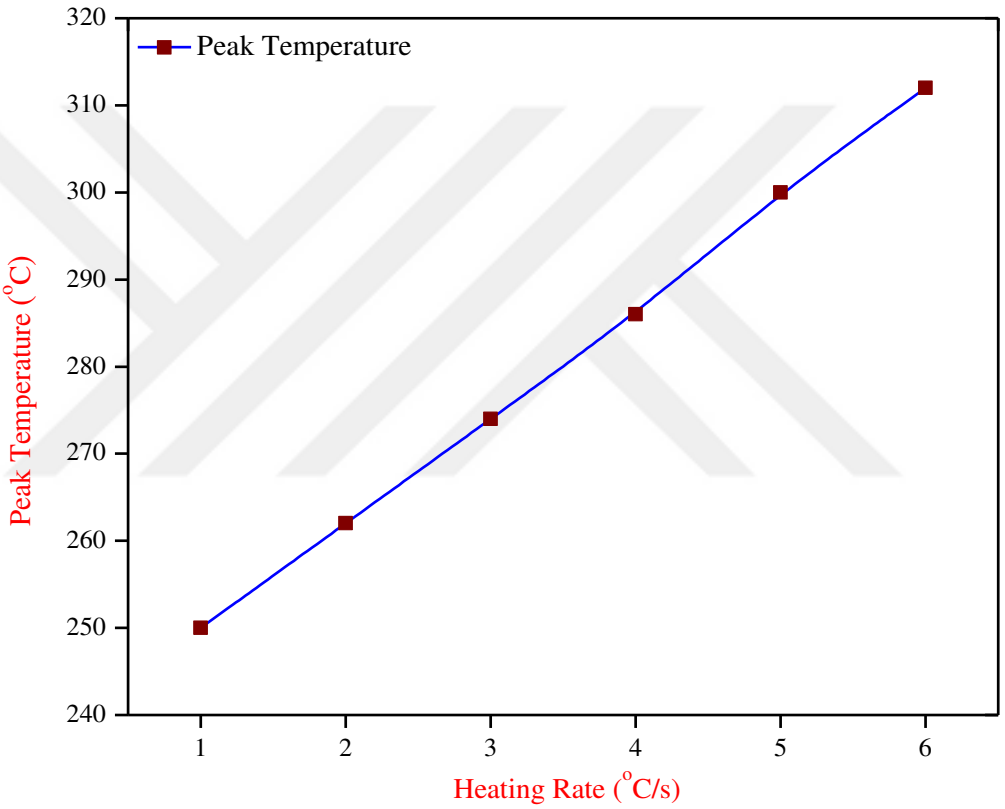

Figure 5.10 Variations of peak temperature for different heating rates for SiC after β irradiation of 36Gy.

5.3.3 Variation of Thermoluminescence Peak Intensity

In this part of the experiment, the effects of the different heating rates on the thermoluminescence peak intensity were examined.

Figure 5.11 shows variation of thermoluminescence peak intensity as a function of heating rate for the SiC sample, if the heating rate increases, the thermoluminescence

peak intensity decreases. The graph generally shows that the TL peak intensity decreases exponentially with increasing heating rate. The results are same as in literature.

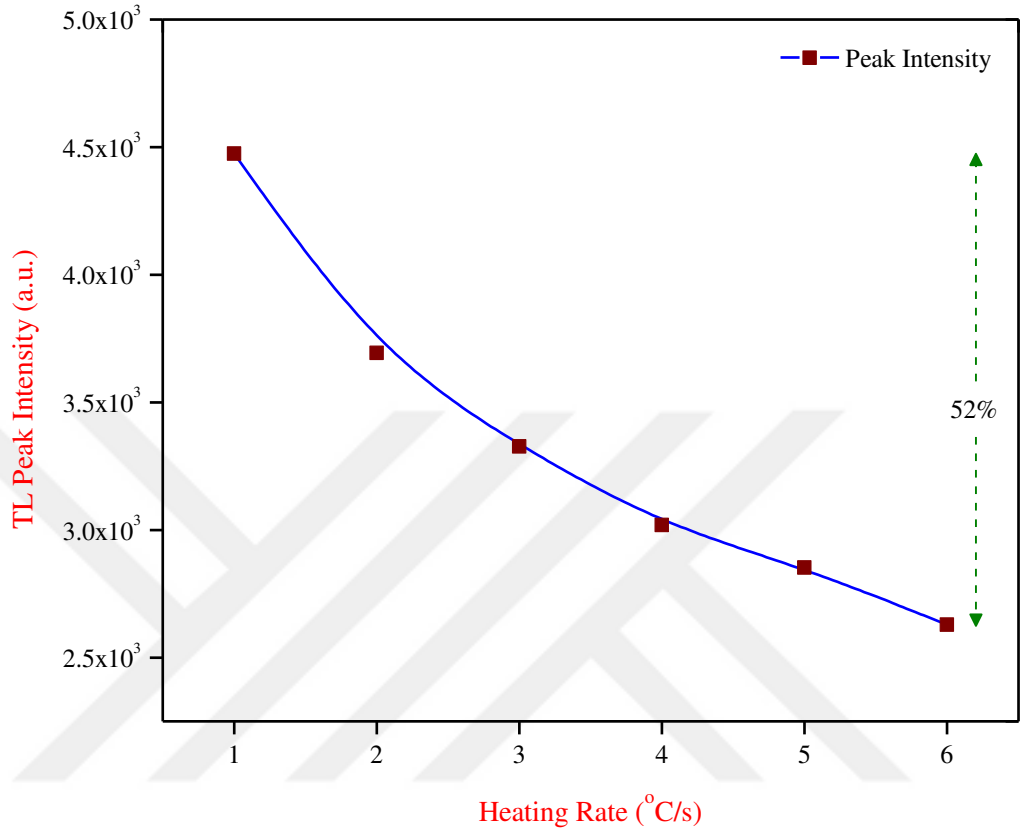

Figure 5.11 Variations of the thermoluminescence peak intensity for different heating rates for SiC after β irradiation of 36Gy.

5.3.4 Variation of Area under the Curve

In this part of the experiment, the effects of the different heating rates on the area under the curve were examined.

Figure 5.12 shows variation of area under the curve as a function of heating rate for the SiC sample, if the heating rate increases, the area decreases with increasing heating rates. It is not linear but it continually decreases. The graph generally shows that the area under the curve decreases exponentially with increasing heating rate.

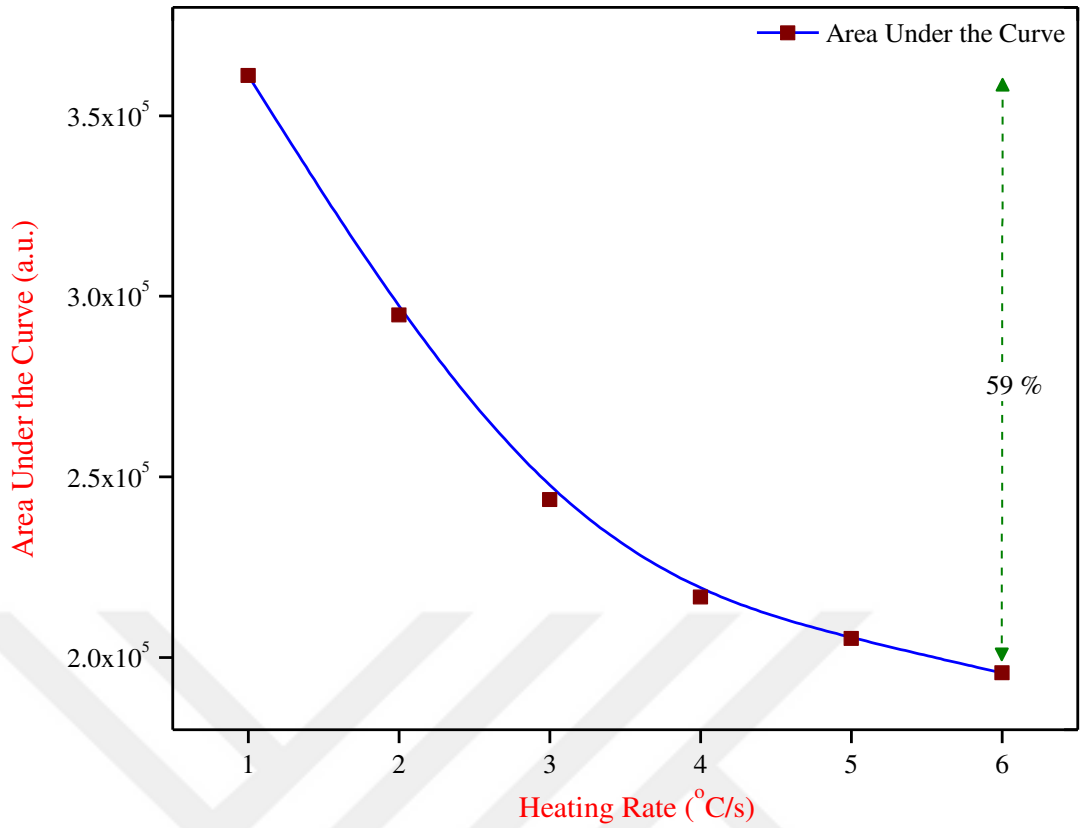

Figure 4.12 Variations of Area under curve for different heating rates for SiC after β irradiation of 36Gy.

5.4 Cycle of Measurements

The reproducibility (cycle of measurements) of samples were investigated with repeated experiments in this part. For a dosimeter, a reproducibility is a more important parameter. The same result is required for a good dosimeter. And by using this following equation the standard deviations for all experimental data were calculated for each cycle of measurement:

$$\sigma = \sqrt{\frac{\sum_i (x_i - M)^2}{n-1}} \quad \ldots\ldots\ldots\ldots\ldots\ldots \quad 5.1$$

Where:

X: Individual measurement.

M: Mean of measurements.

n: Number of measurements.

5.4.1 Variation of Glow Curve

Figure 5.13 shows variation of the glow curve of SiC versus temperature for nine repeats. As a result, the shape of glow curve does not change for nine experiments.

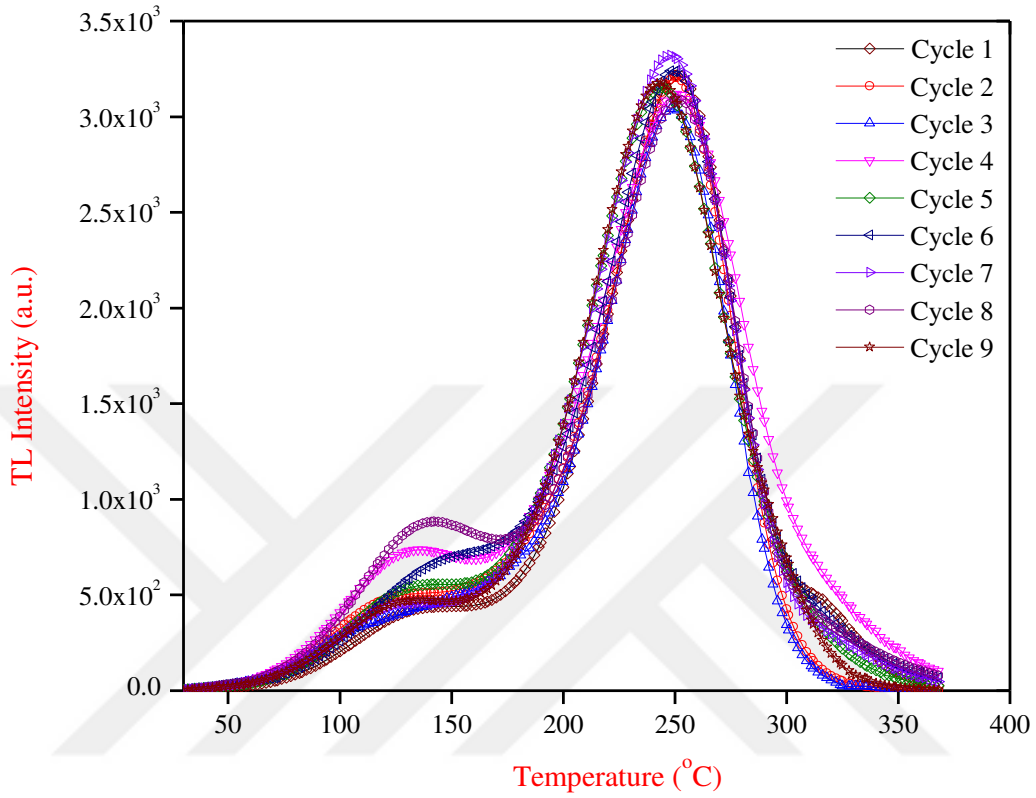

Figure 5.13 A set of TL glow curves of SiC versus temperature for nine repeats after β irradiation of 36Gy.

5.4.2 Normalized Peak Temperature

The peak temperature of each repeat was derived and the normalization was made for a better comparison.

Figure 5.15 shows variation of normalized peak temperature for the SiC sample, each experiment has approximately same result and it is so close to one.

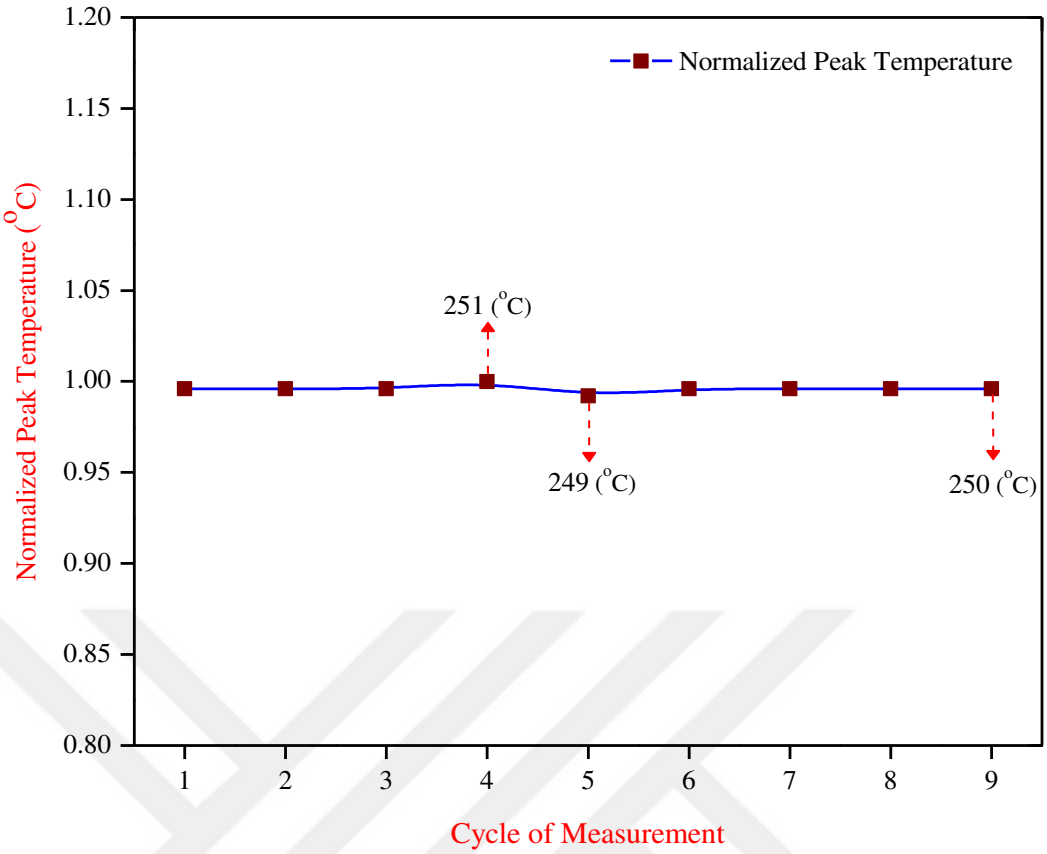

Figure 5.14 Normalized peak temperature versus cycle of measurement for the SiC after β irradiation of 36Gy.

From experimental data of normalized peak temperature, mean (average) and standard deviation, were calculated for SiC sample:

Table 5.1 Mean and standard deviation of SiC sample for normalized peak temperature.

Mean (Average)	0.996018889
Standard deviation	0.001992501

According to the table 5.1 a smaller standard deviation for peak temperature was obtained.

5.3.3 Normalized Thermoluminescence Peak Intensity

The thermoluminescence peak intensity of each sample was examined and normalization was made for a better comparison.

Figure 5.16 shows variations of normalized thermoluminescence peak intensity for the SiC sample, each experiment has approximately the same result and they were close enough to one.

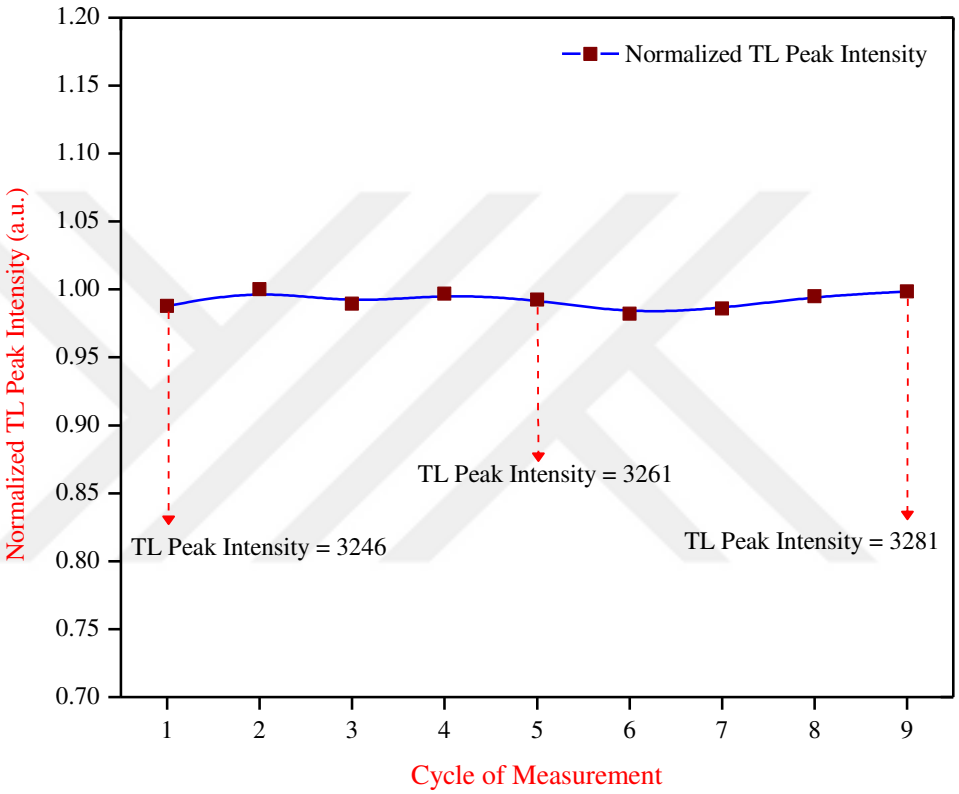

Figure 5.15 Normalized thermoluminescence peak intensity versus cycle of measurement for the SiC after β irradiation of 36Gy.

From experimental data of normalized thermoluminescence peak intensity, good mean (average) and standard deviation, were calculated for SiC sample:

Table 5.2 Mean and standard deviation of SiC sample for normalized thermoluminescence peak intensity.

Mean (Average)	0.991987778
Standard deviation	0.006104973

5.3.4 Normalized Area under the Curve

In this part of the experiment, the area under the curve of each sample was investigated and the normalization was made for a better comparison.

Figure 5.17 shows variations of normalized area under the curve for the SiC sample. At the end of nine cycles of experiment, each experiment for area under curve has approximately same result and they close enough to one.

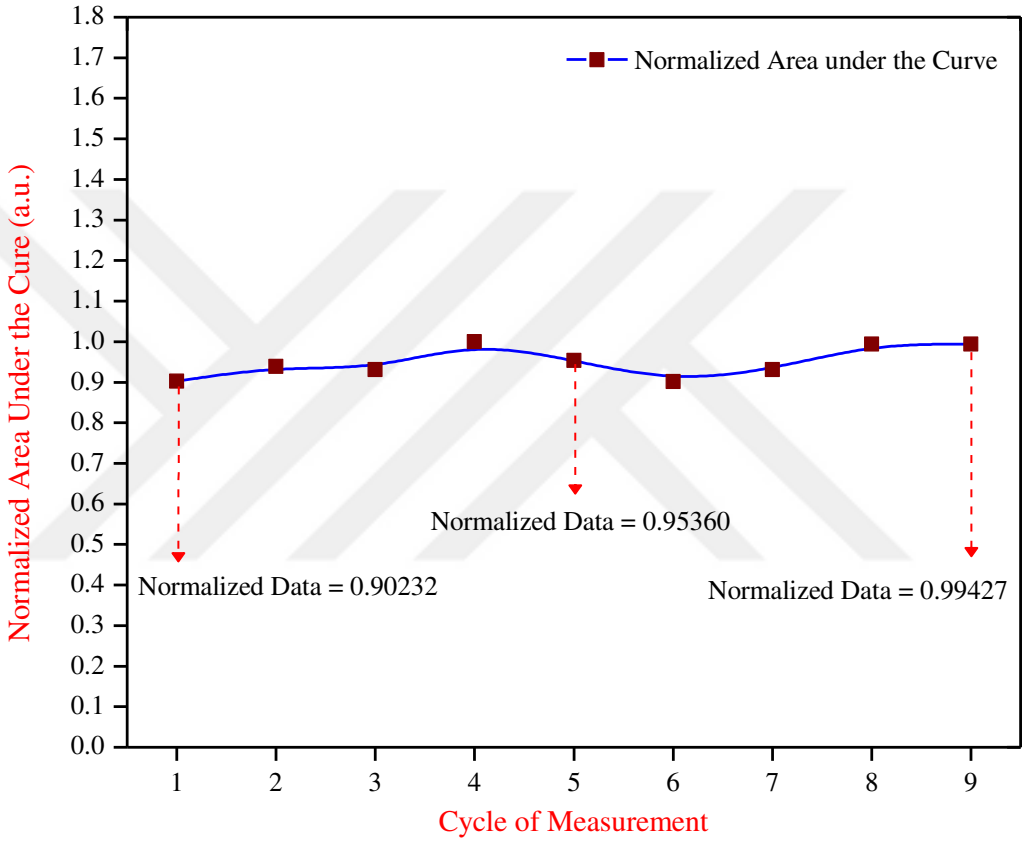

Figure 5.16 Normalized peak temperature versus cycle of measurement for the SiC after β irradiation of 36Gy.

From experimental data of normalized area under the curve, mean (average) and standard deviation, for SiC sample:

Table 5.3 Mean and standard deviation, of SiC sample for normalized area under the curve.

Mean (Average)	0.949548889
Standard deviation	0.03850291

As a result of cycle of measurement experiment the good reproducibility was obtained for the SiC sample.

5.4 Fading Effect

The steadiness of the stored signal at room temperatures is an essential factor in many applications like (Retrospective, personal, environmental, geological and archeological dating dosimetry …etc.). Any significant decreasing in the stored signal at room temperature will destroy the connection between emitted TL and the exposure of radiations that may have been taken at some significant time before readout. The reduction or loss in radiation induced signal in the sample as a function of time is called fading, in this phenomenon in which there is unplanned loss of the hidden information, there are many things that cause the fading process, the main one is temperature and light...etc. The traps which show lower entrapment energy in the thermal fading, will decline faster than the more energetic ones, because of their higher possibility of transition, belongs to this reason it must be keep samples in room temperature to avoid make errors in read out data. Some resources present an unanticipated fading effect unfluctuating, if the materials which are stored at temperatures well below that of the peak temperature of TL glow peak. This phenomenon is identified as the anomalous fading [70].

5.4.1 Variation of Glow Curve

For this experiment, the six samples weighted 100mg were irradiated about 36Gy at room temperature and they were saved in dark place for six different waiting times.

Figure 5.18 shows the variation of glow curve as a function of waiting time in the dark environment for the SiC sample, the shape of glow curves was changed by using different waiting time. The tunneling happens inside energy band gaps, when the electron overcomes and moves to the recombination center. The shape of glow curves changes by using different waiting time and the graph show that the fading effect is anomalous fading [70].

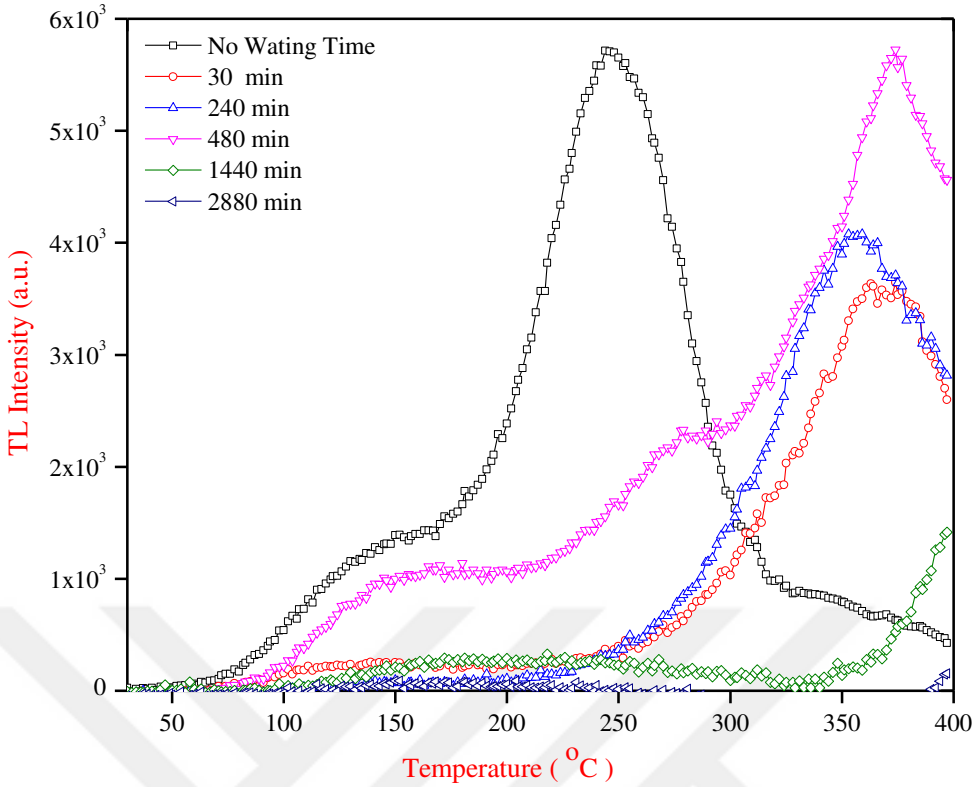

Figure 5.17 TL glow curves for SiC measured after various storage periods at room temperature. Read out all glow curves at β = 1 ºC/s after exposing to an irradiation of 36Gy.

In the figure 5.18, the TL peaks between 30-280 ºC are quickly decreased while a new peak is observed between 280-400 ºC. After 30 munities waiting time, it can be assumed that low and intermediate peaks were completely faded and new peak was taken placed in the high temperature region. In the 240 munities waiting time, the TL peak intensity increases 12%. An increase is observed about 34% after 480 munities. Above this waiting time the higher peak shifts above 400 ºC and not seen in the figure.

5.4.2 Variation of Area under the Curve

In this part of the experiment, the effects of the different waiting time in the dark on the peak area were examined.

Figure 5.19 and Figure 5.20 shows the variations of area under the curve as a function of waiting time in the dark place for the SiC sample.

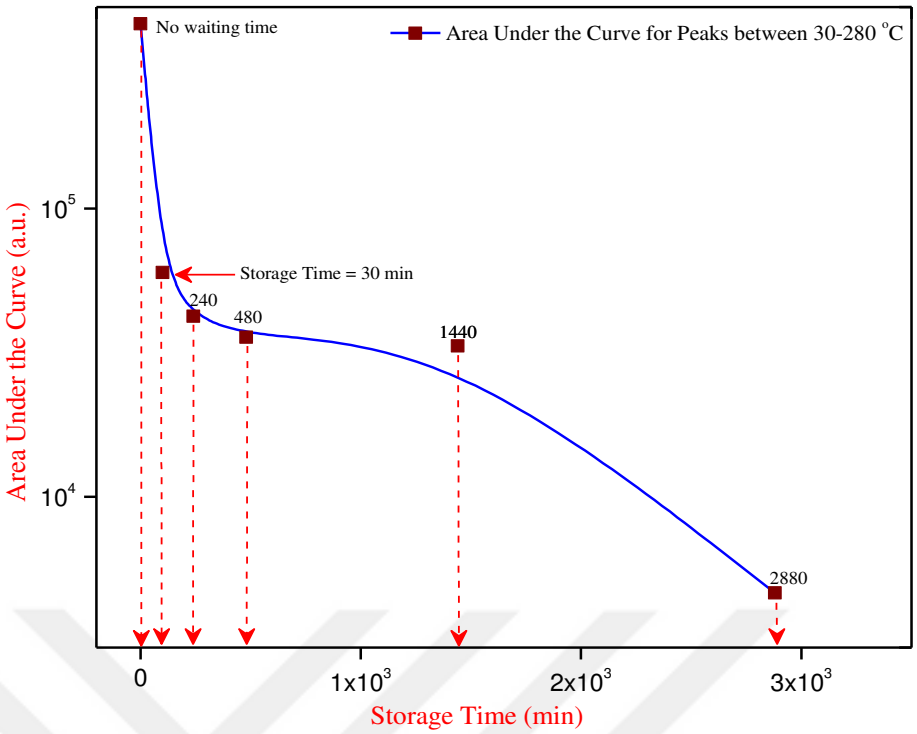

Figure 5.18 Area under curve for different waiting time in the dark for the SiC for peaks between (30-280) ºC

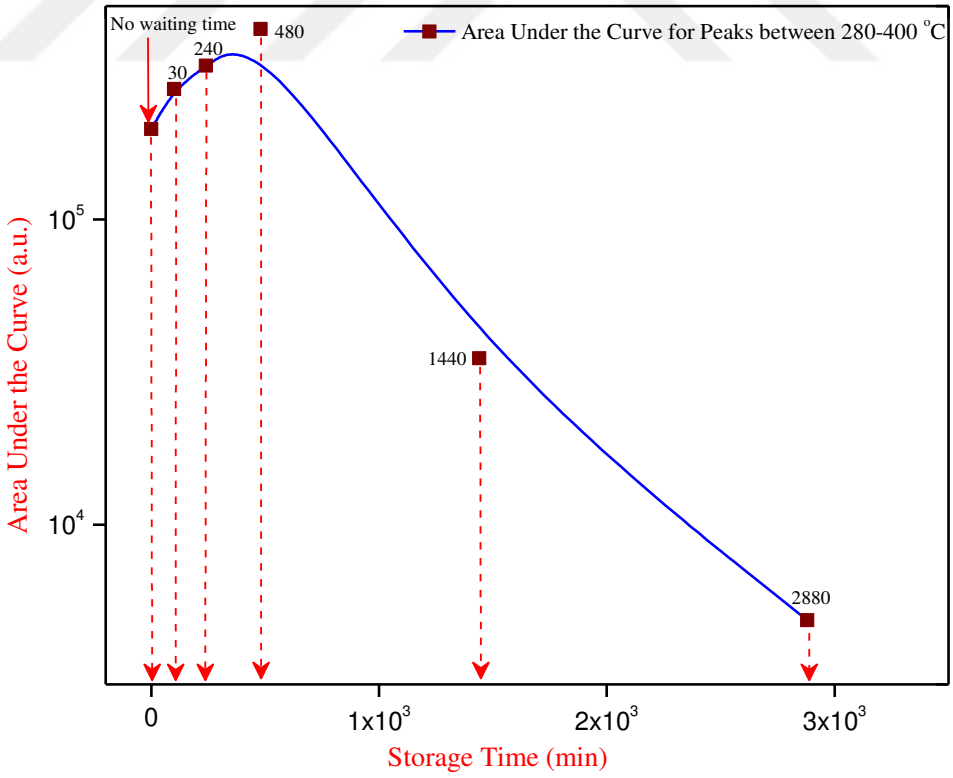

Figure 5.19 Area under curve for different waiting time in the dark for the SiC for peaks between (280-400) ºC.

5.5 Calculation of Trapping Parameters

As clarified in section (3.4) for single glow curve it has several experimental techniques such as (initial rise (IR), various heating rates (VHR), peak shape (PS), etc…) methods for evaluating trapping parameters. In this study, Computerized Glow Curve Deconvolution (CGCD) Method has been utilized to evaluate trapping parameters of the main dosimetric peak of (SiC).

To determine the kinetic parameters and number of peaks related to the TL glow peaks the Computerized Glow Curve Deconvolution (CGCD) methods are used. For the last two decades, this technique has become very favorable for evaluating the trapping parameters [71]. It has extensive superiority when it is compared to the experimental methods because of the coincident evolution of trapping parameters of all peaks without additional thermal treatments and experimental repetitions. Also, this technique can be used for all the data points for one of the glow curves instead of a few points only through the operations of the appropriate curve. If increase one of them the number of data points utilized in the analysis, it is clear that the possibility for right decision of the trapping parameters also increases. [72]

Nevertheless, it should be pointed that various samples, estimations and procedures of minimization may be utilized for the analysis of the glow curves in the computer glow curve deconvolution program. As a result, one may be questioned about if the results of CGCD method reveal the true trapping parameters of the thermoluminescence glow peaks. On the authority of many proficient researchers, in some cases, the results that taken by the method of the computer glow curve deconvolution, look to be unsure [73]. May be weakening the features of the method of CGCD in particular in complex TL glow curves. One may obtain a local minimum of the least square function which may result erroneous trapping parameters as the computerized appropriate routine tries to determine the “best-fit” to the numerical data. As a result, applies many sets of kinetic parameters could be designated to the same glow curve. The utilized program of the CGCD that depend on the procedure of the least square minimization was developed at the Reactor Institute at Delft, The Netherlands. An IRI-CIMAT Report gave the detailed results of these models [74].

The fit goodness for each measured glow curve was tested by using the figure of merit (FOM) [1]. Depends on many studies. It can be interpreted that, the fit is good, if the (FOM) values are among the range of (0.0% and 2.5%), but is fairly fit, if the values of (FOM) are between (2.5% and 3.5%), and the fit is bad if the value of (FOM) greater than (3.5%). It is so important to decide properly in the complex glow curve analyses by the method of CGCD the number of glow peaks exist in the glow curve and which of them have kinetics of the (first or general-order to get real results. [75].

In some cases, when used various peak numbers in the CGCD analysis instead of real numbers of glow peaks to be in the glow curve can be obtained the best-fits. In any way, the kinetic parameter values do not reflect their correct values when suppose that an incorrect number of the glow peaks in the glow curve even if obtain the best-fits. Therefore, first one should be determined the number of glow peaks and their kinetic orders in the glow curve of (SiC). In this study, it was noted that the structure of the glow curve of this model is described well by three general-order glow peaks. Because, the kinetic parameter results are also relying heavily on the input parameters like the individual peak site [76]. The parameters finally so selected were the values that resulted the best overall fit to the features of the certain high priority of the thermoluminescence (TL) results.

5.6 Calculation of Kinetic Parameters for Dose Response Experiment

All of the glow curves of silicon carbide were analyzed by CGCD program. A typical analyzed glow curve of SiC are shown in these figures below. As seen, between room temperature and 400 ºC SiC has three glow peaks.

5.6.1 Calculation of Trapping Parameters for 12 Gy Doses Level

The SiC peaks are located at 147ºC (P1), 273ºC (P2), and 366ºC (P3). The P_2 can be stated as the main peak.

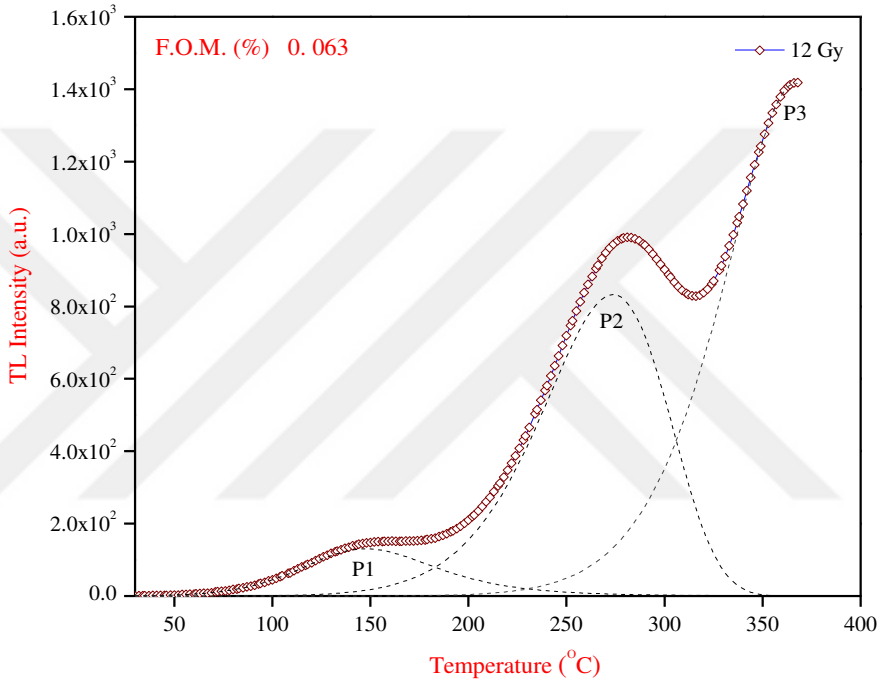

Figure 5.20 An analyzed glow curve of SiC sample measured after 12 Gy irradiation by beta source at room temperature with β =1 ºC/s. The experimental points are represented as open diamonds.

As a result, the measured kinetic parameters which given in the table 5.4 are the result of CGCD method.

Table 5.4 TL parameters of SiC peaks obtained at β =1 ºC/s after exposed to 12 Gy of beta ray at room temperature.

Peaks	T_mºC	***b***	$E_a(ev)$
1	147	2.00	0.80
2	273	1.00	0.96
3	366	1.00	1.85

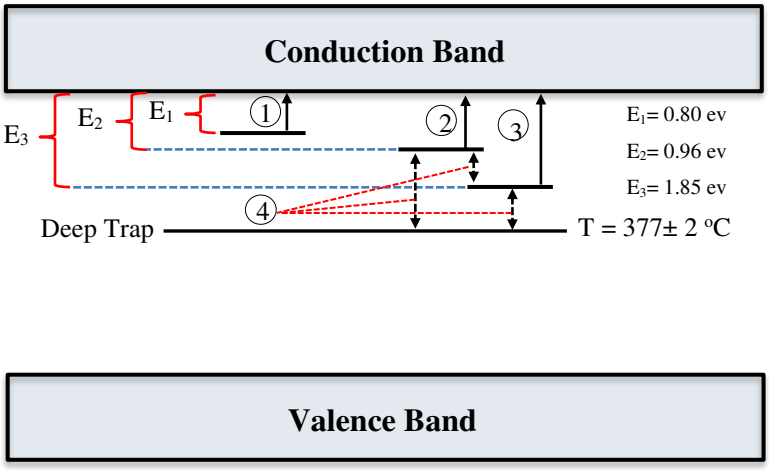

Figure 5.21 Band gap diagram drawn for SiC sample obtained at a β = 1 °C/s after exposed to 12 Gy of beta ray at room temperature.

5.6.2 Calculation of Trapping Parameters for 36 Gy Doses Level

The SiC peaks are located at 143°C (P1), 258°C (P2), and 333°C (P3). The P_2 can be stated as the main peak.

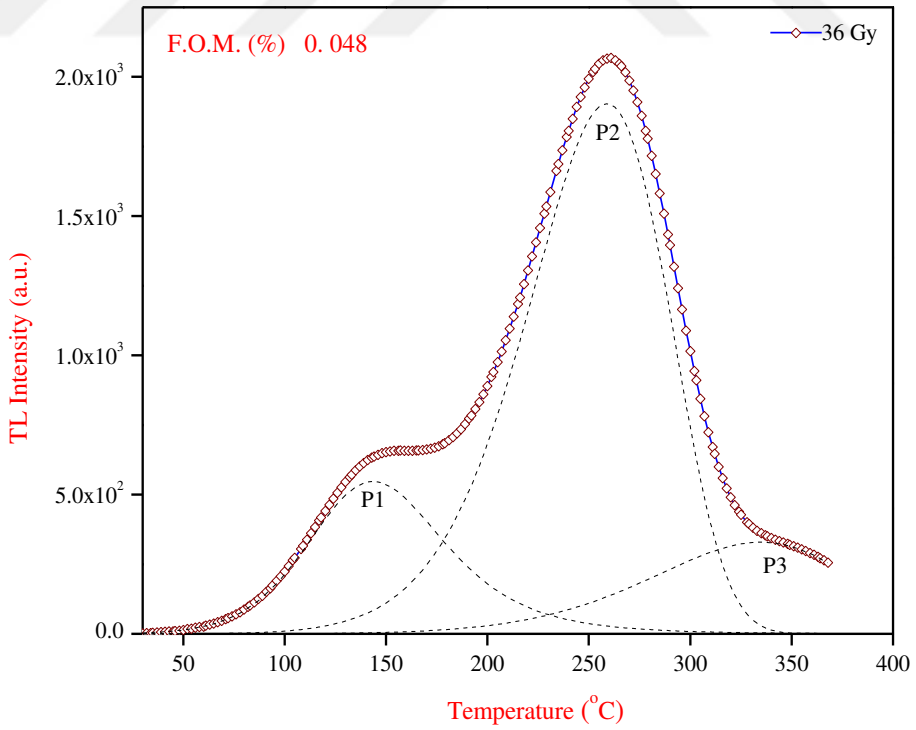

Figure 5.22 An analyzed glow curve of SiC sample measured after 36 Gy irradiation by beta source at room temperature with β =1 °C/s. The experimental points are represented as open diamonds.

As a result, the measured kinetic parameters which given in the table 5.5 are the result of CGCD method.

Table 5.5 TL parameters of SiC peaks obtained at β =1 °C/s after exposed to 36 Gy of beta ray at room temperature.

Peaks	T_m°C	***b***	$E_a(ev)$
1	143	2.00	0.80
2	258	1.00	1.52
3	333	1.00	0.80

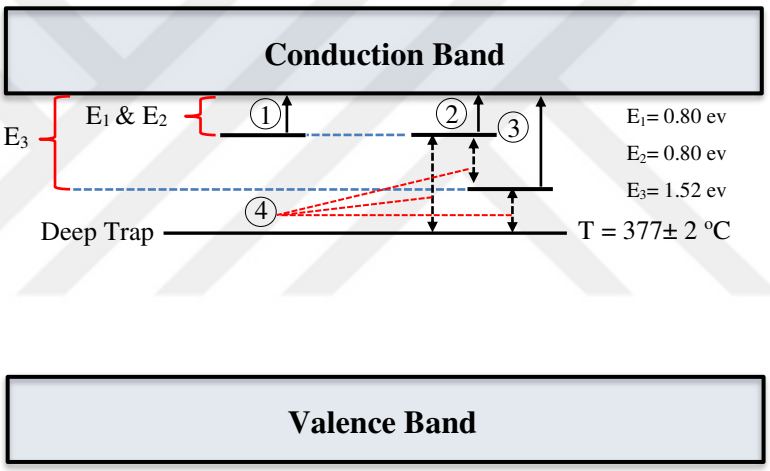

Figure 5.23 Band gap diagram drawn for SiC sample obtained at a β = 1 °C/s after exposed to 36 Gy of beta ray at room temperature.

5.6.3 Calculation of Trapping Parameters for 72Gy Doses Level

The SiC peaks are located at 112°C (P1), 165°C (P2), and 260°C (P3). The P_3 can be stated as the main peak.

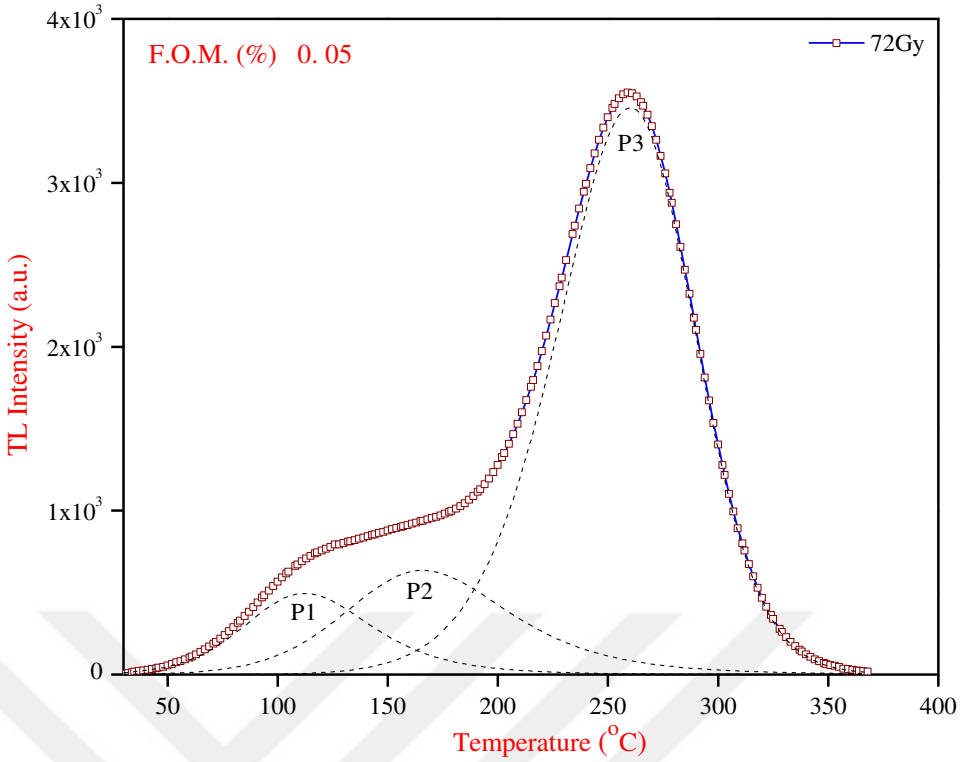

Figure 5.24 An analyzed glow curve of SiC sample measured after 72 Gy irradiation by beta source at room temperature with β =1 °C/s. The experimental points are represented as open diamonds.

As a result, the measured kinetic parameters which given in the table 5.6 are the result of CGCD method.

Table 5.6 TL parameters of SiC peaks obtained at β =1 °C/s after exposed to 72 Gy of beta ray at room temperature.

Peaks	T_m(°C)	***b***	$E_a(ev)$
1	112	2.00	0.80
2	165	2.00	0.80
3	260	1.00	1.72

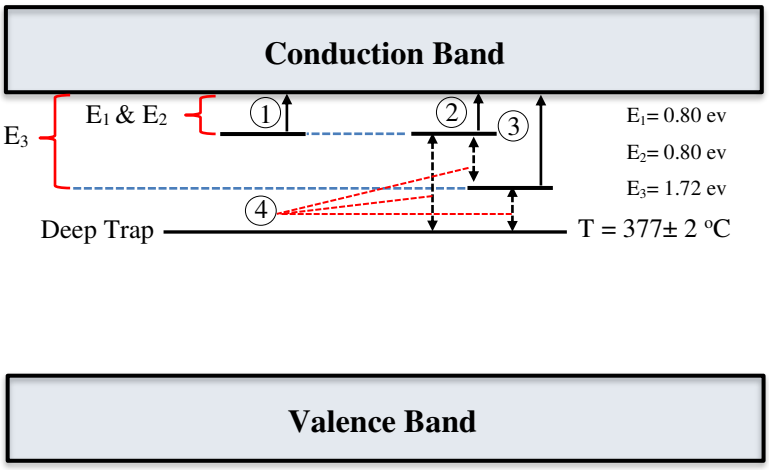

Figure 5.25 Band gap diagram drawn for SiC sample obtained at a β = 1 °C/s after exposed to 72 Gy of beta ray at room temperature.

5.6.4 Calculation of Trapping Parameters for 144 Gy Doses Level

The SiC peaks are located at 140°C (P1), 248°C (P2), and 356°C (P3). The peak two can be stated as the main peak.

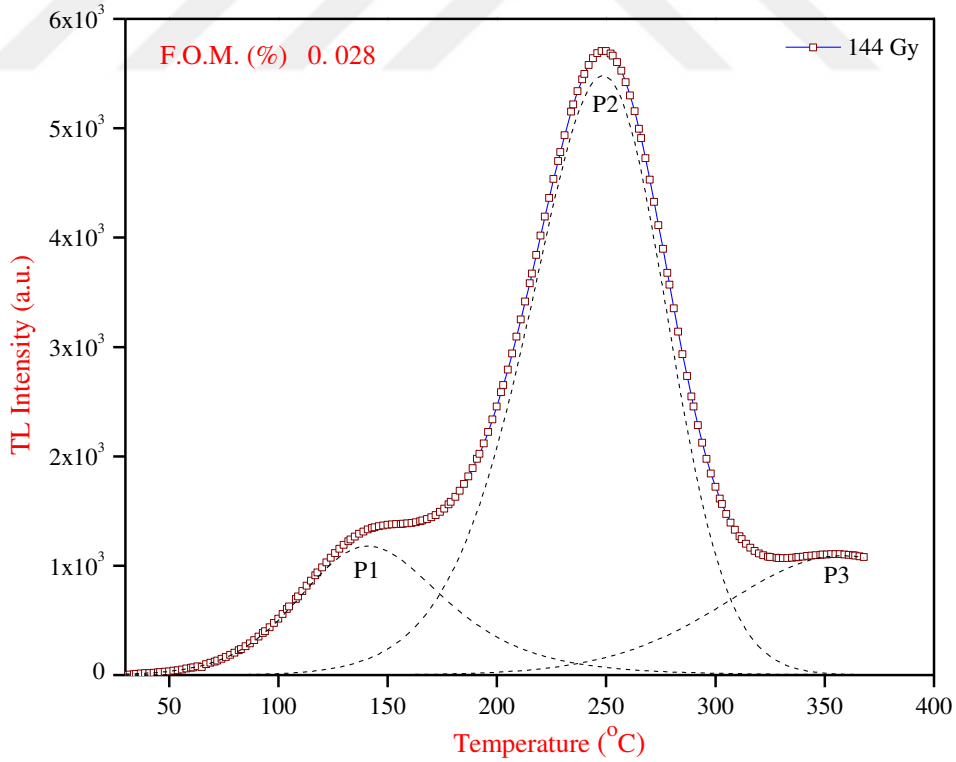

Figure 5.26 An analyzed glow curve of SiC sample measured after 144 Gy irradiation by beta source at room temperature with β =1 °C/s. The experimental points are represented as open diamonds.

As a result, the measured kinetic parameters which given in the table 5.7 are the result of CGCD method.

Table 5.7 TL parameters of SiC peaks obtained at β =1 °C/s after exposed to 144 Gy of beta ray at room temperature.

Peaks	T_m °C	***b***	$E_a(ev)$
1	140	2.00	0.80
2	248	1.23	0.96
3	356	2.00	1.65

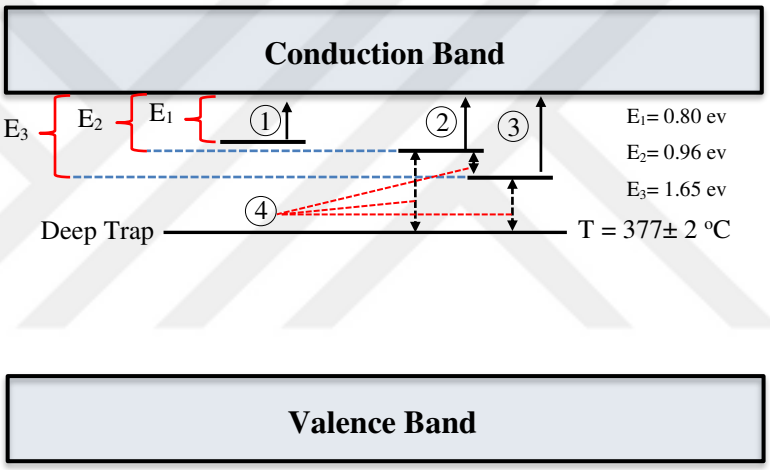

Figure 5.27 Band gap diagram drawn for SiC sample obtained at a β = 1 °C/s after exposed to 144 Gy of beta ray at room temperature.

5.6.5 Calculation of Trapping Parameters for 288 Gy Doses Level

The SiC peaks are located at 145°C (P1), 238°C (P2), and 353°C (P3). The peak two can be stated as the main peak.

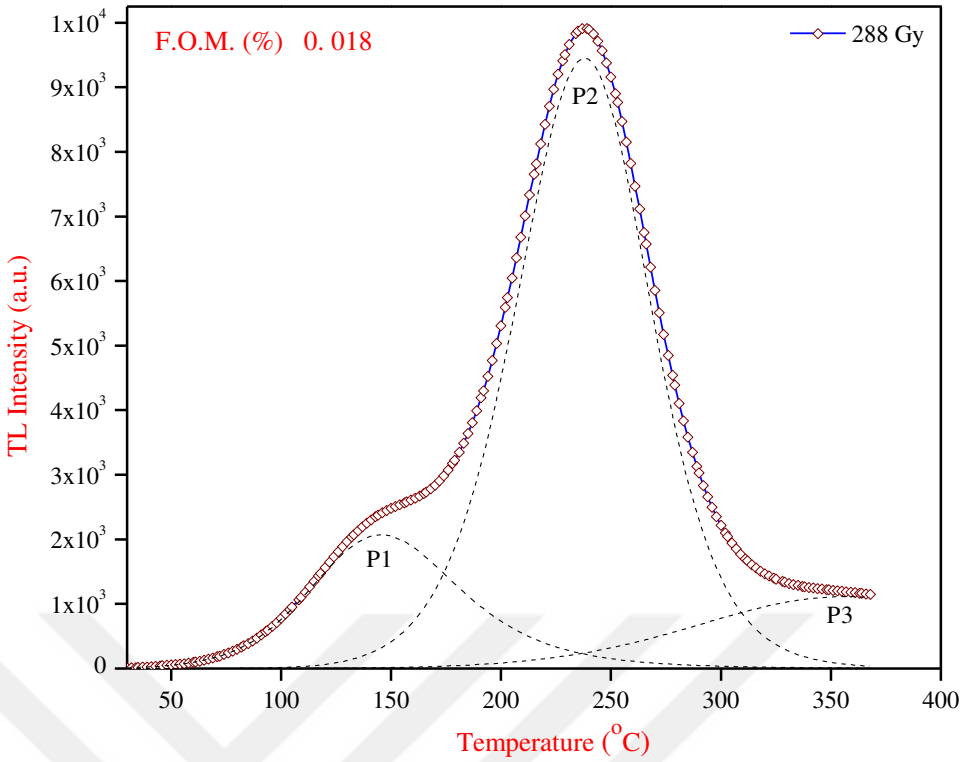

Figure 5.28 An analyzed glow curve of SiC sample measured after 288 Gy irradiation by beta source at room temperature with β =1 °C/s. The experimental points are represented as open diamonds.

As a result, the measured kinetic parameters which given in the table 5.8 are the result of CGCD method.

Table 5.8 TL parameters of SiC peaks obtained at β =1 °C/s after exposed to 288 Gy of beta ray at room temperature.

Peaks	T_m(°C)	***b***	$E_a(ev)$
1	145	2.00	0.80
2	238	1.55	1.54
3	353	1.00	0.80

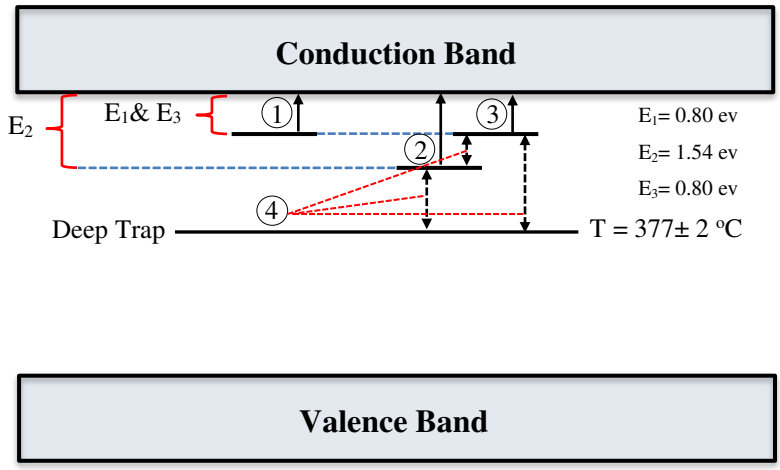

Figure 5.29 Band gap diagram drawn for SiC sample obtained at a β = 1 °C/s after exposed to 288 Gy of beta ray at room temperature.

5.6.6 Calculation of Trapping Parameters for 576 Gy Doses Level

The SiC peaks are located at 148°C (P1), 232°C (P2), and 356°C (P3). The peak two can be stated as the main peak.

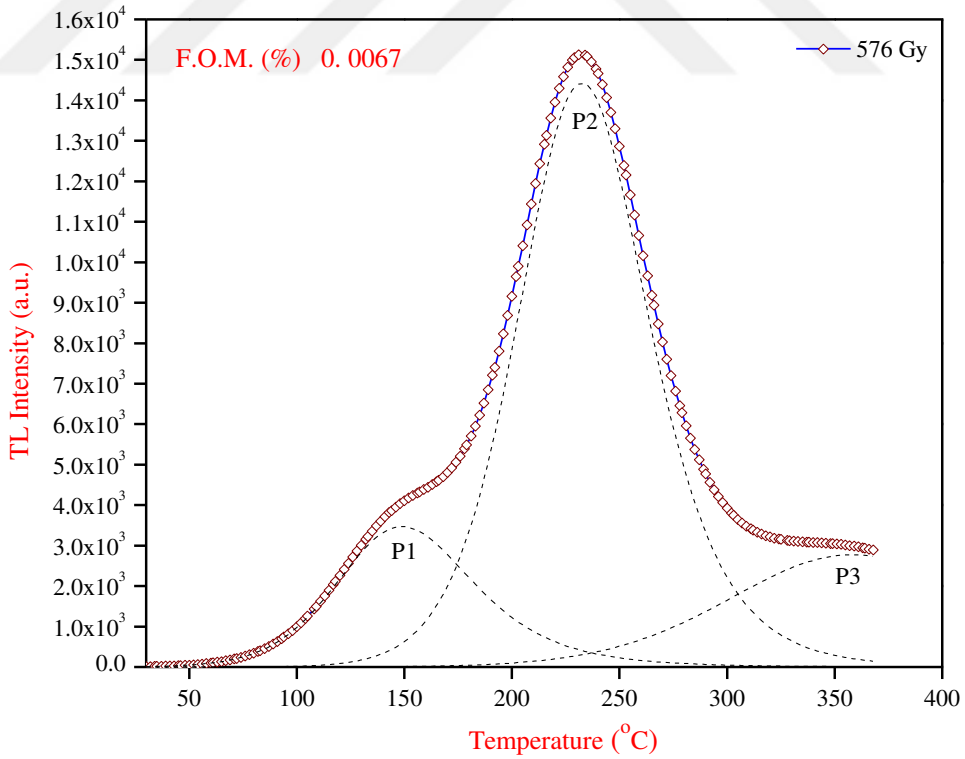

Figure 5.30 An analyzed glow curve of SiC sample measured after 576 Gy irradiation by beta source at room temperature with β =1 °C/s. The experimental points are represented as open diamonds.

As a result, the measured kinetic parameters which given in the table 5.9 are the result of CGCD method.

Table 5.9 TL parameters of SiC peaks obtained at β =1 °C/s after exposed to 576 Gy of beta ray at room temperature.

Peaks	T_m(°C)	***b***	$E_a(ev)$
1	145	2.00	0.80
2	238	1.55	1.86
3	353	1.00	0.87

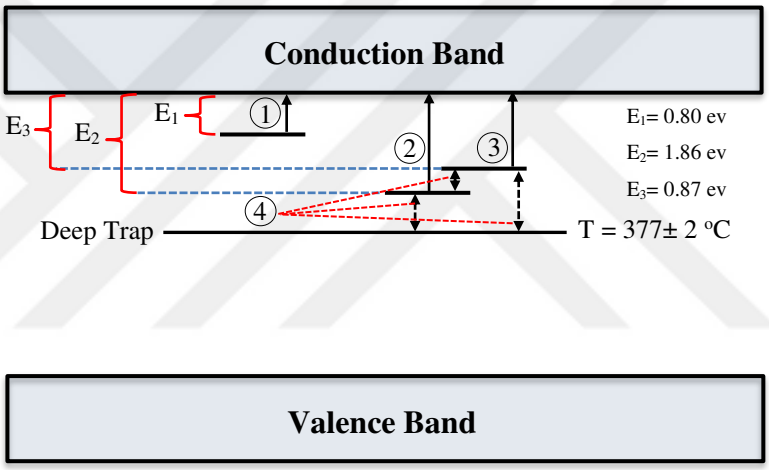

Figure 5.31 Band gap diagram drawn for SiC sample obtained at a β = 1 °C/s after exposed to 576 Gy of beta ray at room temperature.

5.6.7 Calculation of Trapping Parameters for 1152 Gy Doses Level

The SiC peaks are located at 144°C (P1), 225°C (P2), and 341°C (P3). The peak two can be stated as the main peak.

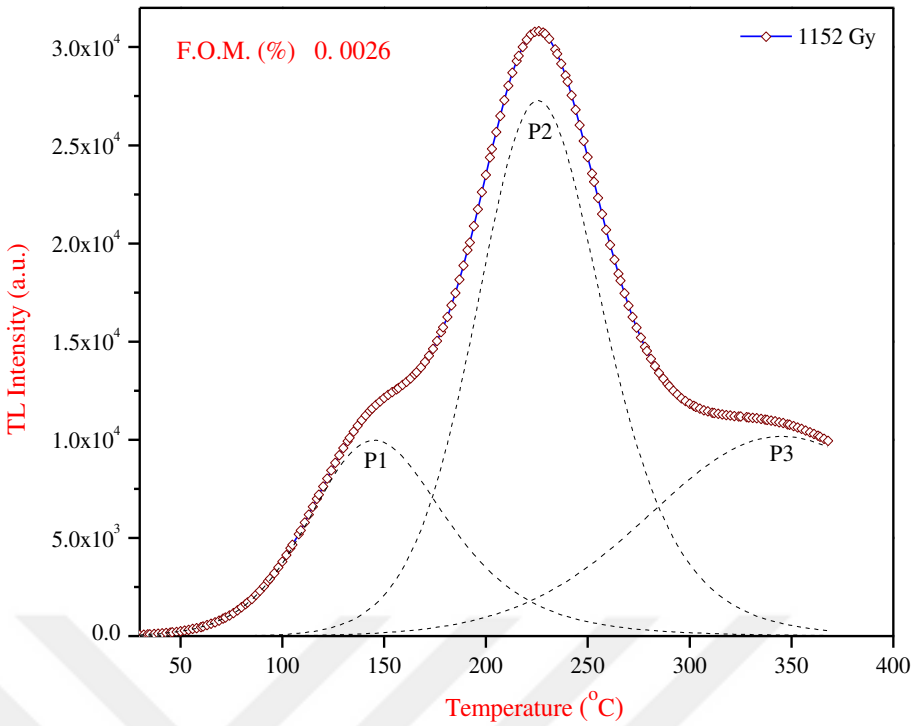

Figure 5.32 An analyzed glow curve of SiC sample measured after 1152 Gy irradiation by beta source at room temperature with β =1 °C/s. The experimental points are represented as open diamonds.

As a result, the measured kinetic parameters which given in the table 5.10 are the result of CGCD method.

Table 5.10 TL parameters of SiC peaks obtained at β =1 °C/s after exposed to 1152 Gy of beta ray at room temperature.

Peaks	T_m(°C)	***b***	$E_a(ev)$
1	144	2.00	0.80
2	225	1.86	1.58
3	341	2.00	0.80

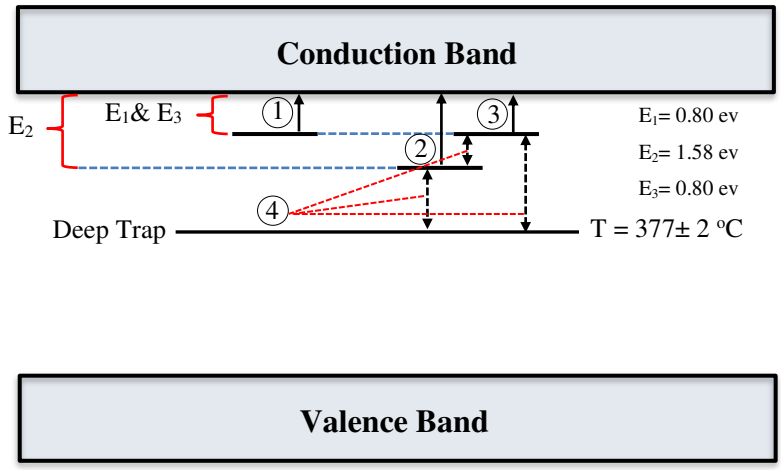

Figure 5.33 Band gap diagram drawn for SiC sample obtained at a β = 1 °C/s after exposed to 1152 Gy of beta ray at room temperature.

5.6.8 Calculation of Trapping Parameters for 2304 Gy Doses Level

The SiC peaks are located at 150°C (P1), 216°C (P2), and 355°C (P3). The peak two can be stated as the main peak.

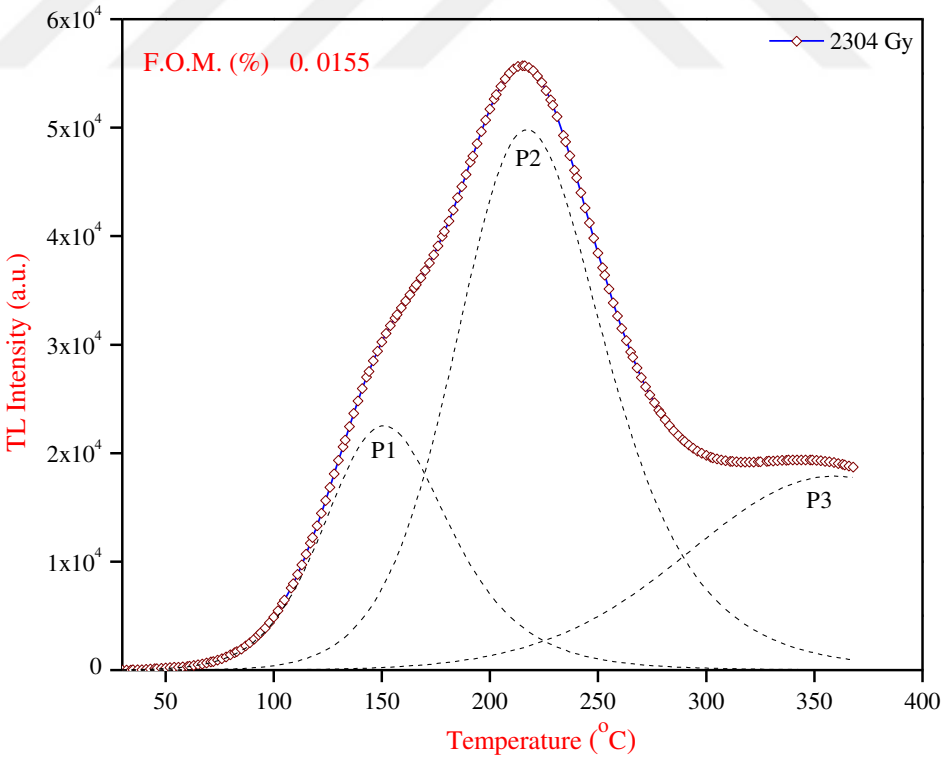

Figure 5.34 An analyzed glow curve of SiC sample measured after 2304 Gy irradiation by beta source at room temperature with β =1 °C/s. The experimental points are represented as open diamonds.

As a result, the measured kinetic parameters which given in the table 5.11 are the result of CGCD method.

Table 5.11 TL parameters of SiC peaks obtained at β =1 °C/s after exposed to 2304 Gy of beta ray at room temperature.

Peaks	T_m(°C)	***b***	$E_a(ev)$
1	150	2.00	0.80
2	216	2.00	1.64
3	355	1.00	0.80

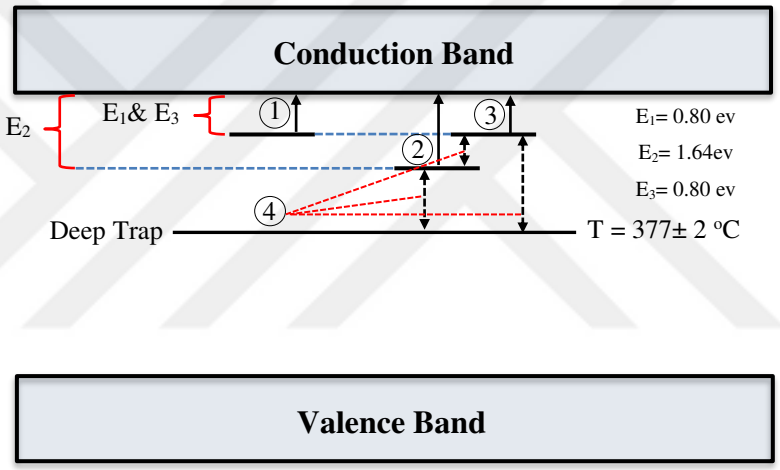

Figure 5.35 Band gap diagram drawn for SiC sample obtained at a β = 1 °C/s after exposed to 2304 Gy of beta ray at room temperature.

5.6.9 Calculation of Trapping Parameters for 4806 Gy Doses Level

The SiC peaks are located at 158°C (P1), 217°C (P2), and 345°C (P3). The peak two can be stated as the main peak.

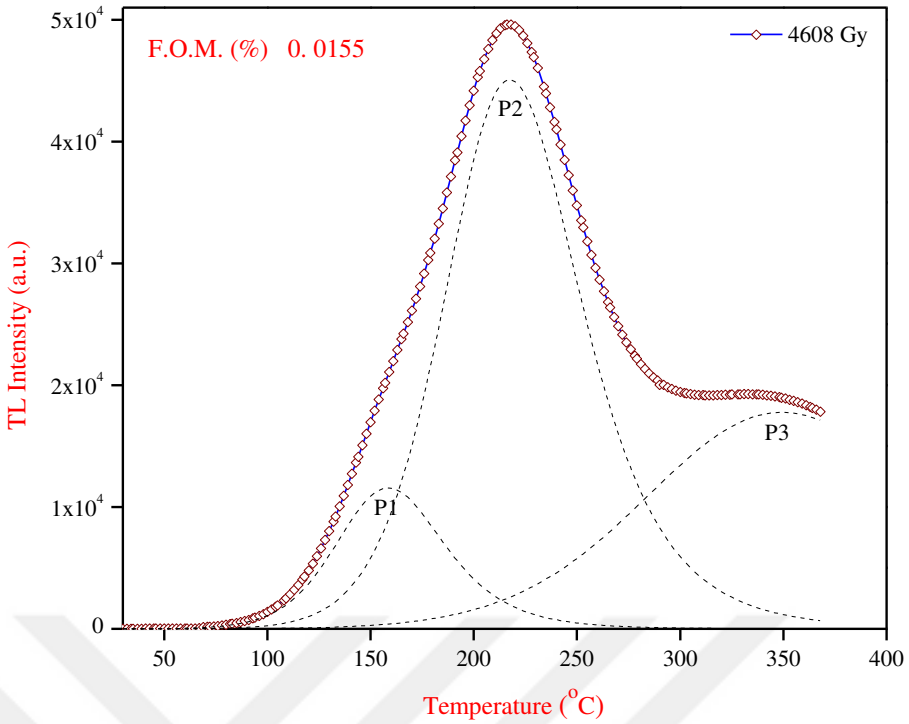

Figure 5.36 An analyzed glow curve of SiC sample measured after 4806 Gy irradiation by beta source at room temperature with β =1 °C/s. The experimental points are represented as open diamonds.

As a result, the measured kinetic parameters which given in the table 5.12 are the result of CGCD method.

Table 5.12 TL parameters of SiC peaks obtained at β =1 °C/s after exposed to 4608 Gy of beta ray at room temperature.

Peaks	T_m(°C)	***b***	$E_a(ev)$
1	144	2.00	0.80
2	225	2.00	1.72
3	341	1.00	0.80

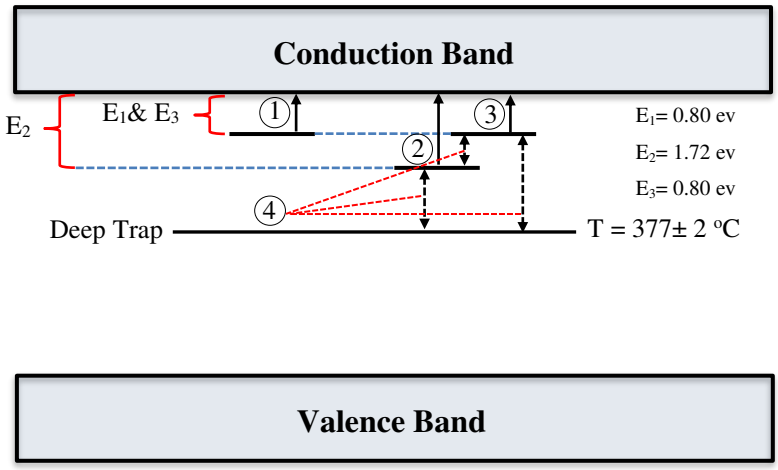

Figure 5.37 Band gap diagram drawn for SiC sample obtained at a β = 1 °C/s after exposed to 4608 Gy of beta ray at room temperature.

5.7 Calculation of kinetic parameters for all cycle of measurement experiments

5.7.1 Calculation of trapping parameters for first cycle of experiment after β irradiation of 36 Gy doses level

The SiC peaks are located at 134°C (P1), 251°C (P2), and 312 °C (P3). The peak two can be stated as the main peak.

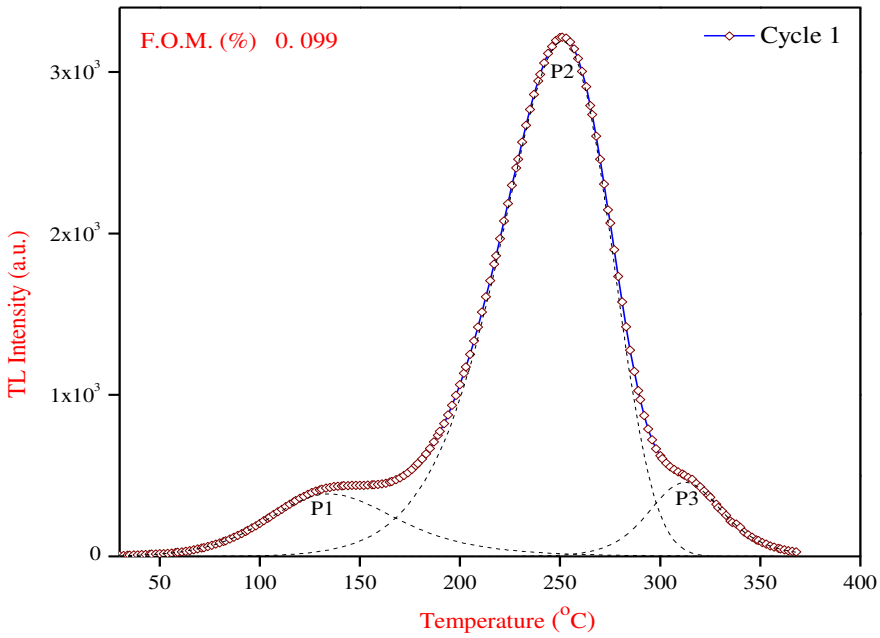

Figure 5.38 An analyzed glow curve of SiC sample measured after 36 Gy irradiation by beta source at room temperature with β =1 °C/s. The experimental points are represented as open diamonds.

As a result, the measured kinetic parameters which given in the table 5.13 are the result of CGCD method.

Table 5.13 TL parameters of SiC peaks obtained at β =1 °C/s after exposed to 36 Gy of beta ray at room temperature.

Peaks	T_m(°C)	***b***	$E_a(ev)$
1	134	2.00	0.80
2	251	1.00	0.95
3	312	1.00	1.96

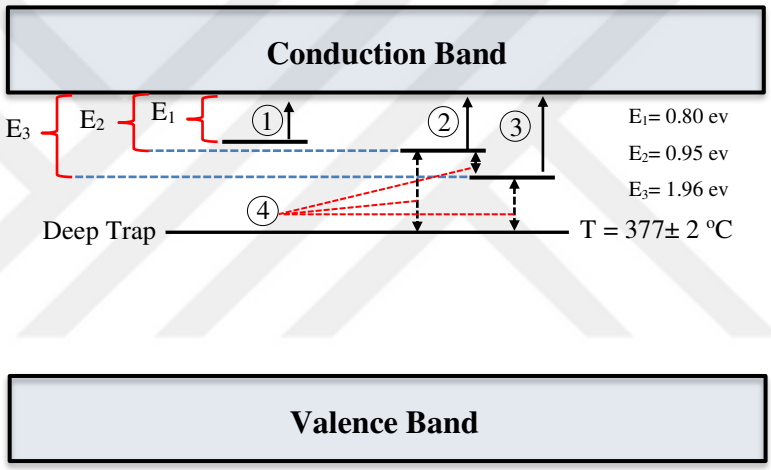

Figure 5.39 Band gap diagram drawn for SiC sample obtained at a β = 1 °C/s after exposed to 36 Gy of beta ray at room temperature.

5.7.2 Calculation of Trapping Parameters for second Cycle of experiment after β irradiation of 36 Gy Doses Level

The SiC peaks are located at 121°C (P1), 190°C (P2), and 251°C (P3). The peak two can be stated as the main peak.

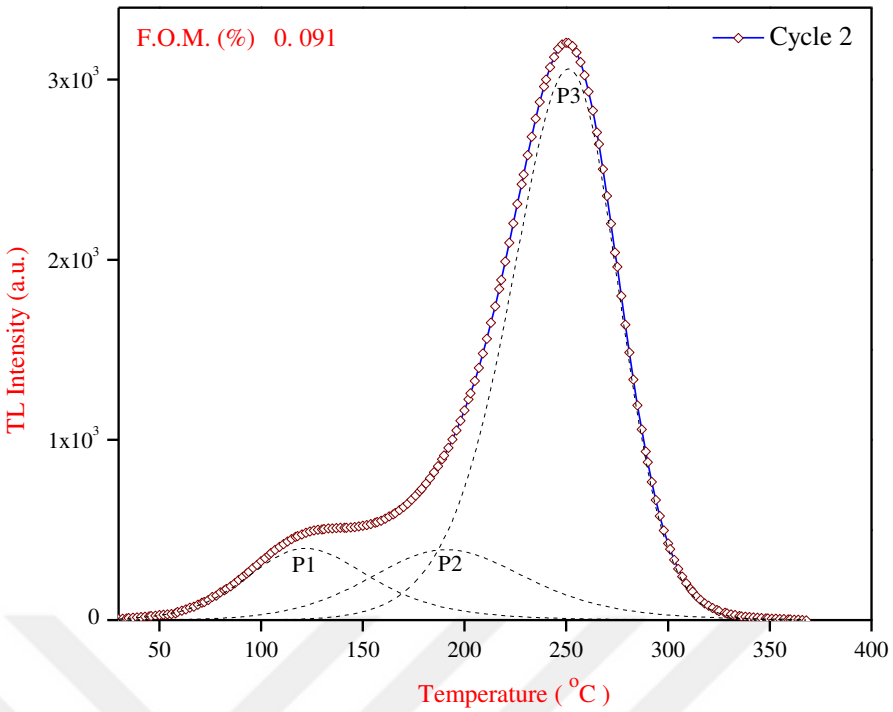

Figure 5.40 An analyzed glow curve of SiC sample measured after 36 Gy irradiation by beta source at room temperature with β =1 °C/s. The experimental points are represented as open diamonds.

As a result, the measured kinetic parameters which given in the table 5.14 are the result of CGCD method.

Table 5.14 TL parameters of SiC peaks obtained at β =1 °C/s after exposed to 36 Gy of beta ray at room temperature.

Peaks	T_m(°C)	***b***	$E_a(ev)$
1	121	2.00	0.80
2	190	1.74	0.80
3	251	2.00	1.84

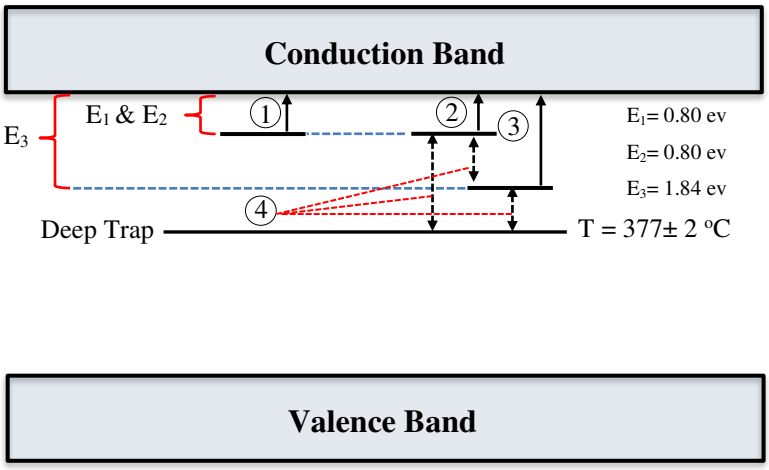

Figure 5.41 Band gap diagram drawn for SiC sample obtained at a β = 1 °C/s after exposed to 36 Gy of beta ray at room temperature.

5.7.3 Calculation of Trapping Parameters for Third Cycle of experiment after β irradiation of 36 Gy Doses Level

The SiC peaks are located at 112°C (P1), 167°C (P2), and 249°C (P3). The peak two can be stated as the main peak.

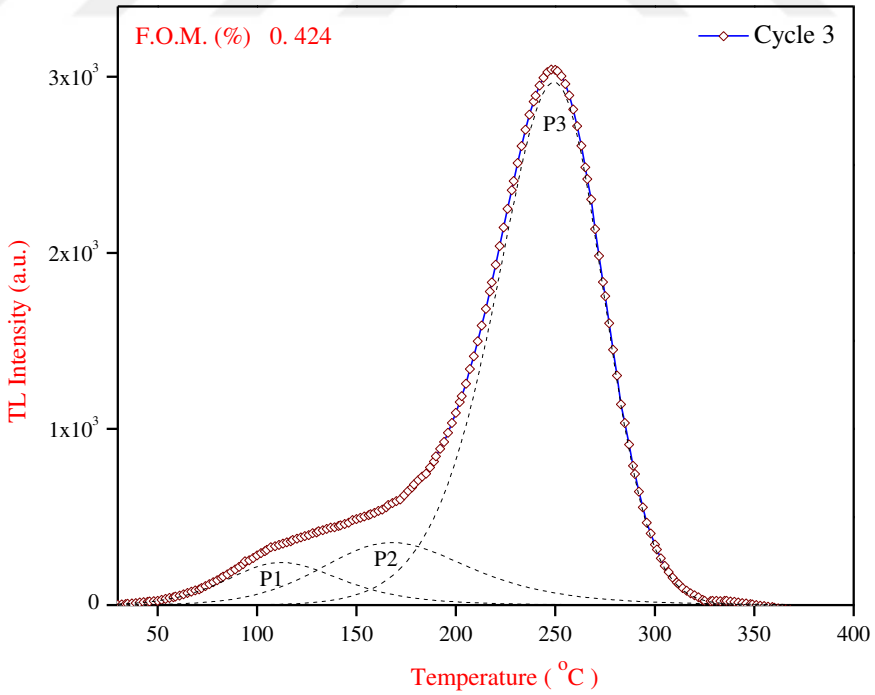

Figure 5.42 An analyzed glow curve of SiC sample measured after 36 Gy irradiation by beta source at room temperature with β =1 °C/s. The experimental points are represented as open diamonds.

As a result, the measured kinetic parameters which given in the table 5.15 are the result of CGCD method.

Table 5.15 TL parameters of SiC peaks obtained at β =1 °C/s after exposed to 36 Gy of beta ray at room temperature.

Peaks	T_m(°C)	***b***	$E_a(ev)$
1	112	2.00	0.80
2	167	2.00	0.80
3	249	2.00	1.70

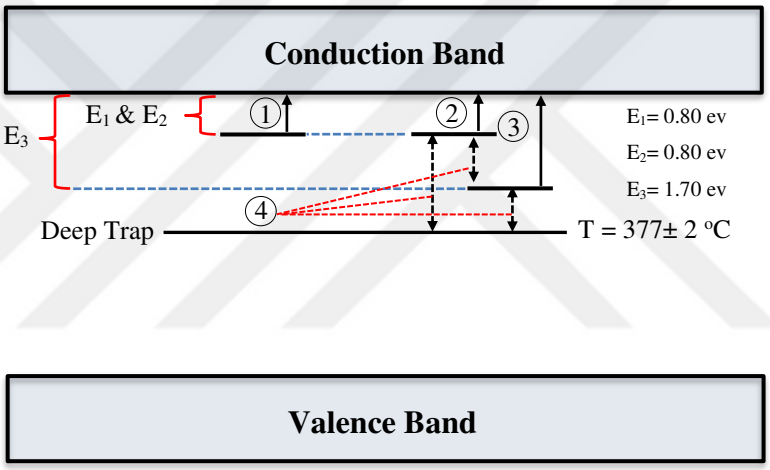

Figure 5.43 Band gap diagram drawn for SiC sample obtained at a β = 1 °C/s after exposed to 36 Gy of beta ray at room temperature.

5.7.4 Calculation of Trapping Parameters for Fourth Cycle of experiment after β irradiation of 36 Gy Doses Level

The SiC peaks are located at 129°C (P1), 249°C (P2), and 308°C (P3). The peak two can be stated as the main peak.

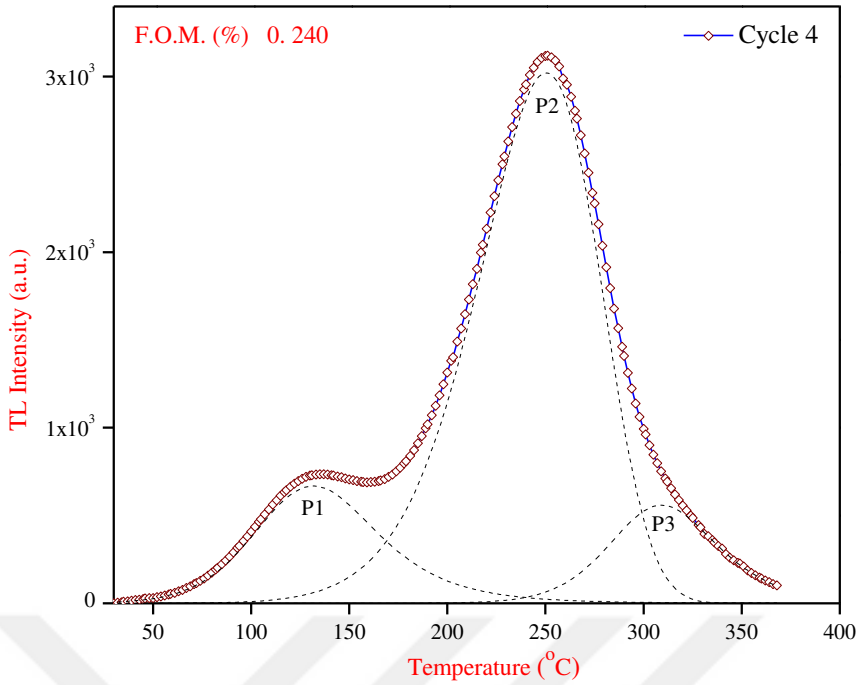

Figure 5.44 An analyzed glow curve of SiC sample measured after 36 Gy irradiation by beta source at room temperature with β =1 °C/s. The experimental points are represented as open diamonds.

As a result, the measured kinetic parameters which given in the table 5.16 are the result of CGCD method.

Table 5.16 TL parameters of SiC peaks obtained at β =1 °C/s after exposed to 36 Gy of beta ray at room temperature.

Peaks	T_m(°C)	***b***	$E_a(ev)$
1	129	2.00	0.80
2	249	1.04	0.99
3	308	1.00	2.01

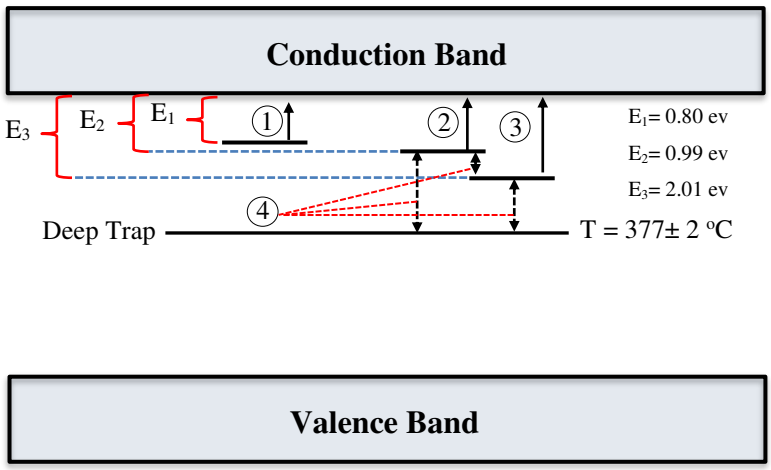

Figure 5.45 Band gap diagram drawn for SiC sample obtained at a β = 1 °C/s after exposed to 36 Gy of beta ray at room temperature.

5.7.5 Calculation of Trapping Parameters for Fifth Cycle of experiment after β irradiation of 36 Gy Doses Level

The SiC peaks are located at 131°C (P1), 242°C (P2), and 287°C (P3). The peak two can be stated as the main peak.

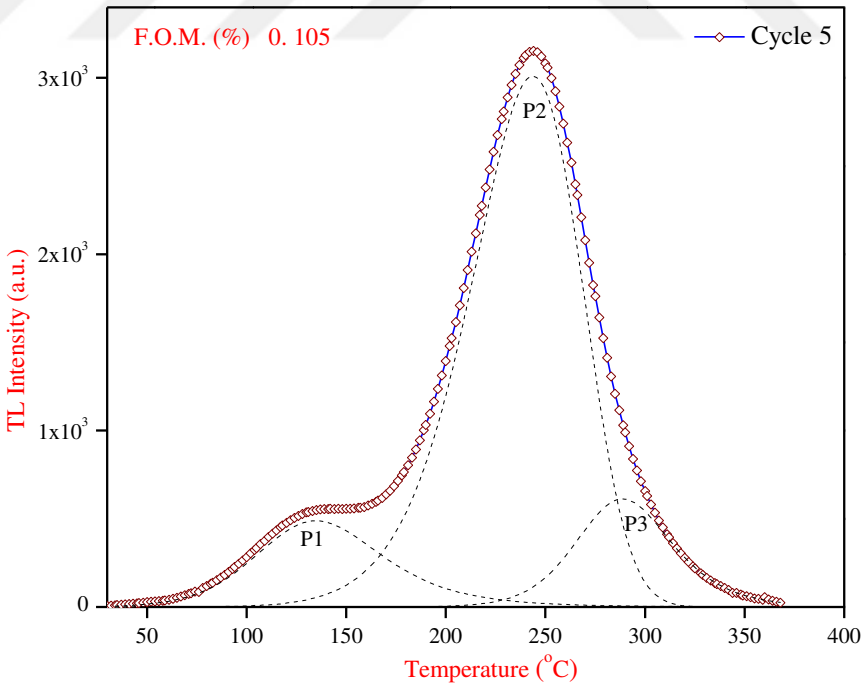

Figure 5.46 An analyzed glow curve of SiC sample measured after 36 Gy irradiation by beta source at room temperature with β =1 °C/s. The experimental points are represented as open diamonds.

As a result, the measured kinetic parameters which given in the table 5.17 are the result of CGCD method.

Table 5.17 TL parameters of SiC peaks obtained at β =1 °C/s after exposed to 36 Gy of beta ray at room temperature.

Peaks	T_m(°C)	***b***	$E_a(ev)$
1	131	2.00	0.80
2	242	1.08	1.02
3	287	1.00	1.87

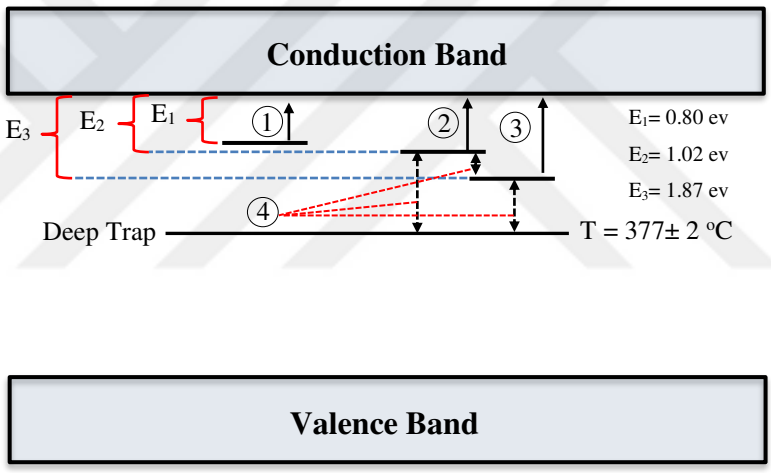

Figure 5.47 Band gap diagram drawn for SiC sample obtained at a β = 1 °C/s after exposed to 36 Gy of beta ray at room temperature.

5.7.6 Calculation of Trapping Parameters for Sixth Cycle of experiment after β irradiation of 36 Gy Doses Level

The SiC peaks are located at 144°C (P1), 247°C (P2), and 289°C (P3). The peak two can be stated as the main peak.

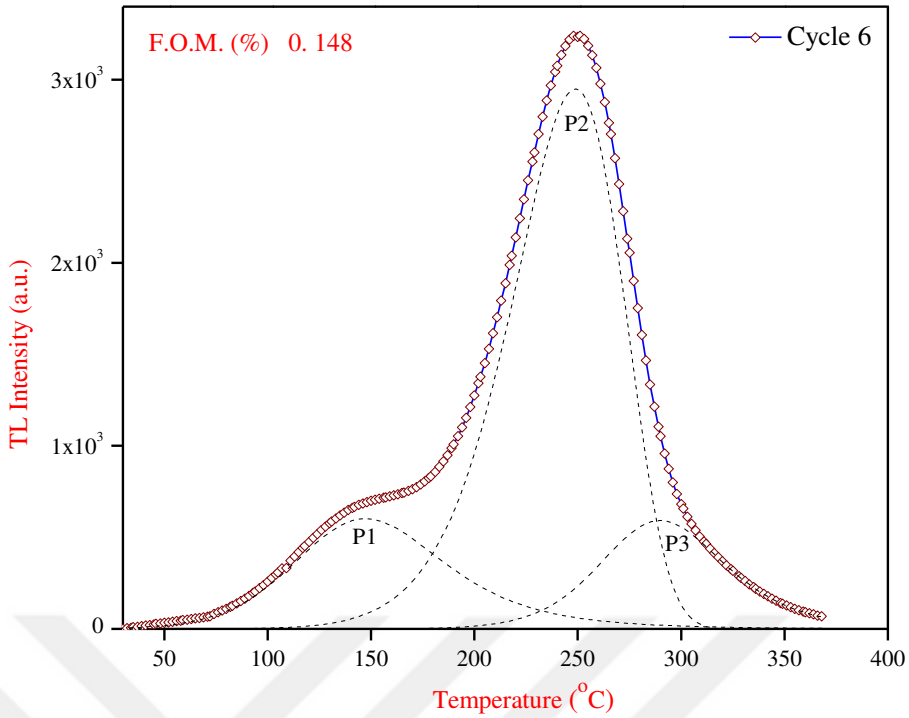

Figure 5.48 An analyzed glow curve of SiC sample measured after 36 Gy irradiation by beta source at room temperature with β =1 °C/s. The experimental points are represented as open diamonds.

As a result, the measured kinetic parameters which given in the table 5.18 are the result of CGCD method.

Table 5.18 TL parameters of SiC peaks obtained at β =1 °C/s after exposed to 36 Gy of beta ray at room temperature.

Peaks	T_m(°C)	***b***	$E_a(ev)$
1	144	2.00	0.80
2	247	1.00	0.92
3	289	1.00	1.67

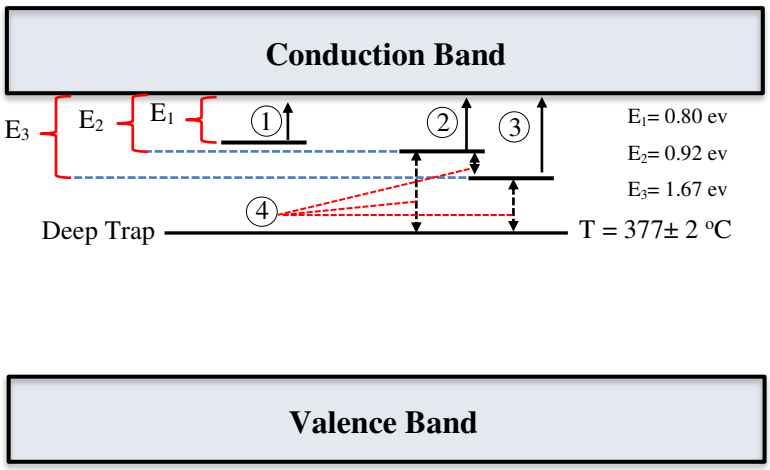

Figure 5.49 Band gap diagram drawn for SiC sample obtained at a β = 1 °C/s after exposed to 36 Gy of beta ray at room temperature.

5.7.7 Calculation of Trapping Parameters for Cycle Seven after β irradiation of 36 Gy Doses Level

The SiC peaks are located at 124°C (P_1), 247°C (P_2), and 309°C (P_3). The peak two can be stated as the main peak.

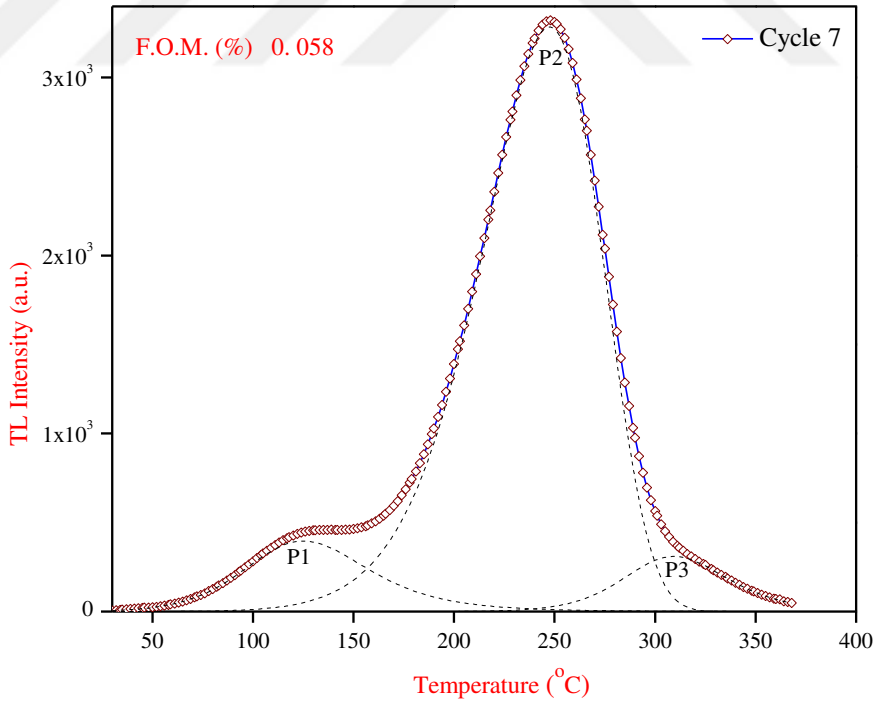

Figure 5.50 An analyzed glow curve of SiC sample measured after 36 Gy irradiation by beta source at room temperature with β =1 °C/s. The experimental points are represented as open diamonds.

As a result, the measured kinetic parameters which given in the table 5.19 are the result of CGCD method.

Table 5.19 TL parameters of SiC peaks obtained at β =1 °C/s after exposed to 36 Gy of beta ray at room temperature.

Peaks	T_m(°C)	***b***	$E_a(ev)$
1	124	2.00	0.80
2	247	1.00	0.98
3	309	1.00	2.00

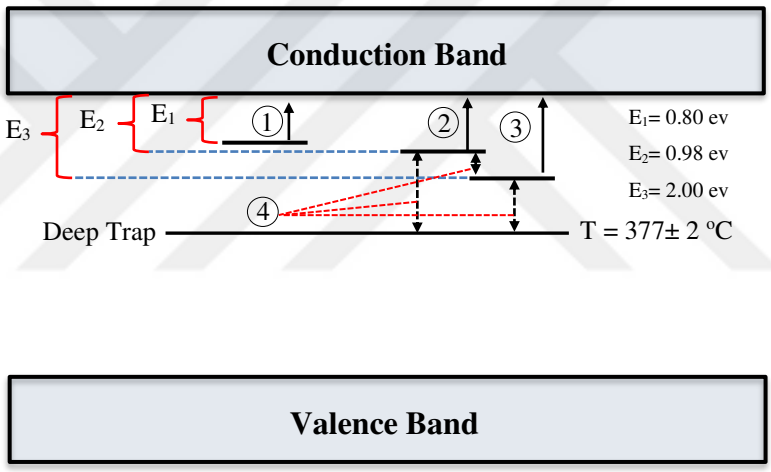

Figure 5.51 Band gap diagram drawn for SiC sample obtained at a β = 1 °C/s after exposed to 36 Gy of beta ray at room temperature.

5.7.8 Calculation of Trapping Parameters for eighth Cycle of experiment after β irradiation of 36 Gy Doses Level

The SiC peaks are located at 137°C (P1), 250°C (P2), and 298°C (P3). The peak two can be stated as the main peak.

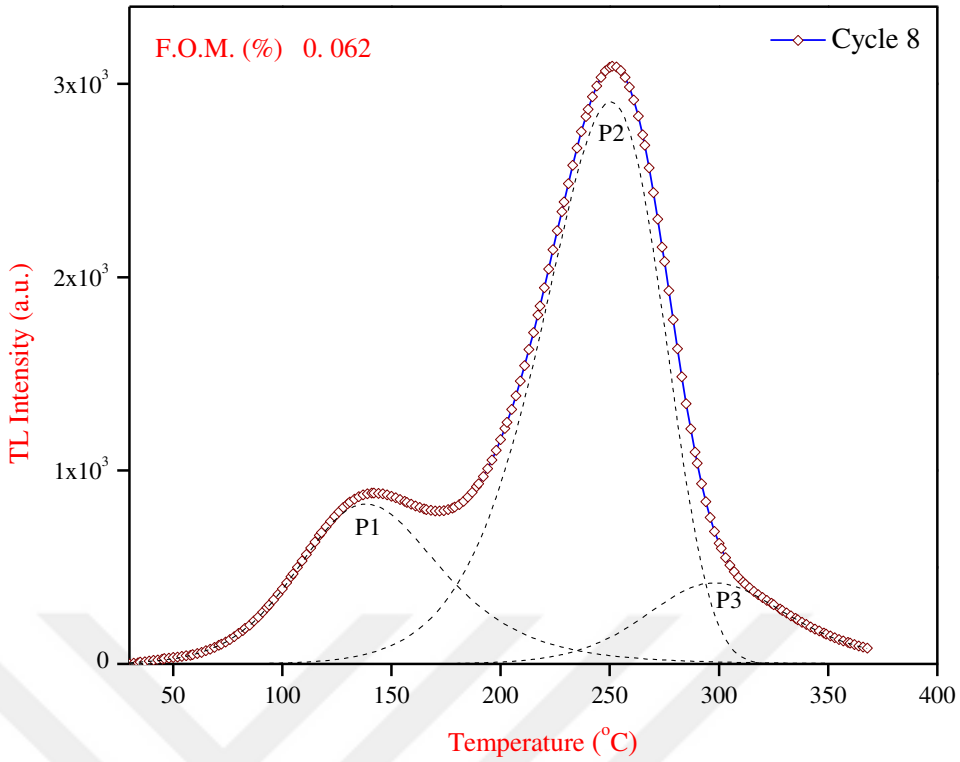

Figure 5.52 An analyzed glow curve of SiC sample measured after 36 Gy irradiation by beta source at room temperature with β =1 °C/s. The experimental points are represented as open diamonds.

As a result, the measured kinetic parameters which given in the table 5.20 are the result of CGCD method.

Table 5.20 TL parameters of SiC peaks obtained at β =1 °C/s after exposed to 36 Gy of beta ray at room temperature.

Peaks	T_m(°C)	***b***	$E_a(ev)$
1	137	2.00	0.80
2	250	1.00	0.95
3	298	1.00	1.86

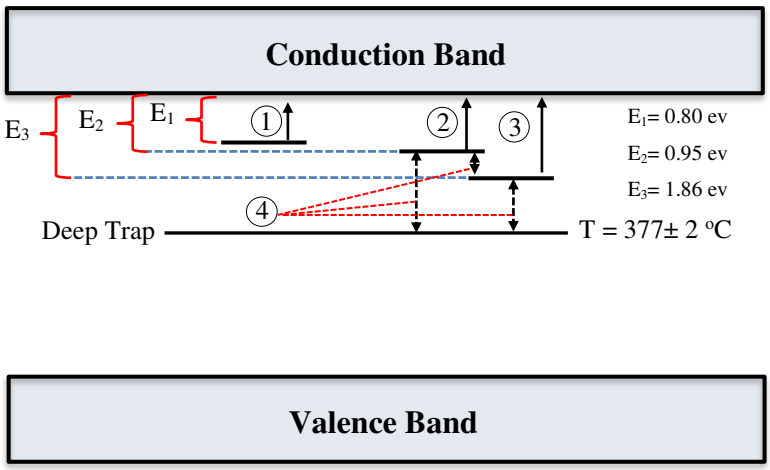

Figure 5.53 Band gap diagram drawn for SiC sample obtained at a β = 1 °C/s after exposed to 36 Gy of beta ray at room temperature.

5.7.9 Calculation of Trapping Parameters for Ninth Cycle of experiment after β irradiation of 36 Gy Doses Level

The SiC peaks are located at 137°C (P1), 243°C (P2), and 295°C (P3). The peak two can be stated as the main peak.

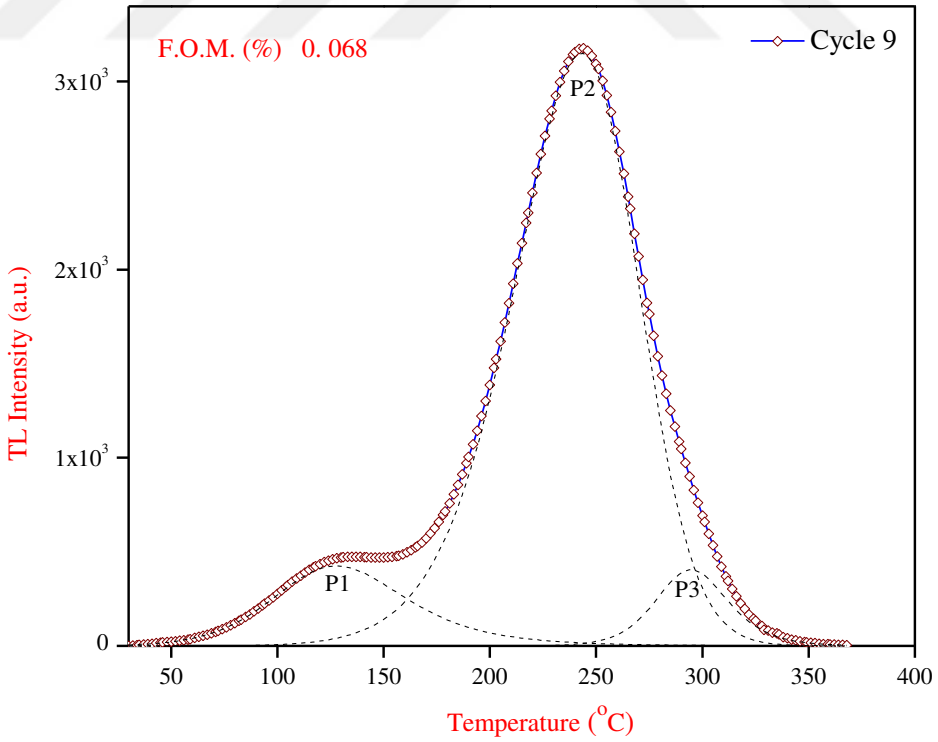

Figure 5.54 An analyzed glow curve of SiC sample measured after 36 Gy irradiation by beta source at room temperature with β =1 °C/s. The experimental points are represented as open diamonds.

As a result, the measured kinetic parameters which given in the table 5.21 are the result of CGCD method.

Table 5.21 TL parameters of SiC peaks obtained at β =1 °C/s after exposed to 36 Gy of beta ray at room temperature.

Peaks	T_m(°C)	***b***	$E_a(ev)$
1	127	2.00	0.80
2	243	1.20	0.93
3	295	1.00	2.30

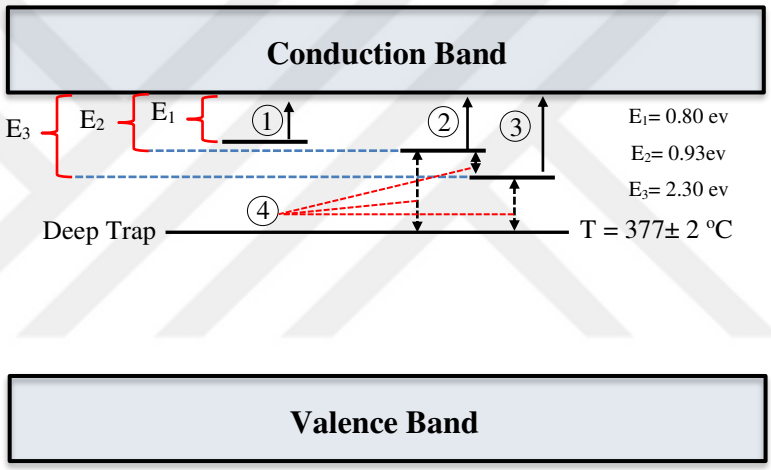

Figure 5.55 Band gap diagram drawn for SiC sample obtained at a β = 1 °C/s after exposed to 36 Gy of beta ray at room temperature.

5.8 Evaluation of all activation energy and peak temperature for all dose responses:

The glow curve of SiC after beta irradiation between 12Gy to 4608Gy at room temperature were investigated, and three main peaks are observed approximately at (145°C), (245 °C), and (349 °C). And the peak 2 can be stated as a main peak, the table chart was clearly show that by increasing the exposed dose levels the TL peak intensity shifted to the low temperature reign.

No important change was observed in activation energy (E_a) in all experiments, and it's situated nearly at (E_1 = 0.8, E_2 = 1.57, and E_3 = 0.8) (eV).

Table 5.22 All activation energy (E_a) and peak temperature of SiC peak obtained at β =1 °C/s after exposed to (12 to 4608) Gy of beta ray at room temperature.

Exposed dose(Gy)	E_1	E_2	E_3	T_1	T_2	T_3
12	0.80	0.96	1.85	147	273*	366
36	0.80	1.52	0.80	143	258*	333
72	0.80	0.80	1.72	112	165	260*
144	0.80	0.96	1.65	139	247*	355
288	0.80	1.54	0.80	145	238*	353
576	0.80	1.86	0.87	148	232*	356
1152	0.80	1.58	0.80	144	225*	341
2304	0.80	1.64	0.80	150	216*	355
4608	0.80	1.72	0.80	158	217*	345

Cells with (*) sign are a main peak

5.9 Evaluation of all activation energy and peak temperature for all cycles:

The calculation of all activation energy and peak temperature of SiC for nine repeats after beta irradiation of 36Gy. And the table chart was clearly show that there are not important changes are observed in activation energy (E_a) in all cycles. and it's situated nearly at (E_1 = 0.8, E_2 = 0.92, and E_3 = 1.93) (eV).

Table 5.23 All activation energy (E_a) and peak temperature of SiC sample for nine repeats obtained at β =1 °C/s after exposed to 36 Gy of beta ray at room temperature.

Reproducibility	E1	E2	E3	T1	T2	T3
Cycle 1	0.80	0.95	1.96	134	251*	312
Cycle 2	0.80	0.80	1.84	121	190	251*
Cycle 3	0.80	0.80	1.70	112	167	249*
Cycle 4	0.80	0.99	2.10	129	249*	308
Cycle 5	0.80	1.02	1.87	131	242*	287
Cycle 6	0.80	0.92	1.67	144	247*	289
Cycle 7	0.80	0.98	2.00	124	247*	309
Cycle 8	0.80	0.95	1.86	137	250*	298
Cycle 9	0.80	0.93	2.30	137	243*	295

cells with signed by (*) are a main peak

CHAPTER 6

CONCLUSION

Thermoluminescence is a useful and sensible method to record radiation information in insulators and it is extensively used in various fields such as; radiation dosimeter and archaeological dating, also to examine the crystalline defects and recently in the sensing of phase transitions [1]. The thermoluminescence (TL) event has also been studied for age determination. It has been done a great deal of study to get a better understanding and enhance the properties of the substances and also to grow a new thermoluminescence material. At the present time, thermoluminescence dosimeter (TLD) is an established dosimetric way with measured dose used in areas like (personnel, clinical and environmental dosimeter). TLD relies on materials which give off light while they are heated. The localized energy levels inside the forbidden energy band gap are generated by putting the impurities in the thermoluminescence (TL) material [26].
In the light of the experimental results, the following conclusions were obtained:

In our experiments, five main cases such as selecting of particle size, dose response, heating rate, cycle of measurements, and fading effect were studied. And according to the experimental results of this study.

- Each sample at different particle size has same TL glow curve shape but with different intensities. The largest TL peak intensity is observed for the sample whose particle size varies between 400-1000 μm. Therefore, the samples with this particle size were used in all experiment.
- The thermoluminescence Peak intensity increase with increasing dose values so the SiC may use as a dosimeter.
- Experimental observations have clearly shown that the peak temperature of intermediate TL peak shifts to lower temperature region with increasing dose level, and the shape of glow curves do not change at different doses. That means no extra peaks are observed.

- The peak temperature gradually shifted to the low temperature sides with increasing dose levels because the position of traps in the forbidden band gap may change with increasing dose. This shifting is about 50ºC. This shifting may be due to charging probability of re-trapping of carrier and also charging in crystal structures by effect of high recombination.
- From 12 Gy, to 2.3 kGy, the TL peak intensity linearly increases and reaches to saturation region between 2.3 kGy to 4.6 kGy . Therefore, SiC sample has a big linear region.

In general, depend on above points dose response experiment show that SiC has a good result.

- The thermoluminescence intensity decreases and peak temperature of glow curve increases with increasing heating rate.
- If heating rate increases, peak temperature increases until heating rate of 6 ℃/s, and it is clearly show that the peak temperature generally increases linearly with heating rate.
- The graph generally shows that the area under the curve decreases exponentially with increasing heating rate.

In general, depend on above points heating rate experiment show that SiC has a good result.

- These experiments show that SiC has a repeatability property that it can be used many times for dosimetric applications. Because the results of dose response, normalized thermoluminescence peak intensity and normalized area under curve are approximately same.
- As a result of cycle of measurement experiment the good reproducibility was obtained for the SiC sample. The obtained standard deviation value is smaller than 2%.

In general, depend on above points reproducibility experiment show that SiC has a good result.

It is well known that the optical treatments highly affect the intensity of the thermoluminescence glow curves. Fading also affects the intensity of the thermoluminescence glow curves.

- The effects of waiting in the dark process on the thermoluminescence glow curves were observed for SiC. Experiments show that SiC doesn't has a good storage capacity. Because the tunneling happens inside energy band gaps. The shape of glow curves changes by using different waiting time and it is anomalous fading.
- The effects of the different waiting time in the dark room on the SiC, the TL peaks between 30-280 ^{o}C are quickly decreased while a new peak is observed between 280-400 ^{o}C. After 30 munities waiting time, it can be assumed that low and intermediate peaks were completely faded and new peak was taken placed in the high temperature region. In the 240 munities waiting time, the TL peak intensity increases 12%. An increase is observed about 34% after 480 munities. Above this waiting time the higher peak shifts above 400 ^{o}C and not seen in the figure.

The main purpose of our study is to investigate the thermoluminescence properties of Silicone Carbide (SiC). In order to understand the properties of a thermoluminescent material the kinetic parameters of the different glow peaks such as the order of kinetics (b), the activation energy (E_a) and frequency factor (s) of the traps must be determined. Therefore, the order of kinetics (b), activation energy (E_a) and the frequency factor (s) associated with the dosimetric thermoluminescent (TL) glow peak of this material were evaluated by using computerized glow deconvolution (CGCD).

In this study, when SiC samples were irradiated doses and SiC sample showed totally one big peak and two little peaks during this study, as seen from Figures above in to the section 5.5. when the evolution of peaks 1, 2, and 3 was carefully followed by CGCD method, second peak clearly was observed at approximately 245^{0}C.

- The goodness of fit for all the measured glow curves was tested using the figure of merit (FOM) the value is between 0.0% and 0.15% and this fit is very good.

- No important change was observed in activation energy (E_a) in all evaluated dose response experiments, and it's situated nearly at (E_1 = 0.8, E_2 = 1.57, and E_3 = 0.8) (eV).

- Three main peaks are observed approximately at (145^{o}C), (245 ^{o}C), and (349 ^{o}C). And the peak 2 can be stated as a main peak.

In general, the results of the experiments and calculation of all kinetic parameters has proved that SiC is a good candidate for TL dosimetry studies.

REFERENCES

[1] McKeever, S.W.S. (1985). Thermoluminescence of Solids. USA: *Cambridge University Press*. p. 374.

[2] Chen, R., And McKeever, S.W.S. (1997). Theory of Thermoluminescence and Related Phenomena. Singapore: *Word Scientific Publishing Co*. Pvt. Ltd.

[3] Randall, J. T., and Wilkins, M. H. F. (1945). Phosphorescence and electron, traps I: The study of trap distributions. Proceedings of Royal Society A 184, 366-389.

[4] Pradhan, A.S. (1981). *Radiation Protection Dosimetry*, **1**, 153.

[5] Pekpak, E., Gülhan, O., Aysen, Y. (2009). Thermoluminescent characteristics of lithium tetraborate, in: Proceedings of the IV International Boron Symposium.

[6] Chen, R., Horowitz, Y.S. (1984). Thermoluminescent and Thermoluminescent Dosimetry, FL*: CRC Press, Boca Raton*, **1**, 49.

[7] Takenaga, M., Yamamoto, O., and Yamashita, T. (1980). Preparation and characteristics of Li2B4O7: Cu phosphor. *Nuclear Instruments and Methods*, **175**, 77-78.

[8] Mahesh, K., Weng, P. S., and Furetta, C. (1989). Thermoluminescence in Solids and its Applications. Ashford, Kent, England: Nuclear Technology Publishing.].

[9] Furetta, C. (2003). Handbook of Thermoluminescence. Singapore: *World Scientific Publishing Co. Pte. Ltd.*

[10] Othman, IE, and Charles, M W. (1999). 12th International Conference on Solid State Dosimetry, held at the Casa del Córdon Conference *Centre, Burgos, Spain*, **84**, 193.

[11] Braunlich, P. (1983). Thermally stimulated relaxation in solids, *Springer- Verlag*

[12] HalpBran A. (1985). Evaluation of thermal activation energies from glow curves, *Phys. Rev*., **117**, 40.

[13] Botter-Jensen L. (1997). Luminescence technique: instrumentation and methods *Rad. Meas*., **17**, 749-768.

[14] McKeever, SWS., Moskovitch, M., and Townsend, P.D. (1995). Thermoluminescence Dosimetry Materials: Properties and Uses. Ashford, England: *Nuclear Technology Publishing*.

[15] Daniels F. and Boyd C. A. (1953). *Thermoluminescence as a research tool. Science*, **117**, 343-349.

[16] Aitken M. J., Tite M. S. and Reid J. (1964). Thermoluminescencent dating of ancient ceramics, *Nature*, **202**, 1032-1033.

[17] Mejdahl V. (1969). Thermoluminescence dating of ancient Danish ceramics. *Archaeometry,* **11,** 99-104.

[18] Wintle A. G. and Huntley D. J. (1985). Thermoluminescencent dating of ocean sediments. *Canadian journal of earth sciences*.

[19] Aitken M. J., Zimerman D. W. and Fleming S. J. (1964). *Thermoluminescencent dating of ancient pottery, Nature*, **219**, 442-444.

[20] Schipper, W.J., Blasse, G., and Leblans, P. (1994). *Chemistry of Materials*, **6**, 1784 – 1789.

[21] Jia, D., and Yen, W.M. (2003). *Journal of Luminescence*, **101**, 115-121, 20].

[22] Pekpak, E. (2009). Synthesis and Characterization of Lithium Tetraborate Doped with Metals, MS Thesis, METU, and Ankara.

[23] Schauer, D., Brodsky, A., and Sayeg, J. (2003). Handbook of Radioactivity Analysis. Second Edition. Great Britain: *Academic Press*.

[24] Meijerink, A., Blasse, G., and Glasbeek, M., (1990). Condensed Matter 2, *Journal of Physics*, 6303-6313.

[25] Yukihara, E.G., Gaza, R., McKeever, S.W.S., and Soares, C.G. (2004). *Radiation Measurement*, **38**, 59-70.

[26] McKeever, S.W.S. (1984). Optical absorption and luminescence in lithium fluoride TLD-100, *Journal of Applied Physics*, **56**, 2883-2889.

[27] E. A. Ainsbury1,*, E. Bakhanova2, J. F. Barquinero3 2011, review of retrospective dosimetry techniques for external ionising radiation exposures *Radiation Protection Dosimetry*, Vol. **147**, No. 4, pp. 573–592.

[28] [D. Mesterházy, M. Osvay, , A. Kovács, , A. Kelemen (September 2012) Accidental and retrospective dosimetry using TL method, *Radiation Physics and Chemistry*, Volume **81**, Issue 9, , Pages 1525-1527.

[29] [H. Y. Göksu, Telephone chip-cards as individual dosimeters, *Radiat. Meas.* **37** (2003), pp. 617-620.

[30] [E. L. Inrig, D. I. Godfrey-Smith and S. Khanna, Optically stimulated luminescence of electronic components for forensic, retrospective and accidental dosimetry, *Radiat. Meas.* **43** (2008), pp. 726-730.

[31] [K. Beerten, C. Woda and F. Vanhavere, Thermoluminescence dosimetry of electronic components for forensic, retrospective and accident dosimetry, *Radiat. Meas.* **44** (2009), pp. 620-625.

[32] A. R. Powell and L. B. Rowland, "SiC Materials Progress, Status, and Potential Roadblocks," *Proc.IEEE*, vol. 90, no. 6, pp. 942-955, 2002.

[33] P. G. Neudeck, R. S. Okojie, and L. Y. Chen, "High-Temperature Electronics-A Role for Wide Bandgap Semiconductors?" *Proc.IEEE*, vol. **90**, no. 6, pp. 1065-1076, 2002.

[34] E. G. Acheson, "Production of Artificial Crystalline Carbonaceous Materials," *United States Patent* **492**,767 (28.02.93), 1893.

[35] H. J. Roound, "A Note on Carborundum," *Elect. World*, vol. **49**, p. 309, 1907.

[36] J. A. Lely, "*Darstellung von Einkristallen von Silicium Carbid und Beherrschung von Art und Menge der eingebauten Verunreinigungen*," Berichte der Deutschen Keramischen Gesellschaft, vol. **32**, pp. 229-236, 1955.

[37] J. A. Lely, "*Sublimation Process for Manufacturing Silicon Carbide Crystals*," United States Patent 2,854,364 (30.09.58), 1958.

[38] Y. M. Tairov and V. F. Tsvetkov, "*General Principles of Growing Large-Size Single Crystals of Various Silicon Carbide Polytypes*," J.Cryst.Growth, vol. **52**, no. 1, pp. 146-150, 1981.

[39] D. L. Barrett, J. P. McHugh, H. M. Hobgood, R. H. Hopkins, P. G. McMullin, and R. C. Clarke, "*Growth of Large SiC Single Crystals*," J.Cryst.Growth, vol. **128**, no. **1**, pp. 358-362, 1993.

[40] D. Hobgood, M. F. Brady, W. H. Brixius, G. Fechko, R. C. Glass, D. Henshall, J. R. Jenny, R. Leonard, D. Malta, S. G. Müller, V. Tsvetkov, and C. H. Carter, Jr., "Status of Large Diameter SiC Crystal Growth for Electronic and Optical Applications," *Materials Science Forum*, vol. 338-342, pp. 3-8, 2000.

[41] T. P. Chow, N. Ramungul, and M. Ghezzo, "Recent Advances in High-Voltage SiC Power Devices," *in Proceedings of the High-Temperature Electronic Materials: Devices and Sensors Conference*, pp. 55-67, 1998.

[42] M. Bhatnagar and B. J. Baliga, "*Comparison of 6H-SiC, 3C-SiC, and Si for Power Devices*," IEEE Trans.Electron Devices, vol. 40, no. **3**, pp. 645-655, 1993.

[43] J. B. Casaday and R. W. Johnson, "*Status of Silicon Carbide (SiC) as a Wide-Bandgap Semiconductor for High-Temperature Applications: A Review*," Solid-State Electron., vol. 39, no. **10**, pp. 1409-1422, 1996.

[44] J. A. Cooper, Jr. and A. Agarwal, "*SiC Power-Switching Devices-The Second Electronics Revolution*?" *Proc.IEEE*, vol. 90, no. **6**, pp. 956-968, 2002.

[45] K. C. Reinhardt and M. A. Marciniak, "Wide-Bandgap Power Electronics for the More Electric Aircraft," in *Transactions of the 3rd International High Temperature Electronics Conference*, pp. I-9, 1996.

[46] T. Burke, K. Xie, J. R. Flemish, R. Singh, T. Podlesak, and J. H. Zhao, "Silicon Carbide Power Devices for High Temperature, High Power Density Switching Applications," *in Proceedings of the Twenty-Second International Power Modulator Symposium*, pp. 18-21, 1996.

[47] R. C. Clarke and J. W. Palmour, "*SiC Microwave Power Technologies*," *Proc.IEEE*, vol. 90, no. 6, pp. 987-992, 2002.

[48] H. Amano, S. Kamiyama, and I. Akasaki, "*Impact of Low-Temperature Buffer Layers on Nitride-Based Optoelectronics*," *Proc.IEEE*, vol. 90, no. 6, pp. 1015-1021, 2002.

[49] L. Patrick, W. J. Choyke, and D. R. Hamilton, "Luminescence of 4H SiC, and Location of Conduction-Band Minima in SiC Polytypes," Phys. Rev., vol. 137, no. 5A, pp. A1515-A1520, 1965.

[50] W. J. Choyke and L. Patrick, "*Absorption of Light in Alpha SiC near the Band Edge*," *Phys. Rev.*, vol. **105**, no. **6**, pp. 1721-1723, 1957.

[51] [R. P. Devaty and W. J. Choyke, "*Optical Characterization of Silicon Carbide Polytypes*," Phys. stat. sol. (a), vol. **162**, no. **1**, pp. 5-38, 1997.

[52] Randall, J. T., and Wilkins, M. H. F. (1945). Phosphorescence and electron traps II: The interpretation of long-period Phosphorescence, *Proceedings of Royal Society London A* **184**, 366-389.

[53] Chen, R., Horowitz, Y.S. (1984). Thermoluminescent and Thermoluminescent Dosimetry. Boca Raton, FL: CRC Press.

[54] Kitis, G., Gomez-Ros, J.M., and Tuyn, J.W.N. (1998). Thermoluminescence glow curve deconvolution functions for first, second and general orders of kinetics, Journal of Physics D: *Applied Physics*, **31**, 2636-2641.

[55] Boss, A.J.J. (2007). Theory of thermoluminescence, *Radiation measurements*, **41**, 45-56.

[56] Hoogenboom, J.R., de Vries, W., Dielhof, J.B., Bos, A.J.J., (1988). Computerized analysis of glow curves from thermally activated processes, *Journal of Applied Physics*. **64** (6), 3193–3200.]

[57] Garlick, G. F. J., and Gibson. A. F. (1948). The electron trap mechanism of luminescence in sulfide and silicate phosphors, *Proceedings of Phyics Society*, **60**, 574.

[58] Bos, A.J.J., and Dielhof, J.B. (1991). The analysis of thermoluminescent glow curves in CaF2: Tm (TLD-300), *Radiation Protection Dosimetry*. **37** (4), 231–239.

[59] May, C.E., and Partridge, J.A. (1964). Thermoluminescence kinetics of alpha irradiated alkali halides, *Journal of Chemical Physics*, **40**, 1401-1415.

[60] Gómez Ros, J.M., Kitis, G., (2002). Computerised glow curve deconvolution using general and mixed order kinetics, *Radiation Protection Dosimetry*. **101** (1–4), 47–52.

[61] Chen, R., and Winer, A.A. (1970). Effects of various heating rates on glow curves, *Journal of Applied Physics*, **41**, 5227-5232.

[62] Azorin, J. (1986). Determination of thermoluminescence parameters from glow curves-I. A review, Nuclear Tracks & Radiation Measurements, 11, 159-166.

[63] Halperin, A., and Braner, A.A. (1960). Evaluation of thermal activation energies from glow curves, *Physical Review Letters*, **117**, 408-415.

[64] Thermo Scientific. (1956). http://www.thermoscientific.com/en/.

[65] 9010 Optical Dating System User Manuel, Dec. 1993.

[66] Gorbics, S. G. Nash. A. E. and Attix F. H. (1969). Thermal Quenching of Luminescence in Six Thermoluminescent Dosimetry Phosphors. In: Proc. 2nd Int. Conf. on Luminescence Dosimetry, Gatlinburg. CONF 680920. pp. 587-608.

[67] Pradhan. A.S. (1996). Thermal Quenching and Two Peak Method –Influence of Heating Rates in TLD. *Radiation Protection Dosimetry*, **65**, 73-78.

[68] Kitis, G. Papadopoulos. J. S., Charalambous, S. and Tuyn, J. W. (1994). The Influence of Heating Rate on the Response and Trapping Parameters of aAl2Os;C. *Radiation Protection Dosimetry*. **55,** 183-190.

[69] Lakshmanan, R., Chandra, B., and Bhatt, R.C. (1981). Dosimetry Characteristics of Thermoluminescent Li2B407: Cu Phospho,. *Radiation Protection Dosimetry*, **3,** 191-198.

[70] C. Bull, G.F.J. Garlick, *Proceedings of the Physical Society of London* **63** (1950) 1283–1291.

[71] Pradhan, A.S. & Bhatt, R. Ch. (1980). Photo thermoluminescence and the behaviors of high-temperature glow peaks in Li2B4O7: Mn and CaSO4: Dyphosphors. *Applied Radiation Isotopes*, **31**, 671-674.

[72] Schulman, J.H., Kirk, R.D. and West, E.J. (1967). Proceedings of the International Conference on Luminescence Dosimetry, Stanford University, CONF-650637, p.113.

[73] Mahesh, K. Weng, P. S. and Furetta, C. (1989). Thermoluminescence in Solids and its Applications. Ashford: *Nuclear Technology Publishing*.

[74] Bos, A.J.J., Piters, J. M., Gomez Ros, J. M. and Delgado, A. (1993). (GLACANIN, and Intercomparision of Glow Curve Analysis Computer Programs) IRI-CIEMAT Report 131-93-005 IRI Delft.

[75] Lorrain, S., David, P., Visocekas, R, and Marinello, G., (1986). A study of new preparations of radiothermoluminescent lithium borates with various activators. *Radiation Protection Dosimetry*, **17**,385-392.

[76] Takenaga, M. Yamamoto, O. And Yamashita, T. (1980). Preparation and characteristics of Li2B4O7: Cu phosphor. *Nuclear Instruments and Methods*, **175**, 77-78.